

# Neutrino Mass Implications for Physics Beyond the Standard Model

Thesis by  
Peng Wang

In Partial Fulfillment of the Requirements  
for the Degree of  
Doctor of Philosophy



California Institute of Technology  
Pasadena, California

2007  
(Defended 23 May, 2007)

© 2007

Peng Wang

All Rights Reserved

TO MY PARENTS

# Acknowledgments

First and foremost, I would like to thank my advisors, Mark Wise, who taught me particle theory and has always been a great mentor to me, and Michael Ramsey-Musolf, who taught me how to write scientific papers and give clear and well-organized presentations, and let me believe that nuclear physics could be as fun as particle physics. I would like to thank them for being great advisors, for constant support and encouragement on my research, and for stimulating discussions. In addition to Mark and Michael, I am grateful to Petr Vogel and Brad Filippone for serving on my thesis committee. I am deeply thankful to Nicole F. Bell, Mikhail Gorchtein, Petr Vogel, Michael Graesser, Rebecca J. Erwin, and Jennifer Kile for inspiring collaborations that have contributed a great portion of what I have learned during my time as a graduate student. I wish to thank my best friends. I don't blame Zhipeng Zhang for abandoning physics for finance since he shows me that finance is not only about money. I want to thank Pengpeng Yu for teaching me a lot about history of CCP. I wish Laingwei and his wife happiness forever. Special thanks go to FC Barcelona, my favorite soccer club. I want to thank them for bringing me many exciting games. Finally, I would like to thank my parents Xuelin Wang and Baiyun Wang. Without their love, support, and encouragement, my accomplishments thus far would have been impossible.

# Abstract

We begin by working out an effective field theory valid below some new physics scale  $\Lambda$  for Dirac neutrinos and Majorana neutrinos, respectively. For Dirac neutrinos, we obtain a complete basis of effective dimension four and dimension six operators that are invariant under the gauge symmetry of the Standard Model. As for Majorana neutrinos, we come up with a complete basis of effective dimension five and dimension seven operators that are invariant under the gauge symmetry of the Standard Model. Using the effective theory, we derive model-independent, "naturalness" upper bounds on the magnetic moments  $\mu_\nu$  of Dirac neutrinos and Majorana neutrinos generated by physics above the scale of electroweak symmetry breaking. In the absence of fine-tuning of effective operator coefficients, for Dirac neutrinos, we find that current information on neutrino mass implies that  $|\mu_\nu| \lesssim 10^{-14} \mu_B$ . This bound is several orders of magnitude stronger than those obtained from analyses of solar and reactor neutrino data and astrophysical observations. As for Majorana neutrinos, the magnetic moment contribution to the mass is Yukawa suppressed. The bounds we derive for magnetic moments of Majorana neutrinos are weaker than present experimental limits if  $\mu_\nu$  is generated by new physics at  $\sim 1$  TeV, and surpass current experimental sensitivity only for new physics scales  $> 10$ – $100$  TeV. The discovery of a neutrino magnetic moment near present limits would thus signify that neutrinos are Majorana particles. Then, we use the scale of neutrino mass to derive model-independent naturalness constraints on possible contributions to muon decay Michel parameters. We show that – in the absence of fine-tuning – the most stringent bounds on chirality-changing operators relevant to muon decay arise from one-loop contributions to neutrino mass. The bounds we obtain on their contributions to the Michel parameters are four or more orders of magnitude stronger than bounds previously obtained in the literature. We also show that, if neutrinos are Dirac fermions, there exist chirality-changing operators that contribute to muon decay but whose flavor structure allows them to evade neutrino mass naturalness bounds. We discuss the im-

plications of our analysis for the interpretation of muon decay experiments. Finally, we use the upper limit on the neutrino mass to derive model-independent naturalness constraints on some non-Standard-Model  $d \rightarrow ue^{-}\bar{\nu}$  interactions. In the absence of fine-tuning of effective operator coefficients, our results yield constraints on scalar and tensor weak interactions one or more orders of magnitude stronger than a recent global fit after combined with the current experimental limits. We also show that, if neutrinos are Majorana fermions, there exist four-fermion operators that contribute to beta decay but whose flavor structure allows them to evade neutrino mass naturalness bounds. We also consider the constraint on the branching ratio of  $\pi \rightarrow \nu\bar{\nu}$  by neutrino mass. Constraints on the beta decay parameters by CKM Unitarity,  $R_{e/\mu}$ , and  $\pi_{\beta}$  are discussed as well.

# Contents

<b>Acknowledgments</b>	<b>iv</b>
<b>Abstract</b>	<b>v</b>
<b>1 Introduction</b>	<b>1</b>
1.1 Some Neutrino Properties . . . . .	1
1.1.1 Types of Neutrino . . . . .	1
1.1.2 Neutrino Oscillations . . . . .	3
1.1.3 Direct Bounds on Neutrino Masses . . . . .	4
1.2 Neutrino Mass Implications . . . . .	6
1.3 Plan of My Dissertation . . . . .	7
<b>2 Effective Field Theory</b>	<b>9</b>
2.1 Introduction . . . . .	9
2.2 The Fields and the Lagrangian $\mathcal{L}_{\text{SM}}$ . . . . .	11
2.3 Operator Basis . . . . .	12
2.3.1 Construction of $\mathcal{L}_6$ for Dirac Neutrinos . . . . .	13
2.3.2 Construction of $\mathcal{L}_5$ and $\mathcal{L}_7$ for Majorana Neutrinos . . . . .	18
<b>3 Operator Matching and Mixing</b>	<b>21</b>
3.1 Introduction . . . . .	21
3.2 Mixing and Matching Considerations for $O_M^{(4,6)}$ and $O_M^{(5,7)}$ . . . . .	23
3.2.1 Diagonalizing Yukawa Couplings . . . . .	23
3.2.2 Dirac Case . . . . .	26
3.2.2.1 Matching with $\mathcal{O}_{M,AD}^{(4)}$ . . . . .	26
3.2.2.2 Mixing with $\mathcal{O}_{M,AD}^{(6)}$ . . . . .	28

3.2.3	Majorana Case . . . . .	34
3.2.3.1	Matching with $\mathcal{O}_{M,AD}^{(5)}$ . . . . .	34
3.2.3.2	Mixing with $\mathcal{O}_{M,AD}^{(7)}$ . . . . .	36
<b>4</b>	<b>Neutrino Mass Constraints</b>	<b>38</b>
4.1	Constraints on Neutrino Magnetic Moment . . . . .	39
4.1.1	Dirac Case . . . . .	39
4.1.2	Majorana Case . . . . .	41
4.2	Implications for Muon Decay Parameters . . . . .	45
4.2.1	Introduction . . . . .	45
4.2.2	Dirac Case . . . . .	46
4.2.3	Majorana Case . . . . .	49
4.2.4	Constraints from Experiments . . . . .	52
4.3	Implications for Beta Decay Parameters . . . . .	53
4.3.1	Introduction . . . . .	53
4.3.2	Correlation coefficients . . . . .	54
4.3.3	Dirac Case . . . . .	56
4.3.3.1	Effective Hamiltonian Below the Weak Scale . . . . .	56
4.3.3.2	$4D$ Case . . . . .	60
4.3.3.3	$6D$ Case . . . . .	63
4.3.4	Majorana Case . . . . .	64
4.3.5	Status of Experiments . . . . .	66
4.3.6	Constraints From CKM Unitarity, $R_{e/\mu}$ , and $\pi_\beta$ . . . . .	67
4.3.6.1	CKM Unitarity . . . . .	68
4.3.6.2	$R_{e/\mu}$ . . . . .	70
4.3.6.3	$\pi_\beta$ . . . . .	71
4.4	Constraints on $\pi \rightarrow \nu\bar{\nu}$ . . . . .	75
	<b>Bibliography</b>	<b>77</b>

# List of Figures

1.1	The most important exclusion limits, as well as preferred parameter regions, from neutrino oscillation experiments assuming two-flavour oscillations . . . . .	5
1.2	a) Generic contribution to the neutrino magnetic moment induced by physics beyond the standard model. b) Corresponding contribution to the neutrino mass. The solid and wavy lines correspond to neutrinos and photons respectively, while the shaded circle denotes physics beyond the SM. . . . .	7
1.3	Scheme of my dissertation . . . . .	8
2.1	Contributions from the operators (a) $\mathcal{O}_{B,AD}^{(6)}$ and (b) $\mathcal{O}_{B,AD}^{(6)}$ (denoted by the shaded box) to the amplitude for $\mu$ -decay or $\beta$ -decay. Solid, dashed, and wavy lines denote fermions, Higgs scalars, and gauge bosons, respectively. After SSB, the neutral Higgs field is replaced by its vev, yielding a four-fermion $\mu$ -decay or $\beta$ -decay amplitude . . . . .	18
3.1	One-loop graphs for the matching of $\mathcal{O}_{B,W}^{(6)}$ , $\mathcal{O}_{\tilde{V}}^{(6)}$ , and $\mathcal{O}_F^{(6)}$ (denoted by the shaded box) into $\mathcal{O}_{M,AD}^{(4)}$ . Solid, dashed, and wavy lines denote fermions, Higgs scalars, and gauge bosons, respectively. Panels (a, b, c) illustrate matching of $\mathcal{O}_{B,W}^{(6)}$ , $\mathcal{O}_{\tilde{V}}^{(6)}$ , and $\mathcal{O}_F^{(6)}$ , respectively, into $\mathcal{O}_{M,AD}^{(4)}$ . . . . .	26
3.2	One-loop graphs for the matching of $\mathcal{O}_{u,d}^{(6)}$ (denoted by the black box) into $\mathcal{O}_{M,AD}^{(4)}$ . Solid and dashed lines denote fermions and Higgs scalars, respectively. . . . .	26
3.3	Self-renormalization of $\mathcal{O}_{B,W}^{(6)}$ . . . . .	29
3.4	Mixing of $\mathcal{O}_{B,W}^{(6)}$ into $\mathcal{O}_M^{(6)}$ . . . . .	29
3.5	Self-renormalization of $\mathcal{O}_M^{(6)}$ . . . . .	29
3.6	One-loop graphs for the mixing among $6D$ operators. Notation is as in previous figures. Various types of mixing (a–g) and self-renormalization (h–j) are as discussed in the text . . . . .	30

3.7	Self renormalizations of $\mathcal{O}_{Q,d1,d2,AD,\alpha\beta}^{(6)}$ (denoted by the black box). Solid, dashed, and wavy lines denote fermion, Higgs scalar, and gauge bosons, respectively . . . . .	30
3.8	Mixing $\mathcal{O}_{Q,d1,d2,AD,\alpha\beta}^{(6)}$ into $\mathcal{O}_{B,W}^{(6)}$ . . . . .	31
3.9	Mixing $\mathcal{O}_{B,W}^{(6)}$ into $\mathcal{O}_{Q,d1,d2,AD,\alpha\beta}^{(6)}$ . . . . .	31
3.10	One-loop graphs for the matching of $\mathcal{O}_{B,W}^{(7)}$ (denoted by the black box) into $\mathcal{O}_{M,AD}^{(5)}$ . . . . .	34
3.11	One-loop graphs for the matching of $\mathcal{O}_{L,u,d}^{(7)}$ (denoted by the shaded box) into $\mathcal{O}_{M,AD}^{(5)}$ . . . . .	35
3.12	Contribution of $O_W^-$ to the 7D neutrino mass operator . . . . .	37
4.1	Representative contribution of $O_W^-$ to the 5D neutrino mass operator . . . .	43
4.2	Constraints on $\tilde{C}_S = C_S/C_V$ and $\tilde{C}'_S = C'_S/C_V$ . The narrow diagonal band at $-45^\circ$ is from this work. The gray circle is a 95% C.L. limit from Ref. [62]. The diagonal band at $45^\circ$ is a 90% C.L. limit from Ref. [60] . . . . .	67
4.3	Constraints on $\tilde{C}_T = C_T/C_A$ and $\tilde{C}'_T = C'_T/C_A$ . The diagonal band at $-45^\circ$ is from this work. The gray circle is a 68% C.L. limit from Ref. [65]. The diagonal band at $45^\circ$ is a 90% C.L. limit from Ref. [61] . . . . .	67

# List of Tables

4.1	Summary of constraints on the magnitude of the magnetic moment of Majorana neutrinos. The upper two lines correspond to a magnetic moment generated by the $O_W$ operator, while the lower two lines correspond to the $O_{\bar{B}}$ operator. . . . .	41
4.2	Constraints on $\mu$ -decay couplings $g_{e\mu}^\gamma$ in the Dirac case. The first eight rows give naturalness bounds in units of $(v/\Lambda)^2 \times (m_\nu/1 \text{ eV})$ on contributions from $6D$ muon decay operators based on one-loop mixing with the $4D$ neutrino mass operators. The ninth row gives upper bounds derived from a recent global analysis of [40], while the last row gives estimated bounds from [44] derived from two-loop mixing of $6D$ muon decay and mass operators. A “-” indicates that the operator does not contribute to the given $g_{e\mu}^\gamma$ , while “None” indicates that the operator gives a contribution unconstrained by neutrino mass. The subscript $D$ runs over the two generations of RH Dirac neutrinos . . . . .	47
4.3	Coefficients $\kappa$ that relate $g_{e\mu}^\gamma$ to the dimension six operator coefficients $C_k^6$ . . . . .	47
4.4	Constraints on $\mu$ -decay couplings $g_{e\mu}^\gamma$ in the Majorana case. The naturalness bounds are given in units of $(v/\Lambda)^2 \times (m_\nu/1 \text{ eV})$ on contributions from $7D$ muon decay operators based on one-loop mixing with the $5D$ neutrino mass operators . . . . .	50
4.5	Coefficients $\kappa$ that relate $g_{e\mu}^\gamma$ to the dimension six operator coefficients $C_k^7$ . . . . .	50
4.6	Constraints on $\beta$ -decay couplings $a_{e\mu}^\gamma$ in the Dirac case. The naturalness bounds are given in units of $(v/\Lambda)^2 \times (m_\nu/1 \text{ eV})$ on contributions from $6D$ beta decay operators based on one-loop mixing with the $4D$ neutrino mass operators . . . . .	63

4.7	Constraints on $\beta$ -decay couplings $a_{e\mu}^\gamma$ in the Majorana case. Naturalness bounds are given in units of $(v/\Lambda)^2 \times (m_\nu/1\text{eV})$ on contributions from $7D$ beta decay operators based on one-loop mixing with the $5D$ neutrino . . . .	65
4.8	Constraints on $\beta$ -decay couplings $a_{e\mu}^\gamma$ . . . . .	68

# Chapter 1

## Introduction

The Standard Model (SM) [1] is the name given in the 1970s to a theory of fundamental particles and how they interact. The SM is very successful at energies up to about hundred GeV. The SM has passed numerous experimental tests. However, despite its tremendous successes, no one finds the SM satisfactory, and it is widely expected that there is physics beyond the SM, with new characteristic mass scale(s), perhaps up to, ultimately, a string scale. In the absence of any direct evidence for their mass, neutrinos were introduced in the SM as truly massless fermions for which no gauge-invariant renormalizable mass term can be constructed. Consequently, in the SM there is no mixing in the lepton sector. However, the evidences of neutrino oscillations were found in the Super-Kamiokande [3], SNO [4], KamLAND [5], and other solar [6, 7, 8, 9] and atmospheric [10, 11] neutrino experiments of neutrino oscillations. Observation of neutrino oscillations gives us the first sign of physics beyond the SM. New physics seems to have manifested itself in the form of neutrino masses and lepton mixing. In this way, neutrino masses can be connected to other new physics.

### 1.1 Some Neutrino Properties

#### 1.1.1 Types of Neutrino

In general, there are two possible types of neutrinos: Dirac and Majorana neutrinos, since neutrinos are neutral fermions. In the following, we consider the simplest case of one generation. Dirac neutrinos could have Dirac mass terms, which couple left- and right-handed fields

$$m_D \bar{\nu}_L \nu_R + h.c., \quad (1.1)$$

where  $m_D$  is the Dirac mass and  $\nu_L$  and  $\nu_R$  are left- and right-handed Weyl spinor fields, respectively.

Majorana neutrinos could have Majorana mass terms which couples a left-handed or a right-handed field to itself. Consider  $\nu_L$ . Its Majorana mass term is

$$m_M \overline{\nu_L^c} \nu_L, \quad \psi^c = C \overline{\psi}^T, \quad (1.2)$$

where  $m_M$  is the Majorana mass and  $C$  is the charge conjugation matrix.

Majorana neutrinos could also have both Dirac and Majorana mass terms. In this way the mass terms, would be:

$$m_D \overline{\nu_R} \nu_L + \frac{1}{2} m_M \overline{\nu_R} \nu_R^c + h.c. = \frac{1}{2} \overline{n_L^c} M n_L + h.c. \quad (1.3)$$

with:

$$M \equiv \begin{pmatrix} 0 & m_D \\ m_D & m_M \end{pmatrix}. \quad (1.4)$$

The eigenvalues of this mass matrix will be the neutrino masses:

$$m_1 \simeq -\frac{(m_D)^2}{m_M}, \quad m_2 \simeq m_M. \quad (1.5)$$

When  $m_M \gg m_D$ , we obtain a very low mass, which would explain the lightness of neutrino, and a very high mass, for a superheavy neutrino, which is the famous see-saw mechanism [15].

Experimentally, there exists no conclusive evidence for or against the presence of light Majorana neutrinos. New searches for neutrinoless double  $\beta$ -decay could provide conclusive proof that the light neutrinos are Majorana, provided the neutrino-mass spectrum has the “inverted” rather than “normal” hierarchy (for recent reviews, see, e.g., [16]). If, on the other hand, future longbaseline oscillation experiments establish the existence of the inverted hierarchy and/or ordinary  $\beta$ -decay measurements indicate a mass consistent with the inverted hierarchy, a null result from the neutrinoless double  $\beta$ -decay searches would imply that neutrinos are Dirac neutrinos. Either way, the investment of substantial experimental resources in these difficult measurements indicates that determining the charge conjugation properties of the neutrino is both an central question for neutrino physics as

well as one that is not settled.

### 1.1.2 Neutrino Oscillations

Neutrino oscillations are similar to the well known oscillations between  $K^0$ - and  $\overline{K^0}$ -mesons. They occur because of the mixing in the charged weak current discussed in the SM. The neutral and charged current weak interactions of neutrinos are described by the Lagrangian

$$\mathcal{L}_{EW} = - \sum_{\alpha,i} \left\{ \frac{g}{2 \cos \theta_W} \bar{\nu}_{L\alpha} \gamma^m \nu_{L\alpha} Z_m + \frac{g}{\sqrt{2}} \bar{e}_{L\alpha} \gamma^m U_{\alpha i} \nu_{Li} W_m^- + h.c. \right\}, \quad (1.6)$$

where the fields  $e_{L\alpha}$ ,  $\alpha = 1 \dots 3$ , represent the mass eigenstates of electron, muon, and tau, and the fields  $\nu_{Li}$ ,  $i = 1 \dots n \geq 3$ , correspond to neutrino mass eigenstates. The flavour eigenstate  $\nu_a$  is a linear superposition of mass eigenstates,

$$\nu_a = \sum_i U_{\alpha i}^* \nu_i. \quad (1.7)$$

Three linear combinations of mass eigenstates have weak interactions, and are therefore called *active*, whereas  $n - 3$  linear combinations are *sterile*, i.e., they don't feel the weak force. In the case  $n = 4$ , for instance, the sterile neutrino is given by

$$\nu_s = \sum_i U_{4i}^* \nu_i. \quad (1.8)$$

In the following we will restrict ourselves to the case of three active neutrinos.

We will consider now the evolution of the flavor state  $\nu_a$  in vacuum. If at  $t = 0$  flavor neutrino  $\nu_\alpha$  is produced, for the neutrino state at a time  $t$  we will have

$$|\nu_\alpha\rangle_t = e^{-iH_0 t} |\nu_\alpha\rangle = \sum_1^2 U_{li}^* e^{-iE_i t} |\nu_i\rangle, \quad (1.9)$$

where  $H_0$  is the free Hamiltonian. Developing  $E_i$  over  $m_i^2$  we have

$$E_i \simeq E + \frac{m_i^2}{2E}, \quad (1.10)$$

where  $E = p$  is the energy of the neutrino in the approximation  $m_i^2 \rightarrow 0$ . From (1.9) and

(1.10) for the neutrino state at the time  $t$  we have

$$|\nu_\alpha\rangle_t = e^{-iEt} \sum_{i=1}^3 e^{-i\frac{m_i^2 t}{2E}} U_{\alpha i}^* |\nu_i\rangle. \quad (1.11)$$

Taking into account the unitarity of the mixing matrix, we find the amplitude of the probability to find a state  $|\nu_{\alpha'}\rangle$  in the state  $|\nu_\alpha\rangle_t$  is

$$A(\nu_\alpha \rightarrow \nu_{\alpha'}) = \langle \nu_{\alpha'} | \nu_\alpha \rangle_t = \sum_{i=1}^3 U_{\alpha' i} e^{-i\frac{m_i^2 t}{2E}} U_{\alpha i}^* \quad (1.12)$$

from which we obtain the transition probability in the form

$$P(\nu_\alpha \rightarrow \nu_{\alpha'}) = |\delta_{\alpha'\alpha} + \sum_{i=2,3} U_{\alpha' i} (e^{-i\Delta m_{i1}^2 \frac{L}{2E}} - 1) U_{\alpha i}^*|^2 \quad (1.13)$$

where  $\Delta m_{i1}^2 = m_i^2 - m_1^2$ ,  $L$  is the distance between neutrino source and neutrino detector, and we label neutrino masses in such a way that  $m_1 < m_2 < m_3$ .

In the simplest case of the transition between two flavor neutrinos index  $i$  in (1.13) takes the value 2. For  $\alpha' \neq \alpha$  we have

$$P(\nu_\alpha \rightarrow \nu_{\alpha'}) = \frac{1}{2} \sin^2 2\theta (1 - \cos \Delta m^2 \frac{L}{2E}); \quad (\alpha' \neq \alpha). \quad (1.14)$$

Here  $\Delta m^2 = m_2^2 - m_1^2$  and  $\theta$  is the mixing angle ( $|U_{\alpha'2}|^2 = \sin^2 \theta$ ,  $|U_{\alpha2}|^2 = \cos^2 \theta$ ).

In matter, a resonance enhancement of neutrino oscillations can take place and transition probabilities can be maximal even for small vacuum mixing angles—this is the Mikheyev-Smirnov-Wolfenstein effect [17], which turns out to be very important in the analysis of solar neutrinos.

In recent years there has been a wealth of experimental data in neutrino physics, and we can look forward to important new results also in the coming years. The present situation is summarized in Fig. 1.1 which is taken from the review of particle physics.

### 1.1.3 Direct Bounds on Neutrino Masses

Neutrinos are expected to have mass, like all other leptons and quarks. The study of the electron energy spectrum in tritium  $\beta$ -decay over many years has led to an impressive bound

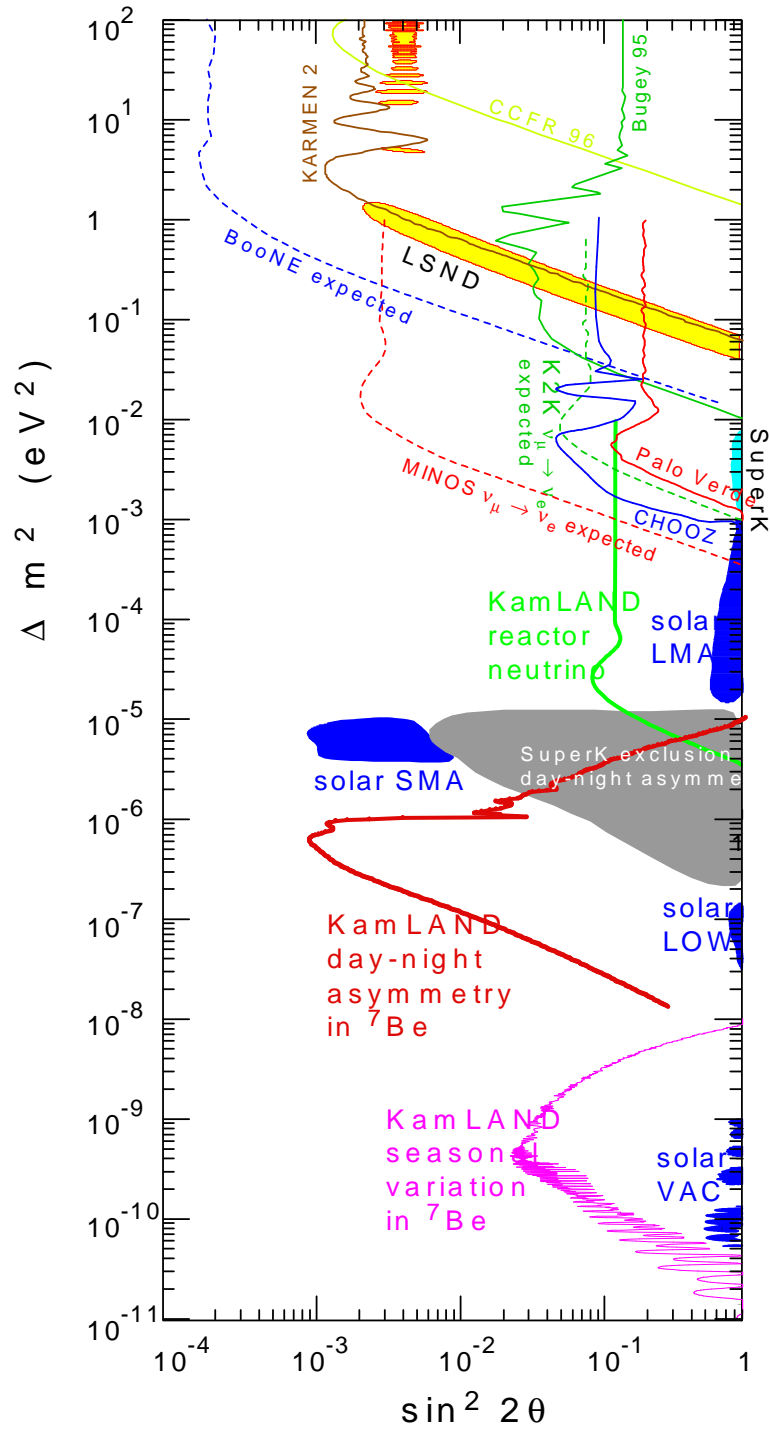


Figure 1.1: The most important exclusion limits, as well as preferred parameter regions, from neutrino oscillation experiments assuming two-flavour oscillations

for the electron-neutrino mass. The strongest upper bound has been obtained by the Mainz collaboration [12]:

$$m_{\nu_e} < 2.2 \text{ eV (95\% CL)}. \quad (1.15)$$

It is based on the analysis of the Kurie plot, where the electron energy spectrum is studied near the maximal energy  $E_0$ :

$$K(E_e) \propto \sqrt{(E_0 - E_e)((E_0 - E_e)^2 - m_n^2)^{1/2}}. \quad (1.16)$$

In the future the bound (1.15) is expected to be improved to 0.3 eV [13].

Direct kinematic limits for tau- and muon-neutrinos have been obtained from the decays of  $\tau$ -leptons and  $\pi$ -mesons, respectively. The present upper bounds are [14],

$$m_{\nu_\tau} < 18.2 \text{ MeV (95\% CL)}, m_{\nu_\tau} < 170 \text{ KeV (90\% CL)}. \quad (1.17)$$

## 1.2 Neutrino Mass Implications

Neutrino mass implications for new physics is the main topic in my dissertation. Here I am just going to use a naïve relationship between the size of  $\mu_\nu$ , neutrino magnetic moment, and  $m_\nu$ , neutrino mass, to illustrate the general picture.

If a magnetic moment is generated by physics beyond the Standard Model (SM) at an energy scale  $\Lambda$ , as in Fig. 1.2a, we can generically express its value as

$$\mu_\nu \sim \frac{eG}{\Lambda}, \quad (1.18)$$

where  $e$  is the electric charge and  $G$  contains a combination of coupling constants and loop factors. Removing the photon from the same diagram (Fig. 1.2b) gives a contribution to the neutrino mass of order

$$m_\nu \sim G\Lambda. \quad (1.19)$$

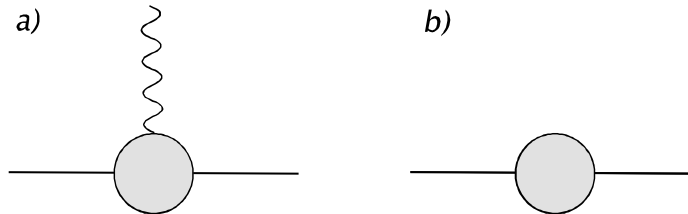


Figure 1.2: a) Generic contribution to the neutrino magnetic moment induced by physics beyond the standard model. b) Corresponding contribution to the neutrino mass. The solid and wavy lines correspond to neutrinos and photons respectively, while the shaded circle denotes physics beyond the SM.

We thus have the relationship

$$\begin{aligned}
 m_\nu &\sim \frac{\Lambda^2}{2m_e} \frac{\mu_\nu}{\mu_B} \\
 &\sim \frac{\mu_\nu}{10^{-18} \mu_B} [\Lambda(\text{TeV})]^2 \text{ eV},
 \end{aligned}
 \tag{1.20}$$

which implies that it is difficult to simultaneously reconcile a small neutrino mass and a large magnetic moment.

However, it is well known that the naïve restriction given in Eq. (1.20) can be overcome via a careful choice for the new physics. For example, we may impose a symmetry to enforce  $m_\nu = 0$  while allowing a non-zero value for  $\mu_\nu$  [18, 19, 20, 21], or employ a spin suppression mechanism to keep  $m_\nu$  small [22].

### 1.3 Plan of My Dissertation

Fig. 1.3 shows the framework of my work here. Above the new physics scale  $\Lambda$ , I expect some form of new physics. In my work, I am going to carry out a model-independent analysis, so I don't specify new physics above  $\Lambda$ . Below  $\Lambda$ , the new physics is integrated out and I have an effective theory which I am going to work with. Since new physics is not specified above  $\Lambda$ ,  $C_j^n$ , the couplings of effective dimension  $n$  operators, cannot be determined by matching the effective theory with the new physics at the scale  $\Lambda$ . Instead, they can only be determined by experiments.

In Chapter 2, I am going to list all  $n = 6$  effective operators for Dirac neutrinos and  $n = 7$  ones for Majorana neutrinos for the effective theory valid below  $\Lambda$ . Also, I focus on the

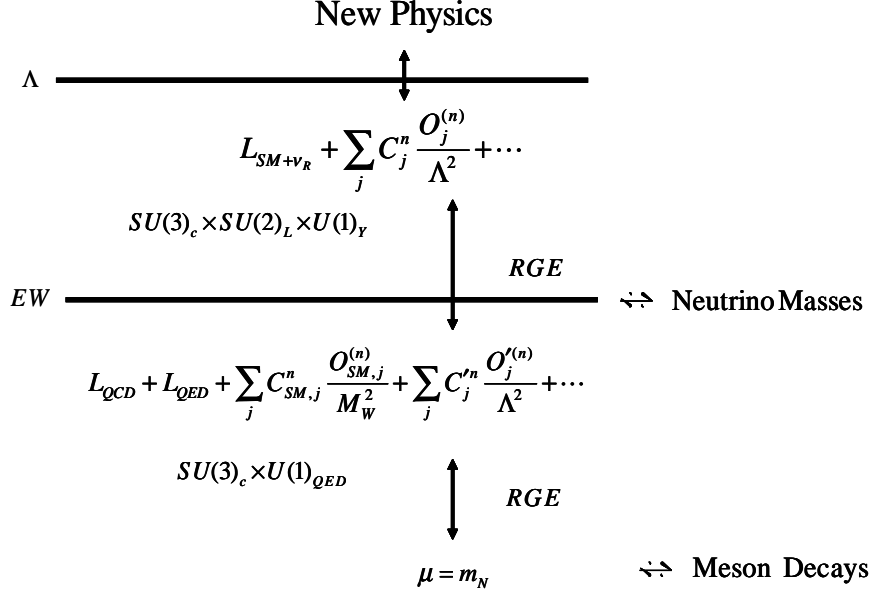


Figure 1.3: Scheme of my dissertation

"interesting" operators that could contribute to neutrino mass through loops and other low energy physics, such as neutrino magnetic moment,  $\mu$ -decay, and  $\beta$ -decay.

In Chapter 3, in order to connect the "interesting" operators with neutrino mass operators, I am going to work on these operators matching with 4D neutrino mass operators and mixing with 6D neutrino mass operators.

In Chapter 4, I am going to use upper bounds on neutrino mass to constrain neutrino magnetic moment [42, 45] and parameters of  $\mu$ -decay [41] and  $\beta$ -decay. I have to evolve the renormalization scale  $\mu$  to characteristic energy of low energy physics to study them. For neutrino magnetic moment and  $\mu$ -decay, I only have QED corrections, which are negligible. However, as for  $\beta$ -decay, QCD corrections could be important and we therefore include them in our analysis of  $\beta$ -decay.

## Chapter 2

# Effective Field Theory

### 2.1 Introduction

Standard Model is the best theory of the ultimate nature of matter available today. To date, almost all experimental tests of the three forces described by the Standard Model have agreed with its predictions, which have resulted in establishing the Standard Model as a very good effective theory at the weak scale given by the Higgs boson vacuum expectation value of  $v \simeq 250$  GeV and below. Although the Standard Model is remarkably successful, there is still some room for new physics, due to many theoretical reasons and deviations from some experiments, which suggests that new physics might be one with a cutoff scale much lower than the Planck scale; perhaps as low as a few TeV. For example, the discovery of neutrino mixing has given us the first sign of new physics beyond  $v$ . The exact nature of the new physics has not been identified yet. However, there are still two approaches we can employ to explore the contributions from new physics. One is the top-down approach, with which one can make a guess at this new physics and engage in constructing consistent models. The top-down approaches can and will be very important for guiding thinking, but are unlikely to lead to detailed serious predictions that really test the ideas, especially for the string theory. The other approach is bottom-up, with which we can proceed by making use of the effective field theory, which is characterized by a scale  $\Lambda$ . Then we only need to take explicitly into account the relevant degrees of freedom, i.e., those states with  $m \ll \Lambda$ , while the heavier states with  $m \gg \Lambda$  are integrated out from the action of new physics. All UV dependence appears directly in the coefficients of the effective Lagrangian, which is a sum of the SM term and non-renormalizable ones which are the results of integrating out the unknown degrees of freedom. However, the effective Lagrangian carries an infinite number

of non-renormalizable terms whose coefficients can only be determined by experiments since the full theory is unknown. This is not as desperate as it seems, the good news is that all the operators can be classified by their dimensions  $d$  and their coefficients are suppressed by  $\frac{1}{\Lambda^d}$ . Generally, we only need to use the lowest-dimension operators, discarding the higher orders.

Since the full theory still stays a mystery to us, we need to identify two crucial ingredients of the effective field theory before we build it. First, we have to identify the symmetry the effect field theory respects. Intense experimental efforts in the search for new physics strongly suggest that we should take the gauge symmetry  $SU_C(3) \times SU_L(2) \times U_Y(1)$  of the Standard Model above the weak scale. Below the weak scale, the gauge symmetry is  $SU_{\text{QCD}}(3) \times U_{\text{QED}}(1)$ . The second ingredient to know is the degrees of freedom. We usually take the minimal set of fields, namely the SM fields of 45 chiral fermions, plus the gauge bosons and one Higgs doublet, plus the necessary fields for certain theoretical motivations. If we assume neutrinos are Dirac particle and are also massive, we need to include the right-handed neutrinos  $\nu_R$  as well. On the other hand, if the neutrinos are assumed to be Majorana particle, the SM fields are enough. Even for the popular see-saw mechanism in which we need very heavy  $\nu_R(s)$  to make  $\nu_Ls$  light enough,  $\nu_R(s)$  are integrated out since they are so heavy.

In this spirit, the total Lagrangian valid up to energies of order  $\Lambda$  can be written as an expansion in  $\frac{1}{\Lambda}$

$$\mathcal{L}_{\text{eff}} = \mathcal{L}_{\text{SM}+\text{new fields}} + \frac{1}{\Lambda}\mathcal{L}_5 + \frac{1}{\Lambda^2}\mathcal{L}_6 + \frac{1}{\Lambda^3}\mathcal{L}_7 \cdots \quad (2.1)$$

where  $\mathcal{L}_{\text{SM}+\text{new fields}}$  are dimension four operators (SM operators plus ones generated by the new fields of the effective field theory),  $\mathcal{L}_5$  is the dimension five operator constructed from the neutrino and Higgs fields which is responsible for generating Majorana neutrino masses for the active neutrinos,  $\mathcal{L}_6$  are dimension six operators, etc. All  $\mathcal{L}_i$  are  $SU_C(3) \times SU_L(2) \times U_Y(1)$  invariant. If  $\mathcal{L}_5$  is non-vanishing then lepton number is not conserved. On the other hand, neutrinos may be Dirac particles, in which case  $\mathcal{L}_5$  vanishes. So for the Dirac neutrino case, we have to include a new field  $\nu_R$  and work out all the dimension six operators. However for the Majorana neutrino case, we don't need any new fields. But we have to find all the dimension seven operators, because  $\mathcal{L}_5$  only includes the Majorana

neutrino mass operator, which is not interesting for our analysis.

In Section 2.2, we review the Standard Model field and  $\mathcal{L}_{\text{SM}}$  to set notations; in Section 2.3 we develop  $\mathcal{L}_6$  and  $\mathcal{L}_7$ .

## 2.2 The Fields and the Lagrangian $\mathcal{L}_{\text{SM}}$

To set notations, we begin with  $\mathcal{L}_{\text{SM}}$ . The fields are

- Matter fields:

$$\text{Left-handed lepton doublets: } L = \begin{pmatrix} \nu_L \\ l_L \end{pmatrix} (\mathbf{1}, \mathbf{2}, -1)$$

$$\text{Right-handed charged leptons: } l_R (\mathbf{1}, \mathbf{1}, -2)$$

$$\text{Left-handed quark doublets: } Q = \begin{pmatrix} u_L \\ d_L \end{pmatrix} (\mathbf{3}, \mathbf{2}, \frac{1}{3})$$

$$\text{Right-handed quark singlets: } u_R (\mathbf{3}, \mathbf{1}, \frac{4}{3}), d_R (\mathbf{3}, \mathbf{1}, -\frac{2}{3})$$

- Gauge fields:

$$\text{Gluons: } G_\mu^A, \quad A = 1 \cdots 8, \quad (\mathbf{8}, \mathbf{1}, 0)$$

$$\text{W bosons: } W_\mu^a, \quad a = 1, 2, 3 \quad (\mathbf{1}, \mathbf{3}, 0)$$

$$\text{B bosons: } B_\mu \quad (\mathbf{1}, \mathbf{1}, 0)$$

- Higgs boson doublets:  $\phi (\mathbf{1}, \mathbf{2}, 1), \tilde{\phi} = i\tau^2 \phi^* (\mathbf{1}, \mathbf{2}, -1)$

where we indicate how fields transform under  $SU_C(3) \times SU_L(2) \times U_Y(1)$  in the brackets. The gauge couplings of  $SU_C(3) \times SU_L(2) \times U_Y(1)$  are denoted by  $g_3$ ,  $g_2$ , and  $g_1$ . The latter are often expressed in terms of the weak mixing angle,  $\theta_W$ , and the electric unit charge,  $e$ :

$$\sin^2 \theta_W = \frac{g_1^2}{g_1^2 + g_2^2} \tag{2.2}$$

$$e = g_2 \sin \theta_W = g_1 \cos \theta_W.$$

The  $SU_C(3) \times SU_L(2) \times U_Y(1)$  Lagrangian is

$$\begin{aligned}
\mathcal{L}_{\text{SM}} = & -\frac{1}{4}G_{\mu\nu}^A G^{A\mu\nu} - \frac{1}{4}W_{\mu\nu}^a W^{a\mu\nu} - \frac{1}{4}B_{\mu\nu}B^{\mu\nu} \\
& + i\bar{L}\not{D}L + i\bar{Q}\not{D}Q + i\bar{u}_R\not{D}u_R + i\bar{d}_R\not{D}d_R + i\bar{l}_R\not{D}l_R \\
& + f_e\bar{L}\phi l_R + f_d\bar{Q}\phi d_R + f_u\bar{Q}\tilde{\phi}u_R \\
& + (D_\mu\phi)(D^\mu\phi) + m_\phi^2\phi^\dagger\phi + \frac{\lambda}{2}(\phi^\dagger\phi)^2.
\end{aligned} \tag{2.3}$$

Assuming  $m_\phi^2 < 0$ ,  $\phi$  develops a vacuum expectation value (VEV)

$$\phi \rightarrow \begin{pmatrix} 0 \\ v/\sqrt{2} \end{pmatrix} \tag{2.4}$$

and the Higgs potential spontaneously breaks part of the gauge symmetry,

$$SU_C(3) \times SU_L(2) \times U_Y(1) \rightarrow SU(3)_{\text{QCD}} \times U(1)_{\text{QED}}.$$

The one remaining physical Higgs degree of freedom,  $H = (0, \phi^0/\sqrt{2})$ , acquires a mass given by  $M_H = \lambda v$ .

Quarks and charged leptons receive masses through Yukawa interactions. In the three-generation SM, the Yukawa couplings  $f_e$ ,  $f_u$ , and  $f_d$  become matrix valued. The mass matrices for charged leptons,  $u$ -type quarks, and  $d$ -type quarks are given by, respectively,

$$m_e = f_e \frac{v}{\sqrt{2}}, \quad m_u = f_u \frac{v}{\sqrt{2}}, \quad m_d = f_d \frac{v}{\sqrt{2}}. \tag{2.5}$$

Normally,  $m_e$ ,  $m_u$ , and  $m_d$  are general matrices. We can use fields' redefinition to make some of them diagonal; will discuss this in Section 3.2.

## 2.3 Operator Basis

We are going to list all the effective operators with dimension six for the case of Dirac neutrinos in Section 2.3.1 and all the effective operators with dimension five and dimension seven for the case of Majorana neutrinos in Section 2.3.2. We find that it is useful to group

them according to the number of fermion, Higgs, and gauge boson fields that enter. And we will make use of the equations of motion to express some operators in terms of other ones and hence exclude them in the operator basis. In the process of listing all operators, we will single out the operators which can contribute to both  $m_\nu$  through radiative corrections and muon decay, beta decay, or neutrino magnetic moment in order to carry out our analysis in Chapter 4.

### 2.3.1 Construction of $\mathcal{L}_6$ for Dirac Neutrinos

In this case, the effective Lagrangian turns out to be

$$\mathcal{L}_{\text{eff}} = \mathcal{L}_{\text{SM}+\text{new fields}} + \frac{1}{\Lambda^2} \mathcal{L}_6 \cdots + \text{h.c.} \quad (2.6)$$

The lowest dimension neutrino mass operator is

$$\mathcal{O}_M^{(4)} = \bar{L} \tilde{\phi} \nu_R. \quad (2.7)$$

After spontaneous symmetry breaking, one has

$$\begin{aligned} C_M^4 \mathcal{O}_M^{(4)} &\rightarrow -m_\nu \bar{\nu}_L \nu_R \\ m_\nu &= -C_M^4 v / \sqrt{2}. \end{aligned} \quad (2.8)$$

The other operators with dimension four are those of the SM which we already have in Section 2.2.

For the case of Dirac neutrinos that we consider here, there exist no gauge-invariant operators with dimension five. So we move to operators with dimension six.

Four-lepton:

$$\begin{aligned} \bar{L} \gamma^\mu L \bar{L} \gamma_\mu L & \quad \bar{l}_R \gamma^\mu l_R \bar{l}_R \gamma_\mu l_R & \quad \bar{l}_R \gamma^\mu l_R \bar{\nu}_R \gamma_\mu \nu_R & \quad \bar{\nu}_R \gamma^\mu \nu_R \bar{\nu}_R \gamma_\mu \nu_R \\ \bar{L} l_R \bar{l}_R L & \quad \bar{L} \nu_R \bar{\nu}_R L & \quad \epsilon^{ij} \bar{L}_i l_R \bar{L}_j \nu_R \end{aligned} \quad (2.9)$$

Several of the operators appearing in this list can contribute to  $\mu$ -decay, but only the last one can also contribute to  $m_\nu$  through radiative corrections. Including flavor indices, we

refer to this operator as

$$\mathcal{O}_{F,ABCD}^{(6)} = \epsilon^{ij} \bar{L}_i^A \bar{L}_R^C \bar{L}_j^B \nu_R^D \quad (2.10)$$

where the indices  $i, j$  refer to the weak isospin components of the LH doublet fields and  $\epsilon^{12} = -\epsilon^{21} = 1$ .

Semi-leptonic four-fermion:

$$\begin{array}{llll} \epsilon_{ij} \bar{Q}_i d_R \bar{L}_j \nu_R & \epsilon_{ij} \bar{Q}_i l_R \bar{L}_j u_R & \bar{L} \gamma^\mu L \bar{Q} \gamma_\mu Q & \bar{L} u_R \bar{u}_R L \\ \epsilon_{ij} \bar{Q}_i \nu_R \bar{L}_j d_R & \epsilon_{ij} \bar{Q}_i u_R \bar{L}_j l_R & \bar{l}_R \gamma^\mu l_R \bar{u}_R \gamma_\mu u_R & \bar{L} d_R \bar{d}_R L \\ \bar{L} \nu_R \bar{u}_R Q & \bar{L} \gamma^\mu \tau^a L \bar{Q} \gamma_\mu \tau^a Q & \bar{\nu}_R \gamma^\mu \nu_R \bar{u}_R \gamma_\mu u_R & \bar{Q} l_R \bar{l}_R Q \\ \bar{L} l_R \bar{d}_R Q & & \bar{l}_R \gamma^\mu l_R \bar{d}_R \gamma_\mu d_R & \bar{Q} \nu_R \bar{\nu}_R Q \\ \bar{l}_R \gamma^\mu \nu_R \bar{u}_R \gamma_\mu d_R & & \bar{\nu}_R \gamma^\mu \nu_R \bar{d}_R \gamma_\mu d_R & \end{array} \quad (2.11)$$

The first and the second column could contribute to the  $\beta$ -decay at tree level while the third and fourth column couldn't. Only the first column can contribute radiatively to  $\delta m_\nu$  through loop graphs. Since  $\nu_R$  doesn't exist in SM, operators of a given dimension with the same number of  $\nu_R$  can only mix with each other. The relevant operators are

$$\begin{aligned} \mathcal{O}_{Q,AD,\alpha\beta}^{(6)} &= \bar{L}^A \nu_R^D \bar{u}_R^\alpha Q^\beta \\ \mathcal{O}_{d1,AD,\alpha\beta}^{(6)} &= \epsilon_{ij} \bar{L}^A_i d_R^\beta \bar{Q}^\alpha_j \nu_R^D \\ \mathcal{O}_{d2,AD,\alpha\beta}^{(6)} &= \epsilon_{ij} \bar{Q}^\alpha_i d_R^\beta \bar{L}^A_j \nu_R^D \end{aligned} \quad (2.12)$$

where we already specify flavor indices for the fermion fields and these operators don't mix with the other four-fermion operators.

Four-quark:

$$\bar{Q} \gamma^\mu Q \bar{Q} \gamma_\mu Q \quad \bar{Q} \gamma^\mu \lambda^A Q \bar{Q} \gamma_\mu \lambda^A Q \quad (2.13)$$

These operators don't contribute to the beta decay, muon decay, or neutrino magnetic moment. They don't contribute radiatively to  $\delta m_\nu$  through loop graphs, either.

Lepton-Higgs:

$$\begin{aligned}
i(\bar{L}\gamma^\mu L)(\phi^+ D_\mu \phi) & \quad i(\bar{L}\gamma^\mu \tau^a L)(\phi^+ \tau^a D_\mu \phi) & (2.14) \\
i(\bar{l}_R \gamma^\mu l_R)(\phi^+ D_\mu \phi) & \quad i(\bar{\nu}_R^A \gamma^\mu \nu_R^B)(\phi^+ D_\mu \phi) \\
& \quad i(\bar{l}_R \gamma^\mu \nu_R^B)(\phi^+ D_\mu \tilde{\phi})
\end{aligned}$$

Neither of the first two operators in the list can contribute significantly to  $m_\nu$  since they contain no RH neutrino fields. Any loop graph through which they radiatively induce  $m_\nu$  would have to contain operators that contain both LH and RH fields, such as  $\mathcal{O}_M^{(4)}$  or other  $n = 6$  operators. In either case, the resulting constraints on the operator coefficients will be weak. For similar reasons, the third and fourth operators cannot contribute substantially because they contain an even number of neutrino fields having the same chirality and since the neutrino mass operator contains one LH and one RH neutrino field. Only the last operator

$$\mathcal{O}_{\tilde{V}, AD}^{(6)} \equiv i(\bar{l}_R^A \gamma^\mu \nu_R^D)(\phi^+ D_\mu \tilde{\phi}) \quad (2.15)$$

can contribute significantly to  $m_\nu$ , since it contains a single RH neutrino. It also contributes to the  $\mu$ -decay amplitude after SSB *via* the graph of Fig. 2.1a, since the covariant derivative  $D_\mu$  contains charged  $W$ -boson fields. We also write down the  $n = 6$  neutrino mass operators

$$\mathcal{O}_{M, AD}^{(6)} = (\bar{L}^A \tilde{\phi} \nu_R^D)(\phi^+ \phi). \quad (2.16)$$

Quark-Higgs:

$$\begin{aligned}
i(\bar{u}_R \gamma^\mu d_R)(\phi^+ D_\mu \tilde{\phi}) & \quad i(\bar{Q} \gamma^\mu \tau^a Q)(\phi^+ \tau^a D_\mu \phi) & (2.17) \\
i(\bar{Q} \gamma^\mu Q)(\phi^+ D_\mu \phi) & \quad i(\bar{d}_R \gamma^\mu d_R)(\phi^+ D_\mu \phi) \\
& \quad i(\bar{u}_R \gamma^\mu u_R)(\phi^+ D_\mu \phi)
\end{aligned}$$

Here we also list operators having two quark fields within because they might contribute to  $\beta$ -decay at tree level combining some SM operator. Actually the first two operators do contribute to  $\beta$ -decay. But they don't include  $\nu_R$  and therefore won't contribute to  $\delta m_\nu$ .

Fermion-Higgs-Gauge:

$$\begin{aligned}
& \bar{L}\tau^a\gamma^\mu D^\nu L W_{\mu\nu}^a & \bar{L}\gamma^\mu D^\nu L B_{\mu\nu} & \bar{l}_R\gamma^\mu D^\nu l_R B_{\mu\nu} & \bar{\nu}_R\gamma^\mu D^\nu \nu_R B_{\mu\nu} & (2.18) \\
& g_2(\bar{L}\sigma^{\mu\nu}\tau^a\phi)l_R W_{\mu\nu}^a & g_1(\bar{L}\sigma^{\mu\nu}\phi)l_R B_{\mu\nu} & & & \\
& g_2(\bar{L}\sigma^{\mu\nu}\tau^a\tilde{\phi})\nu_R W_{\mu\nu}^a & g_1(\bar{L}\sigma^{\mu\nu}\tilde{\phi})\nu_R B_{\mu\nu} & & & 
\end{aligned}$$

As for the fermion-Higgs operators, the operators in (2.18) that contain an even number of  $\nu_R$  fields will not contribute significantly to  $m_\nu^{AB}$ , so only the last two in the list are relevant:

$$\begin{aligned}
\mathcal{O}_{B,AD}^{(6)} &= g_1(\bar{L}^A\sigma^{\mu\nu}\tilde{\phi})\nu_R^D B_{\mu\nu} & (2.19) \\
\mathcal{O}_{W,AD}^{(6)} &= g_2(\bar{L}^A\sigma^{\mu\nu}\tau^a\tilde{\phi})\nu_R^D W_{\mu\nu}^a.
\end{aligned}$$

These also contribute to the neutrino magnetic moment. We also observe that the operator  $\mathcal{O}_{W,AD}^{(6)}$  will also contribute to the  $\mu$ -decay or  $\beta$ -decay amplitude *via* graphs as in Fig. 2.1b. We have computed its contributions to the Michel parameters of  $\mu$ -decay and find that they are suppressed by  $\sim (\frac{m_\mu}{\Lambda})^2$  relative to the effects of the other  $n = 6$  operators. We think the same suppression still exists for  $\beta$ -decay. This suppression arises from the presence of the derivative acting on the gauge field and the absence of an interference between the corresponding amplitude and that of the SM.

Two-quark-Higgs-Gauge:

$$\begin{aligned}
& i\bar{Q}\lambda^A\gamma_\mu D_\nu Q G^{A\mu\nu} & i\bar{Q}\tau^a\gamma_\mu D_\nu Q W^{a\mu\nu} & i\bar{Q}\gamma_\mu D_\nu Q B^{\mu\nu} & (2.20) \\
& i\bar{d}_R\lambda^A\gamma_\mu D_\nu d_R G^{A\mu\nu} & i\bar{d}_R\gamma_\mu D_\nu d_R B^{\mu\nu} & i\bar{u}_R\lambda^A\gamma_\mu D_\nu u_R G^{A\mu\nu} & \\
& i\bar{u}_R\gamma_\mu D_\nu u_R B^{\mu\nu} & (\bar{Q}\sigma_{\mu\nu}\lambda^A u_R)\tilde{\phi}G^{A\mu\nu} & (\bar{Q}\sigma_{\mu\nu}\tau^a u_R)\tilde{\phi}W^{a\mu\nu} & \\
& (\bar{Q}\sigma_{\mu\nu}u_R)\tilde{\phi}B^{\mu\nu} & (\bar{Q}\sigma_{\mu\nu}\lambda^A d_R)\phi G^{A\mu\nu} & (\bar{Q}\sigma_{\mu\nu}\tau^a d_R)\phi W^{a\mu\nu} & \\
& & (\bar{Q}\sigma_{\mu\nu}d_R)\phi B^{\mu\nu} & & 
\end{aligned}$$

We list these operators for the same reason as above Quark-Higgs operators. However, even if they may contribute to the  $\beta$ -decay, their contributions will be suppressed by derivatives on the gauge bosons just as  $\mathcal{O}_{W,AD}^{(6)}$ . What is more, they don't contribute to  $\delta m_\nu$  due to

that fact they contain no  $\nu_R$ .

In addition to these operators, there exist additional operators with dimension six which don't contribute to  $m_\nu$  through radiative corrections and muon decay, beta decay or neutrino magnetic moment. They won't mix with the "interesting operators" due to mismatch of the number of  $\nu_R$ . These operators are not interesting in our case. We list them as follows for completeness.

### Two-fermion-Gauge

$$\begin{aligned}
& i\bar{Q}\tau^a\gamma_\mu D_\nu QW^{a\mu\nu} \quad i\bar{Q}\gamma_\mu D_\nu QB^{\mu\nu} \quad i\bar{d}_R\lambda^A\gamma_\mu D_\nu d_RG^{A\mu\nu} \\
& i\bar{d}_R\gamma_\mu D_\nu d_RB^{\mu\nu} \quad i\bar{u}_R\lambda^A\gamma_\mu D_\nu u_RG^{A\mu\nu} \quad i\bar{u}_R\gamma_\mu D_\nu u_RB^{\mu\nu} \\
& i\bar{l}_R\gamma_\mu D_\nu l_RB^{\mu\nu} \quad i\bar{L}\tau^a\gamma_\mu D_\nu LW^{a\mu\nu} \quad i\bar{L}\gamma_\mu D_\nu LB^{\mu\nu} \\
& i\bar{Q}\lambda^A\gamma_\mu D_\nu QG^{A\mu\nu}
\end{aligned} \tag{2.21}$$

### Gauge-only

$$\begin{aligned}
& f_{ABC}G_\mu^{A\nu}G_\nu^{B\lambda}G_\lambda^{C\mu} \quad f_{ABC}\tilde{G}_\mu^{A\nu}G_\nu^{B\lambda}G_\lambda^{C\mu} \\
& \epsilon_{abc}W_\mu^{a\nu}W_\nu^{b\lambda}W_\lambda^{c\mu} \quad \epsilon_{abc}\tilde{W}_\mu^{a\nu}W_\nu^{b\lambda}W_\lambda^{c\mu}
\end{aligned} \tag{2.22}$$

### Higgs-only

$$(\phi^+\phi)^3 \quad \partial_\mu(\phi^+\phi)\partial^\mu(\phi^+\phi) \tag{2.23}$$

### Fermion-Higgs

$$(\phi^+\phi)(\bar{L}l_R\phi) \quad (\phi^+\phi)(\bar{Q}d_R\phi) \quad (\phi^+\phi)(\bar{Q}u_R\tilde{\phi}) \tag{2.24}$$

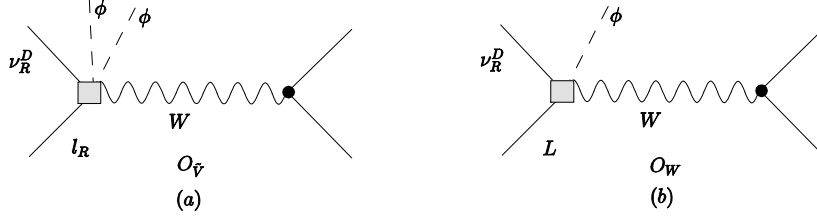


Figure 2.1: Contributions from the operators (a)  $\mathcal{O}_{B,AD}^{(6)}$  and (b)  $\mathcal{O}_{B,AD}^{(6)}$  (denoted by the shaded box) to the amplitude for  $\mu$ -decay or  $\beta$ -decay. Solid, dashed, and wavy lines denote fermions, Higgs scalars, and gauge bosons, respectively. After SSB, the neutral Higgs field is replaced by its vev, yielding a four-fermion  $\mu$ -decay or  $\beta$ -decay amplitude

### Higgs-Gauge

$$\begin{aligned}
(\phi^+ \phi) G_{\mu\nu}^A G^{A\mu\nu} & \quad (\phi^+ \phi) \tilde{G}_{\mu\nu}^A G^{A\mu\nu} & (2.25) \\
(\phi^+ \phi) W_{\mu\nu}^a W^{a\mu\nu} & \quad (\phi^+ \phi) \tilde{W}_{\mu\nu}^a W^{a\mu\nu} \\
(\phi^+ \phi) B_{\mu\nu} B^{\mu\nu} & \quad (\phi^+ \phi) \tilde{B}_{\mu\nu} B^{\mu\nu} \\
(\phi^+ \tau^a \phi) W_{\mu\nu}^a B^{\mu\nu} & \quad (\phi^+ \tau^a \phi) \tilde{W}_{\mu\nu}^a B^{\mu\nu} \\
(\phi^+ \phi) (D_\mu \phi^+ D^\mu \phi) & \quad (\phi^+ D^\mu \phi) (D_\mu \phi^+ \phi)
\end{aligned}$$

### 2.3.2 Construction of $\mathcal{L}_5$ and $\mathcal{L}_7$ for Majorana Neutrinos

Now, we don't need any new fields and therefore the effective Lagrangian is

$$\mathcal{L}_{\text{eff}} = \mathcal{L}_{\text{SM}} + \frac{1}{\Lambda} \mathcal{L}_5 + \frac{1}{\Lambda^3} \mathcal{L}_7 \cdots + \text{h.c.} \quad (2.26)$$

The lowest-order contribution to the neutrino (Majorana) mass arises from the usual five dimensional operator containing  $\phi$  and  $L$

$$\mathcal{O}_M^{(5)} = \epsilon^{ik} \epsilon^{jm} (\bar{L}_i^c L_j) \phi_k \phi_m \quad (2.27)$$

where  $\bar{L}^c = L^T C$ , and  $C$  denotes charge conjugation. After spontaneous symmetry breaking,

one has

$$\begin{aligned} \frac{C_M^5 \mathcal{O}_M^{(5)}}{\Lambda} &\rightarrow -m_\nu \bar{\nu}_L^c \nu_L \\ m_\nu &= -C_M^4 \frac{v^2}{2\Lambda} \quad . \end{aligned} \quad (2.28)$$

The lowest-order contribution to muon decay, beta decay, and neutrino magnetic moment arises at dimension seven. We are going to group the operator with dimension seven according to the number of fermion, Higgs, and gauge boson fields that enter, as before.

Two-fermion-Higgs-Gauge:

$$\begin{aligned} \mathcal{O}_{B,AB}^{(7)} &= \left( \overline{L^{Ac}} \epsilon \phi \right) \sigma_{\mu\nu} \left( H^T \epsilon L^B \right) B^{\mu\nu} \\ \mathcal{O}_{W,AB}^{(7)} &= \left( \overline{L^{Ac}} \epsilon H \right) \sigma_{\mu\nu} \left( H^T \epsilon \tau^a L^B \right) W_a^{\mu\nu} \end{aligned} \quad (2.29)$$

These contain the neutrino magnetic moment operator. They will also contribute to the  $\mu$ -decay and  $\beta$ -decay as  $\mathcal{O}_{W,AD}^{(6)}$  in the Dirac case. Their contributions are also suppressed.

Two-fermion-Higgs-derivative:

$$\mathcal{O}_{\tilde{V},AB}^{(7)} = i \epsilon^{ik} e^{jm} \overline{L^{Ac}} \gamma^\mu l_R^B \phi_j \phi_k D_\mu \phi_m \quad (2.30)$$

This is analogous to  $\mathcal{O}_{\tilde{V},AB}^{(6)}$  in the Dirac case, it also contributes to  $\mu$ -decay and  $\beta$ -decay in the way  $\mathcal{O}_{\tilde{V},AB}^{(6)}$  does.

Four-lepton-Higgs:

$$\begin{aligned} \mathcal{O}_{L1,AB,CD}^{(7)} &= \epsilon^{ij} \epsilon^{km} \left( \overline{L^{Ac}} \epsilon L_j^B \right) \left( \overline{l_R^C} L_k^D \right) \phi_m \\ \mathcal{O}_{L2,AB,CD}^{(7)} &= \epsilon^{ij} \epsilon^{km} \left( \overline{L^{Ac}} \epsilon L_k^B \right) \left( \overline{l_R^C} L_j^D \right) \phi_m \end{aligned} \quad (2.31)$$

These will contribute to  $\mu$ -decay. In Section 3.2, we will find  $\mathcal{O}_{L1,AB,CD}^{(7)}$  contributes to  $m_\nu$  through radiative corrections, while  $\mathcal{O}_{L2,AB,CD}^{(7)}$  won't. They are analogous to  $\mathcal{O}_{F,ABCD}^{(6)}$  in the Dirac case.

Four-quark-Higgs:

$$\begin{aligned}
\mathcal{O}_{d1,AB,\alpha\beta}^{(7)} &= \epsilon^{ij} \epsilon^{km} (\overline{L}^{Ac}_i L_j^B) (\overline{d}_R^\alpha Q_k^\beta) \phi_m & (2.32) \\
\mathcal{O}_{d2,AB,\alpha\beta}^{(7)} &= \epsilon^{ik} \epsilon^{jm} (\overline{L}^{Ac}_i L_j^B) (\overline{d}_R^\alpha Q_k^\beta) \phi_m \\
\mathcal{O}_{d1,A\beta,\alpha B}^{(7)} &= \epsilon^{ij} \epsilon^{km} (\overline{L}^{Ac}_i Q_k^\beta) (\overline{d}_R^\alpha L_j^B) \phi_m \\
\mathcal{O}_{d2,A\beta,\alpha B}^{(7)} &= \epsilon^{ik} \epsilon^{jm} (\overline{L}^{Ac}_i Q_k^\beta) (\overline{d}_R^\alpha L_j^B) \phi_m \\
\mathcal{O}_{u1,AB,\alpha\beta}^{(7)} &= \epsilon^{ij} \delta_k^m (\overline{L}^{Ac}_i L_j^B) (\overline{Q}^{\alpha k} u_R^\beta) \phi_m \\
\mathcal{O}_{u2,AB,\alpha\beta}^{(7)} &= \epsilon^{jm} \delta_k^i (\overline{L}^{Ac}_i L_j^B) (\overline{Q}^{\alpha k} u_R^\beta) \phi_m \\
\mathcal{O}_{R,AB,\alpha\beta}^{(7)} &= \epsilon^{ij} (\overline{L}^{Ac}_i \gamma^\mu l_R^B) (\overline{d}_R^\alpha \gamma_\mu u_R^\beta) \phi_j
\end{aligned}$$

$\mathcal{O}_{d,AB,\alpha\beta}^{(7)}$  is the counterpart of  $\mathcal{O}_{d,AD,\alpha\beta}^{(6)}$  in the Dirac case and  $\mathcal{O}_{d,AB,\alpha\beta}^{(7)}$  is one of  $\mathcal{O}_{d,AD,\alpha\beta}^{(6)}$  in the Dirac case, they will all contribute to  $\beta$ -decay. However, in Section 3.2, we will find that  $\mathcal{O}_{u1,AB,\alpha\beta}^{(7)}$  and  $\mathcal{O}_{d1,AB,\alpha\beta}^{(7)}$  don't contribute to  $m_\nu$  *via* loops. As for  $\mathcal{O}_{R,AB,\alpha\beta}^{(7)}$ , it won't contribute to neutrino mass through loops because of Dirac structure.

Two-leptons-Higgs-two-derivatives:

$$\mathcal{O}_{2D}^1 = (\overline{L}^c \epsilon H) (D_\mu H^T \epsilon D^\mu L) \quad (2.33)$$

$$\mathcal{O}_{2D}^2 = (\overline{L}^c \epsilon D_\mu H) (D^\mu H^T \epsilon L) \quad (2.34)$$

These operators are not interesting to us since they don't contribute to  $m_\nu$  through radiative corrections and muon decay, beta decay, or neutrino magnetic moment.

## Chapter 3

# Operator Matching and Mixing

### 3.1 Introduction

We start with the effective Lagrangian which follows [45] and takes the following form

$$\mathcal{L}_{\text{eff}} = \sum_{n,j} \frac{C_j^n(\mu)}{\Lambda^{n-4}} \mathcal{O}_j^{(n)}(\mu) + h.c. \quad (3.1)$$

where  $\mu$  is renormalization scale,  $n \geq 4$  is the corresponding operator's dimension,  $j$  is the index running over all independent operators of a given dimension and  $\Lambda$  is the new physics cutoff. In analyzing the renormalization of an operator, say  $\mathcal{O}_i^{(n)}(\mu)$ , it is useful to consider separately two cases:

- $\mathcal{O}_i^{(n)}$  receives contributions at the scale  $\Lambda$  associated with loop graphs containing an operator  $\mathcal{O}_j^{(m)}$  with  $m > n$ .

Above the weak scale, all the fields are massless, and  $\mu$  itself appears only logarithmically. If  $\mathcal{O}_i^{(n)}$  and  $\mathcal{O}_j^{(m)}$  can exist for zero external momentum, these graphs will vanish in dimensional regularization (DR) since they must be proportional to  $M^{m-n}$  where  $M$  is some mass scale. If we use brutal cutoff, these graphs turn out proportional to  $\Lambda^{m-n}$ . However, they might be cancelled by the contributions from new physics. Since we don't know anything about new physics, we have to be cautious, and thus are going to follow the argument found in [56] and use NDA to estimate these contributions. Simple power counting shows that these contributions go as  $\sim \frac{\Lambda^{m-n}}{16\pi^2}$  times a product of  $\mathcal{O}_j^{(m)}$  operator coefficient  $\frac{C_j^m}{\Lambda^{m-4}}$  and the gauge couplings  $g_1, \dots, g_l$  appearing in the loop. Thus, matching of the effective theory with the full theory (unspecified) at the scale  $\Lambda$  implies the presence

of a contribution to  $C_j^n$  of order  $\frac{g_1 \cdots g_l}{16\pi^2} C_j^m$ . As emphasized in [56], the precise numerical coefficient that enters this matching contribution cannot be computed without knowing the theory above the scale.

- $\mathcal{O}_i^{(n)}$  mixes with a set of operators  $\{\mathcal{O}_j^{(n)}\}$  which have the same dimension as  $\mathcal{O}_i^{(n)}$ .

We can carry out exact calculations on mixing among these operators by employing a renormalization group (RG) analysis. We will compute all the one-loop graphs that contribute by using DR and background field gauge [23] in  $d = 4 - 2\epsilon$ , and introduce the renormalization scale  $\mu$ . Due to operator mixing, the renormalized operators  $\mathcal{O}_{jR}^{(n)}$  can be expressed in terms of the un-renormalized operators  $\mathcal{O}_j^{(n)}$  *via*

$$\mathcal{O}_{jR}^{(n)} = \sum_k Z_{jk}^{-1} Z_L^{n_L/2} Z_\phi^{n_\phi/2} Z_{l_R}^{n_{l_R}/2} Z_Q^{n_Q/2} Z_{d_R}^{n_{d_R}/2} Z_{u_R}^{n_{u_R}/2} \mathcal{O}_k^{(n)} = \sum_k Z_{jk}^{-1} \mathcal{O}_{k0}^{(n)} \quad (3.2)$$

where

$$\mathcal{O}_{k0}^{(n)} = Z_L^{n_L/2} Z_\phi^{n_\phi/2} Z_{l_R}^{n_{l_R}/2} Z_Q^{n_Q/2} Z_{d_R}^{n_{d_R}/2} Z_{u_R}^{n_{u_R}/2} \mathcal{O}_k^{(n)} \quad (3.3)$$

are the  $\mu$  independent bare operators;  $Z_L^{1/2}$ ,  $Z_\phi^{1/2}$ ,  $Z_{l_R}^{1/2}$ ,  $Z_Q^{1/2}$ ,  $Z_{d_R}^{1/2}$ , and  $Z_{u_R}^{1/2}$  are the wave-function renormalization constants for the fields  $L^A$ ,  $\phi$ ,  $l_R^A$ ,  $Q^\alpha$ ,  $d_R^\alpha$ , and  $u_R^\alpha$ , respectively;  $n_L$ ,  $n_\phi$ ,  $n_{l_R}$ ,  $n_Q$ ,  $n_{d_R}$ , and  $n_{u_R}$  are the number of left-handed lepton, Higgs fields, right-handed leptons, left-handed quarks, right-handed down quarks, and right-handed up quarks appearing in a given operator. In the minimal subtraction scheme that we adopt here, the products of renormalization constants  $Z_{jk}^{-1} Z_L^{n_L/2} Z_\phi^{n_\phi/2} Z_{l_R}^{n_{l_R}/2} Z_Q^{n_Q/2} Z_{d_R}^{n_{d_R}/2} Z_{u_R}^{n_{u_R}/2}$  simply remove the  $1/\epsilon$  terms arising from the loop graphs.

Since the bare operators  $\mathcal{O}_{j0}^{(n)}$  do not depend on the renormalization scale, whereas the  $Z_{jk}^{-1}$  and the  $\mathcal{O}_{jR}^{(n)}$  do, the operator coefficients  $C_j^n$  must carry a compensating  $\mu$ -dependence to ensure that  $\mathcal{L}_{\text{eff}}$  is independent of scale. This requirement leads to the RG equation for the operator coefficients:

$$\mu \frac{d}{d\mu} C_j^n + \sum_k C_k^n \gamma_{kj} = 0 \quad (3.4)$$

where

$$\gamma_{kj} = \sum_l \left( \mu \frac{d}{d\mu} Z_{kl}^{-1} \right) Z_{lj} \quad (3.5)$$

is the anomalous dimension matrix.

Using the anomalous dimension matrix  $\gamma$  and the one-loop running of the couplings in  $\gamma$ , we can solve the RG equation. If the couplings in  $\gamma$  don't change drastically—just as  $\alpha_1, \alpha_2, \alpha_3$ , and Yukawa couplings which run from  $\Lambda$  to  $v$ —their runnings have a negligible impact on the solutions to RGE so it's safe to assume these couplings are constant. If we

define the column vector  $\mathbf{C} = \begin{pmatrix} C_1^n \\ \vdots \\ C_j^n \\ \vdots \end{pmatrix}$ , the RGE will take a simple form:

$$\mu \frac{d}{d\mu} \mathbf{C} + \gamma^T \mathbf{C} = 0 \quad (3.6)$$

where  $\gamma$  is the anomalous dimension matrix. Since  $\gamma$  is assumed constant, the solution is

$$\mathbf{C}(\mu) = \exp\left(-\gamma^T \ln \frac{\mu}{\Lambda}\right) \mathbf{C}(\Lambda). \quad (3.7)$$

Keeping only the leading logarithms  $\ln \frac{\mu}{\Lambda}$ , we find

$$\mathbf{C}(\mu) = \mathbf{C}(\Lambda) - \gamma^T \ln \frac{\mu}{\Lambda} \mathbf{C}(\Lambda). \quad (3.8)$$

In the following section, we are going to apply the above results to  $O_{M,AD}^{(4)}$  and  $O_{M,AD}^{(6)}$  in the Dirac case and  $O_{M,AD}^{(5)}$ , and  $O_{M,AD}^{(7)}$  in the Majorana case.

## 3.2 Mixing and Matching Considerations for $O_M^{(4,6)}$ and $O_M^{(5,7)}$

### 3.2.1 Diagonalizing Yukawa Couplings

To simplify our analysis, we can redefine the lepton fields  $L$  and  $l_R$  so that the charged lepton Yukawa  $f_e^{AB}$  coupling matrix is diagonal. Specifically, we take

$$\begin{aligned} L^A &\rightarrow L^{A'} = S_{AB} L^B \\ l_R^C &\rightarrow l^{C'} = T_{CD} l^D \end{aligned} \quad (3.9)$$

with  $S_{AB}$  and  $T_{CD}$  chosen so that

$$\bar{L} f_e l = \bar{L}' f_e^{\text{diag}} l' \quad (3.10)$$

where  $L, L'$  denote vectors in flavor space,  $f_e$  denotes the Yukawa matrix in the original basis, and  $f_e^{\text{diag}} = \tilde{S}^\dagger f_e \tilde{T}$ . We note that the field redefinition Eq. (3.9) differs from the conventional flavor rotation used for quarks, since we have performed identical rotations on both isospin components of the left-handed doublet. Specifically, the charged lepton Yukawa operator is  $f_e^{AB} \bar{L}^A \phi l_R^B$  where  $f_e^{AB} = \frac{m_A}{v/\sqrt{2}} \delta_{AB}$  with  $m_A$  being the mass for the charge lepton of flavor  $A$  and  $v$  being the vacuum expectation value of the Higgs scalar field.

However, there are some subtleties in diagonalizing quark Yukawa matrices. The two quark Yukawa matrices  $f_u^{\alpha\beta}$  and  $f_d^{\alpha\beta}$  can't be diagonalized simultaneously by redefining  $Q^\alpha$ ,  $u_R^\alpha$ , and  $d_R^\alpha$ . Specifically, the redefinitions of  $Q^\alpha$ ,  $u_R^\alpha$ , and  $d_R^\alpha$

$$\begin{aligned} Q^\alpha &\rightarrow T^{\alpha\beta} Q^\beta \\ u_R^\alpha &\rightarrow S_u^{\alpha\beta} u_R^\beta \\ d_R^\alpha &\rightarrow S_d^{\alpha\beta} d_R^\beta \end{aligned} \quad (3.11)$$

yield

$$\begin{aligned} f_u &\rightarrow T^+ f_u S_u \\ f_d &\rightarrow T^+ f_d S_d \end{aligned} \quad (3.12)$$

where the unitary matrices  $T$ ,  $S_u$ , and  $S_d$  can be chosen so that  $f_u$  and  $f_d$  are diagonal. Since there is only one matrix  $T$  acting on the left side of  $f_u$  and  $f_d$  which are generally independent, we can either make  $f_u$  diagonal or make  $f_d$  diagonal but not both.

In literature, people always choose  $T$  and  $S_u$  so that  $f_u$  is diagonal, i.e., we have

$$f_u \rightarrow f_u^{\text{diag}} = T^+ f_u S_u = \begin{pmatrix} m_u & 0 & 0 \\ 0 & m_c & 0 \\ 0 & 0 & m_t \end{pmatrix} \frac{\sqrt{2}}{v} \quad (3.13)$$

while  $S_d$  and  $U$ , a unitary matrix acting on the left side of  $f_d$ , are chosen to diagonalize  $f_d$ ,

namely

$$U f_u S_d = f_u^{\text{diag}} = \begin{pmatrix} m_d & 0 & 0 \\ 0 & m_s & 0 \\ 0 & 0 & m_b \end{pmatrix} \frac{\sqrt{2}}{v} \quad (3.14)$$

$$f_u \rightarrow T f_u S_d = T U^+ U f_u S_d = T U^+ f_u^{\text{diag}} = V_{\text{CKM}} f_u^{\text{diag}}$$

$$Q^\alpha \rightarrow T^{\alpha\beta} Q^\beta = \begin{pmatrix} u_L^\alpha \\ (T U^+)^{\alpha\beta} d_L^\beta \end{pmatrix} = \begin{pmatrix} u_L^\alpha \\ V_{\text{CKM}}^{\alpha\beta} d_L^\beta \end{pmatrix}$$

where  $u_L^\alpha$  and  $d_L^\beta$  are mass eigenstates after SSB and  $T U^+$  is just  $V_{\text{CKM}}$ , which is the famous Cabibbo-Kobayashi-Maskawa matrix. We will adopt this choice in the remainder of the paper and use notations  $Q^\alpha$ ,  $u_R^\alpha$ , and  $d_R^\alpha$  as the corresponding basis.

Consequently, gauge interactions in the new basis entail no transitions between generations. We also note redefinition of fields also implies a redefinition of the operator coefficients  $C_{M,AD}^4$ ,  $C_{F,ABCD}^6$ , etc.. For example, one has

$$C_{M,A'D}^{4,6} = C_{M,AD}^{4,6} S_{M,A'A} \quad (3.15)$$

$$C_{F,A'B'C'D}^{6'} = C_{F,ABCD}^6 S_{A'A} S_{B'B} T_{C'C}^*$$

where a sum over repeated indices is implied.

However, we note that we can also choose  $T$ ,  $S_d$ , and  $S_u$  to make  $f_u$  diagonal. The transformation between the new basis  $Q'^\alpha$ ,  $u_R'^\alpha$ , and  $d_R'^\alpha$  and  $Q^\alpha$ ,  $u_R^\alpha$ , and  $d_R^\alpha$  are given by

$$Q'^\alpha = (V_{\text{CKM}}^+)^{\alpha\beta} Q^\beta \quad (3.16)$$

$$u_R'^\alpha = u_R^\alpha$$

$$d_R'^\alpha = d_R^\alpha$$

which imply a redefinition of the  $6D$  operator coefficients

$$C_{Q,AD,\alpha\beta}^6 = C_{Q,AD,\alpha\lambda}^6 V_{\text{CKM}}^{\lambda\beta} \quad (3.17)$$

$$C_{d1,AD,\alpha\beta}^6 = C_{d1,AD,\lambda\beta}^6 (V_{\text{CKM}}^+)^{\alpha\lambda} \quad (3.18)$$

$$C_{d2,AD,\alpha\beta}^6 = C_{d2,AD,\lambda\beta}^6 (V_{\text{CKM}}^+)^{\alpha\lambda}. \quad (3.19)$$

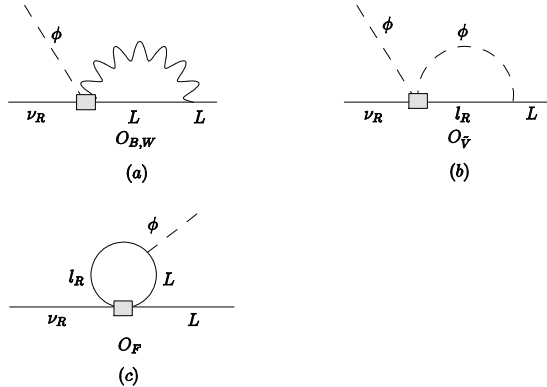


Figure 3.1: One-loop graphs for the matching of  $\mathcal{O}_{B,W}^{(6)}$ ,  $\mathcal{O}_{\tilde{V}}^{(6)}$ , and  $\mathcal{O}_F^{(6)}$  (denoted by the shaded box) into  $\mathcal{O}_{M,AD}^{(4)}$ . Solid, dashed, and wavy lines denote fermions, Higgs scalars, and gauge bosons, respectively. Panels (a, b, c) illustrate matching of  $\mathcal{O}_{B,W}^{(6)}$ ,  $\mathcal{O}_{\tilde{V}}^{(6)}$ , and  $\mathcal{O}_F^{(6)}$ , respectively, into  $\mathcal{O}_{M,AD}^{(4)}$ .

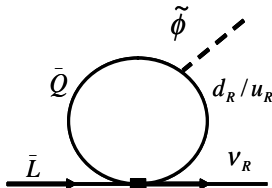


Figure 3.2: One-loop graphs for the matching of  $\mathcal{O}_{u,d}^{(6)}$  (denoted by the black box) into  $\mathcal{O}_{M,AD}^{(4)}$ . Solid and dashed lines denote fermions and Higgs scalars, respectively.

We are going to use these transformations in Section 4.2. Diagonalization of the neutrino mass matrix requires additional, independent rotations of the  $\nu_{L,R}^D$  fields after inclusion of radiative contributions to the coefficients  $C_{M,AD}^{4,6}$  generated by physics above the weak scale. Since we are concerned only with contributions generated above the scale of SSB, we will not perform the latter diagonalization, and will carry out computations using the  $L'$ ,  $l'_R$  basis.

### 3.2.2 Dirac Case

#### 3.2.2.1 Matching with $\mathcal{O}_{M,AD}^{(4)}$

The one-loop graphs for matching  $\mathcal{O}_{F,ABCD}^{(6)}$ ,  $\mathcal{O}_{\tilde{V},AB}^{(6)}$ ,  $\mathcal{O}_{W,AD}^{(6)}$  and  $\mathcal{O}_{B,AD}^{(6)}$ , with  $\mathcal{O}_{M,AD}^{(4)}$  are shown in Fig. 3.1. For mixing the four-fermion operators  $\mathcal{O}_{F,ABCD}^{(6)}$  into  $\mathcal{O}_{M,AD}^{(4)}$ , two

topologies are possible, associated with either the fields  $(\bar{L}^A, \nu_R^D)$  or  $(\bar{L}^B, \nu_R^D)$  living on the external lines. For mixing  $\mathcal{O}_{F,ABCD}^{(6)}$ , as well as of  $\mathcal{O}_{\tilde{V},AB}^{(6)}$ , into  $\mathcal{O}_{M,AD}^{(4)}$ , one insertion of the Yukawa interaction  $f_e^{AC*} \bar{l}_R^C L^A$  is needed to convert the internal RH lepton into a LH one. In contrast, no Yukawa insertion is required for the mixing of  $\mathcal{O}_{B,AD}^{(6)}$  and  $\mathcal{O}_{W,AD}^{(6)}$  into  $\mathcal{O}_{M,AD}^{(4)}$ . The interesting six dimensional operators  $\mathcal{O}_{Q,AD,\alpha\beta}^{(6)}$ ,  $\mathcal{O}_{d1,AD,\alpha\beta}^{(6)}$ , and  $\mathcal{O}_{d2,AD,\alpha\beta}^{(6)}$  can contribute to  $\mathcal{O}_{M,AD}^{(4)}$  through the one-loop graphs of Fig. 3.2. Using NDA we can estimate the contributions from the coefficients of six dimensional operators to the coefficient of the four dimensional neutrino mass operator

$$\begin{aligned}
\mathcal{O}_{B,AD}^{(6)} &\rightarrow C_{M,AD}^4 \sim \frac{\alpha}{4\pi \cos^2 \theta_W} C_{B,AD}^6 \\
\mathcal{O}_{W,AD}^{(6)} &\rightarrow C_{M,AD}^4 \sim \frac{3\alpha}{4\pi \sin^2 \theta_W} C_{W,AD}^6 \\
\mathcal{O}_{\tilde{V},AD}^{(6)} &\rightarrow C_{M,AD}^4 \sim \frac{f_e^{AA}}{16\pi^2} C_{\tilde{V},AD}^6 = \frac{1}{16\pi^2} \frac{m_A}{v/\sqrt{2}} C_{\tilde{V},AD}^6 \\
\mathcal{O}_{F,ABAD}^{(6)} &\rightarrow C_{M,AD}^4 \sim \frac{f_e^{AA}}{8\pi^2} C_{F,ABAD}^6 = \frac{1}{8\pi^2} \frac{m_A}{v/\sqrt{2}} C_{F,ABAD}^6 \\
\mathcal{O}_{F,ABB D}^{(6)} &\rightarrow C_{M,AD}^4 \sim \frac{f_e^{BB}}{16\pi^2} C_{F,ABB D}^6 = \frac{1}{16\pi^2} \frac{m_B}{v/\sqrt{2}} C_{F,ABB D}^6 \\
\mathcal{O}_{Q,AD,\alpha\beta}^{(6)} &\rightarrow C_{M,AD}^4 \sim \frac{N_C}{8\pi^2} f_u^{\alpha\beta} C_{Q,AD,\alpha\beta}^6 = \frac{N_C}{8\pi^2} \frac{m_u^\alpha}{v/\sqrt{2}} \delta^{\alpha\beta} C_{Q,AD,\alpha\beta}^6 \\
\mathcal{O}_{d1,AD,\alpha\beta}^{(6)} &\rightarrow C_{M,AD}^4 \sim \frac{N_C}{16\pi^2} f_d^{\alpha\beta} C_{d1,AD,\alpha\beta}^6 = \frac{N_C}{16\pi^2} \frac{m_d^\beta}{v/\sqrt{2}} V_{CKM}^{*\alpha\beta} C_{d1,AD,\alpha\beta}^6 \\
\mathcal{O}_{d2,AD,\alpha\beta}^{(6)} &\rightarrow C_{M,AD}^4 \sim \frac{N_C}{8\pi^2} f_d^{\alpha\beta} C_{d2,AD,\alpha\beta}^6 = \frac{N_C}{8\pi^2} \frac{m_d^\beta}{v/\sqrt{2}} V_{CKM}^{*\alpha\beta} C_{d2,AD,\alpha\beta}^6
\end{aligned} \tag{3.20}$$

where  $\theta_W$  is the weak mixing angle,  $N_C$  is the quark's number of color and  $m_u^\alpha$ ,  $m_d^\alpha$ ,  $m_A$ , and  $m_B$  are the masses for up quark of flavor  $\alpha$ , down quark of flavor  $\alpha$ , and charged lepton of flavor  $A$  and  $B$ , respectively. The relative factor of  $3 \cot^2 \theta_W$  for the mixing of  $\mathcal{O}_{W,AD}^{(6)}$  compared to the mixing of  $\mathcal{O}_{B,AD}^{(6)}$  arises from the ratio of gauge couplings  $(g_2/g_1)^2$  and the presence of a  $\vec{\tau} \cdot \vec{\tau}$  appearing in Fig. 3.1a. The factor of two that enters the mixing of  $\mathcal{O}_{F,ABAD}^{(6)}$  compared to that of  $\mathcal{O}_{F,ABB D}^{(6)}$  arises from the trace associated with the closed chiral fermion loop that does not arise for  $\mathcal{O}_{F,ABB D}^{(6)}$ , so as the factor of two of  $\mathcal{O}_{d2,AD,\alpha\beta}^{(6)}$ .

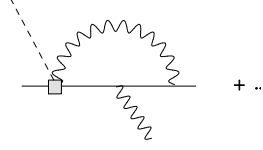
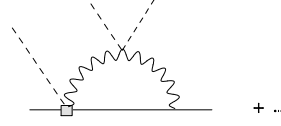
### 3.2.2.2 Mixing with $\mathcal{O}_{M,AD}^{(6)}$

In order to start the renormalization of  $\mathcal{O}_{M,AD}^{(6)}$ , we need to come up with a basis of operators close under renormalizations. We find that the minimal set consists of 10 operators that contribute to  $\mu$ -decay,  $\beta$ -decay, neutrino magnetic moment, and  $m_\nu^{AD}$ :

$$\begin{aligned} \mathcal{O}_{B,AD}^{(6)}, \mathcal{O}_{W,AD}^{(6)}, \mathcal{O}_{M,AD}^{(6)}, \mathcal{O}_{\tilde{V},AD}^{(6)}, \mathcal{O}_{F,AB,BD}^{(6)}, \mathcal{O}_{F,AA,AD}^{(6)}, \mathcal{O}_{F,BA,BD}^{(6)}, \\ \mathcal{O}_{Q,AD,\alpha\beta}^{(6)}, \mathcal{O}_{d1,AD,\alpha\beta}^{(6)}, \mathcal{O}_{d2,AD,\alpha\beta}^{(6)} \end{aligned} \quad (3.21)$$

We only keep the one-loop graphs up to the first order in the Yukawa couplings because all the Yukawa couplings except top quark's are small and hence the higher powers are highly suppressed. As for the top quark's Yukawa coupling, it always comes together with the tiny CKM matrix element  $V_{td}$  in our calculations, since  $\beta$ -decays always involve up or down quarks.

These graphs of the mixing between  $\mathcal{O}_{M,AD}^{(6)}$  and  $\mathcal{O}_{B,AD}^{(6)}, \mathcal{O}_{W,AD}^{(6)}$ , which are illustrated in Fig. 3.3–Fig. 3.5, were computed by the authors of [45]. The remaining classes of graphs relevant to mixing among the first row of the basis Eq. (3.21) are illustrated in Fig. 3.6, where we show representative contributions to operator self-renormalization and mixing among the various operators. The latter include mixing of all operators into  $\mathcal{O}_{M,AD}^{(6)}$  (a–c); mixing of  $\mathcal{O}_{M,AD}^{(6)}, \mathcal{O}_{B,AD}^{(6)}$ , and  $\mathcal{O}_{W,AD}^{(6)}$  into  $\mathcal{O}_{\tilde{V},AD}^{(6)}$  (d, e); and mixing between the four-fermion operators and the magnetic moment operators (f, g). Representative self-renormalization graphs are given in Fig. 3.6(h–j). The representative Feynman diagrams of the graphs mixing between the first seven and the last three and among the last three are shown in Fig. 3.7–Fig. 3.9. The graphs of Fig. 3.7 involve renormalization of  $\mathcal{O}_{Q,AB,\alpha\beta}^{(6)}, \mathcal{O}_{d1,AB,\alpha\beta}^{(6)}$ , and  $\mathcal{O}_{d2,AB,\alpha\beta}^{(6)}$ , where  $\mathcal{O}_{d1,AB,\alpha\beta}^{(6)}$  and  $\mathcal{O}_{d2,AB,\alpha\beta}^{(6)}$  mix into each other under renormalizations. The graphs of Fig. 3.8 show how  $\mathcal{O}_{Q,AB,\alpha\beta}^{(6)}, \mathcal{O}_{d1,AB,\alpha\beta}^{(6)}$ , and  $\mathcal{O}_{d2,AB,\alpha\beta}^{(6)}$  mix into  $\mathcal{O}_{B,W}^{(6)}$ . Contributions from  $\mathcal{O}_{Q,AB,\alpha\beta}^{(6)} \propto \overline{L^A} D^2 \tilde{\phi} \nu_R$ , which is zero by the equation of motion for  $\phi$ , and  $\mathcal{O}_{d1,AB,\alpha\beta}^{(6)}$  and  $\mathcal{O}_{d2,AB,\alpha\beta}^{(6)}$  do contribute to  $\mathcal{O}_{B,W}^{(6)}$ . The graphs mixing  $\mathcal{O}_{B,W}^{(6)}$  into  $\mathcal{O}_{Q,AB,\alpha\beta}^{(6)}, \mathcal{O}_{d1,AB,\alpha\beta}^{(6)}$ , and  $\mathcal{O}_{d2,AB,\alpha\beta}^{(6)}$  are illustrated in Fig. 3.9. As noted in [44], the mixing of the the four-fermion operators into  $\mathcal{O}_{M,AD}^{(6)}$  contains three powers of the lepton Yukawa couplings and is highly suppressed. In contrast, all other mixing contains, at most, one Yukawa insertion.

Figure 3.3: Self-renormalization of  $\mathcal{O}_{B,W}^{(6)}$ Figure 3.4: Mixing of  $\mathcal{O}_{B,W}^{(6)}$  into  $\mathcal{O}_M^{(6)}$ 

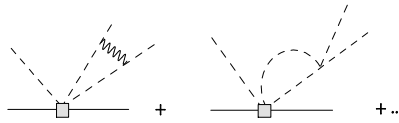
After calculating all the graphs, we obtain the anomalous dimension matrix which is

$$\gamma = \begin{pmatrix} \gamma_L & \gamma_1 & \gamma_2 & \gamma_3 \\ \gamma'_1 & A1 & 0 & 0 \\ \gamma'_2 & 0 & A2 & A3 \\ \gamma'_3 & 0 & A4 & A5 \end{pmatrix} \quad (3.22)$$

where  $\gamma_L$  is the  $7 \times 7$  anomalous dimension matrix for the first seven operators

$$\gamma_L = \begin{pmatrix} -\frac{3(\alpha_1-3\alpha_2)}{16\pi} & \frac{3\alpha_1}{8\pi} & -6\alpha_1(\alpha_1+\alpha_2) & -\frac{9\alpha_1 f_e^{AA*}}{8\pi} & -\frac{9\alpha_1 f_e^{AA}}{4\pi} & -\frac{9\alpha_1 f_e^{BB}}{2\pi} & \frac{9\alpha_1 f_e^{BB}}{4\pi} \\ \frac{9\alpha_2}{8\pi} & \frac{3(\alpha_1-3\alpha_2)}{16\pi} & 6\alpha_2(\alpha_1+3\alpha_2) & \frac{27\alpha_2 f_e^{AA*}}{8\pi} & -\frac{9\alpha_2 f_e^{AA}}{4\pi} & -\frac{9\alpha_2 f_e^{BB}}{2\pi} & \frac{9\alpha_2 f_e^{BB}}{4\pi} \\ 0 & 0 & \frac{9(\alpha_1+3\alpha_2)}{16\pi} - \frac{3\lambda}{2\pi^2} & 0 & 0 & 0 & 0 \\ 0 & 0 & \frac{9\alpha_2 f_e^{AA}}{8\pi} - \frac{3f_e^{AA}\lambda}{8\pi^2} & \frac{3\alpha_1}{4\pi} & 0 & 0 & 0 \\ -\frac{3f_e^{AA*}}{128\pi^2} & -\frac{f_e^{AA*}}{128\pi^2} & 0 & 0 & \frac{3(3\alpha_1-\alpha_2)}{8\pi} & 0 & 0 \\ -\frac{3f_e^{BB*}}{128\pi^2} & -\frac{f_e^{BB*}}{128\pi^2} & 0 & 0 & 0 & \frac{3(\alpha_1+\alpha_2)}{8\pi} & \frac{3(\alpha_1-\alpha_2)}{4\pi} \\ 0 & 0 & 0 & 0 & 0 & \frac{3(\alpha_1-\alpha_2)}{4\pi} & \frac{3(\alpha_1+\alpha_2)}{8\pi} \end{pmatrix}.$$

$\gamma_1, \gamma_2$ , and  $\gamma_3$  are the  $7 \times 1$  column vector mixing the first seven operators into  $\mathcal{O}_{Q,AD,\alpha\beta}^{(6)}$ ,  $\mathcal{O}_{d1,AD,\alpha\beta}^{(6)}$ ,

Figure 3.5: Self-renormalization of  $\mathcal{O}_M^{(6)}$

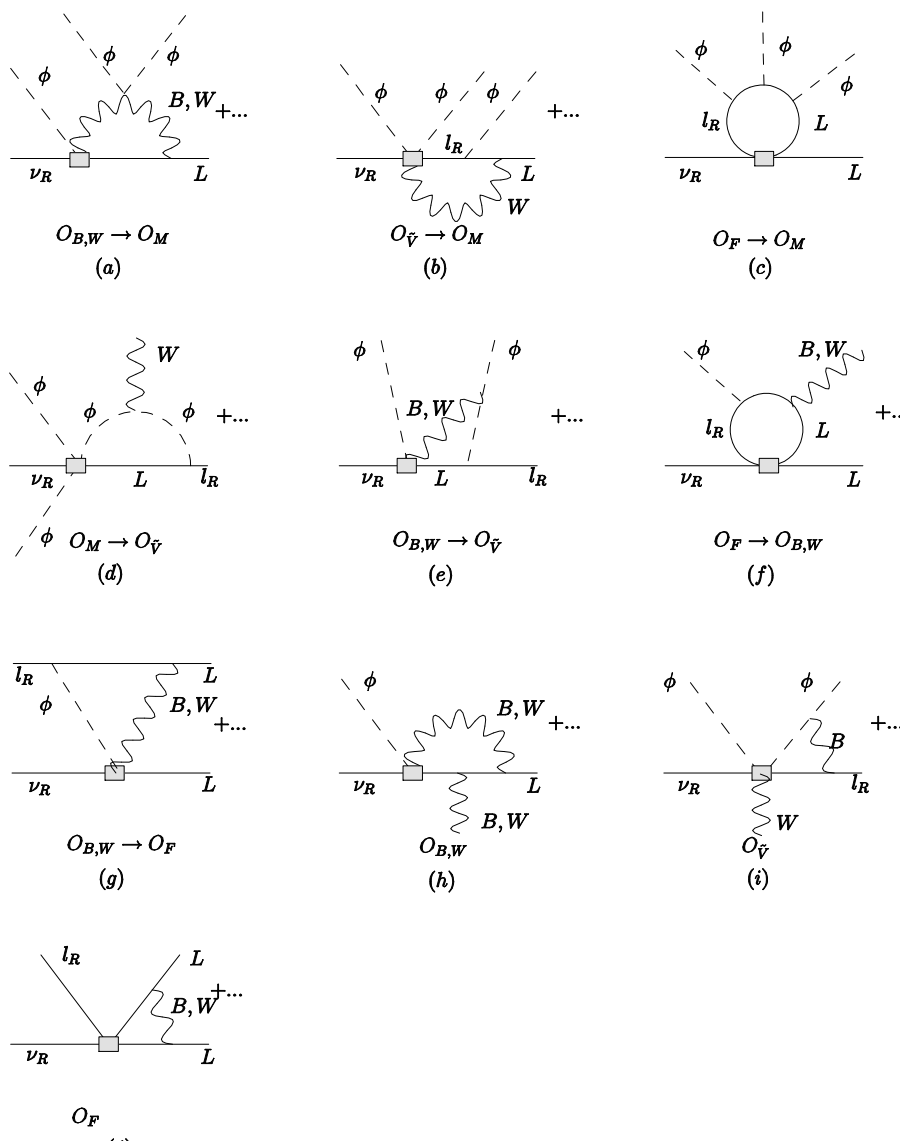


Figure 3.6: One-loop graphs for the mixing among  $6D$  operators. Notation is as in previous figures. Various types of mixing (a–g) and self-renormalization (h–j) are as discussed in the text

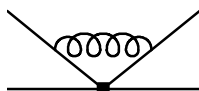


Figure 3.7: Self renormalizations of  $\mathcal{O}_{Q,d1,d2,AD,\alpha\beta}^{(6)}$  (denoted by the black box). Solid, dashed, and wavy lines denote fermion, Higgs scalar, and gauge bosons, respectively

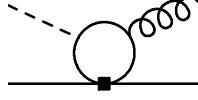


Figure 3.8: Mixing  $\mathcal{O}_{Q,d1,d2,AD,\alpha\beta}^{(6)}$  into  $\mathcal{O}_{B,W}^{(6)}$



Figure 3.9: Mixing  $\mathcal{O}_{B,W}^{(6)}$  into  $\mathcal{O}_{Q,d1,d2,AD,\alpha\beta}^{(6)}$

and  $\mathcal{O}_{d2,AD,\alpha\beta}^{(6)}$ , respectively,

$$\gamma_1 = \begin{pmatrix} 0 \\ 0 \\ 0 \\ 0 \\ 0 \\ 0 \\ 0 \\ 0 \end{pmatrix}, \gamma_2 = \begin{pmatrix} \frac{\alpha_1 f_d^{\alpha\beta}}{3\pi} \\ -\frac{3\alpha_2 f_d^{\alpha\beta}}{2\pi} \\ 0 \\ 0 \\ 0 \\ 0 \\ 0 \\ 0 \end{pmatrix}, \gamma_3 = \begin{pmatrix} -\frac{\alpha_1 f_d^{\alpha\beta}}{3\pi} \\ \frac{3\alpha_2 f_d^{\alpha\beta}}{4\pi} \\ 0 \\ 0 \\ 0 \\ 0 \\ 0 \\ 0 \end{pmatrix}. \quad (3.23)$$

$\gamma'_1, \gamma'_2,$  and  $\gamma'_3$  are the  $1 \times 7$  row vector mixing  $\mathcal{O}_{Q,AD,\alpha\beta}^{(6)}, \mathcal{O}_{d1,AD,\alpha\beta}^{(6)},$  and  $\mathcal{O}_{d2,AD,\alpha\beta}^{(6)}$  into the first seven operators, respectively,

$$\begin{aligned} \gamma'_1 &= (0 \ 0 \ 0 \ 0 \ 0 \ 0 \ 0) \\ \gamma'_2 &= \left(-\frac{f_d^{\alpha\beta*}}{128\pi^2} \quad -\frac{3f_d^{\alpha\beta*}}{128\pi^2} \quad 0 \ 0 \ 0 \ 0 \ 0\right) \\ \gamma'_3 &= (0 \ 0 \ 0 \ 0 \ 0 \ 0 \ 0) \end{aligned} \quad (3.24)$$

and

$$\begin{aligned}
A1 &= -\frac{173\alpha_1}{576\pi} + \frac{2\alpha_3}{\pi} \\
A2 &= A5 = -\frac{13\alpha_1}{576\pi} + \frac{3\alpha_2}{8\pi} - \frac{2\alpha_3}{3\pi} \\
A3 &= -\frac{5\alpha_1}{36\pi^2} - \frac{3\alpha_2}{4\pi} + \frac{4\alpha_3}{3\pi} \\
A4 &= -\frac{5\alpha_1}{36\pi^2} - \frac{3\alpha_2}{4\pi} + \frac{4\alpha_3}{3\pi}.
\end{aligned} \tag{3.25}$$

We find that the running of the gauge and Yukawa couplings has a negligible impact on the evolution of the  $C_k^6(\mu)$ . Eq. (3.8) gives us the solution to the RGE up to the leading logarithms  $\ln(\mu/\Lambda)$ . We find

$$\begin{aligned}
C_{M,AD}^6(\mu) &= C_{M,AD}^6(\Lambda) \left[ 1 - \gamma_{33} \ln \frac{\mu}{\Lambda} \right] \\
&\quad - \left[ \gamma_- C_-^6(\Lambda) + \gamma_+ C_+^6(\Lambda) + \gamma_{43} C_{\tilde{V},AD}^6(\Lambda) \right] \ln \frac{\mu}{\Lambda}
\end{aligned}$$

$$\begin{aligned}
C_+^6(\mu) &= C_+^6(\Lambda) \left[ 1 - \tilde{\gamma} \ln \frac{\mu}{\Lambda} \right] \\
&\quad + \left[ (f_e^{AA^*}/32\pi^2) C_{F,AAAD}^6(\Lambda) + (f_e^{BB^*}/32\pi^2) C_{F,ABBD}^6(\Lambda) \right] \ln \frac{\mu}{\Lambda} \\
&\quad + \left[ (f_d^{\alpha\beta^*}/32\pi^2) C_{d1,AD,\alpha\beta}^6(\Lambda) \right] \ln \frac{\mu}{\Lambda}
\end{aligned}$$

$$\begin{aligned}
\tilde{C}^6(\mu) &= \tilde{C}^6(\Lambda) \left[ 1 + \tilde{\gamma} \ln \frac{\mu}{\Lambda} \right] \\
&\quad + 3/128\pi^2 (\alpha_1 - \alpha_2) [f_e^{AA^*} C_{F,AAAD}^6(\Lambda) + f_e^{BB^*} C_{F,ABBD}^6(\Lambda) \\
&\quad + f_d^{\alpha\beta^*} C_{d1,AD,\alpha\beta}^6(\Lambda)] \ln \frac{\mu}{\Lambda}
\end{aligned}$$

$$C_{\tilde{V},AD}^6(\mu) = C_{\tilde{V},AD}^6(\Lambda) \left[ 1 - \gamma_{44} \ln \frac{\mu}{\Lambda} \right] + (9f_e^{AA}/8\pi) \tilde{C}^6(\Lambda) \ln \frac{\mu}{\Lambda}$$

$$\begin{aligned}
C_{F,AAAD}^6(\mu) &= C_{F,AAAD}^6(\Lambda) \left[ 1 + \frac{3(\alpha_2 - 3\alpha_1)}{8\pi} \ln \frac{\mu}{\Lambda} \right] \\
&\quad + (9f_e^{AA}/4\pi) [C_{B,AD}^6(\Lambda)\alpha_1 + C_{W,AD}^6(\Lambda)\alpha_2] \ln \frac{\mu}{\Lambda}
\end{aligned}$$

$$\begin{aligned}
C_{F, ABBD}^6(\mu) &= C_{F, ABBD}^6(\Lambda) \left[ 1 - \frac{3(\alpha_1 + \alpha_2)}{8\pi} \ln \frac{\mu}{\Lambda} \right] \\
&\quad - \frac{3(\alpha_1 - \alpha_2)}{4\pi} C_{F, BABD}^6(\Lambda) \ln \frac{\mu}{\Lambda} \\
&\quad + (9f_e^{BB}/2\pi) [C_{B, AD}^6(\Lambda)\alpha_1 + C_{W, AD}^6(\Lambda)\alpha_2] \ln \frac{\mu}{\Lambda}
\end{aligned}$$

$$\begin{aligned}
C_{F, BABD}^6(\mu) &= C_{F, BABD}^6(\Lambda) \left[ 1 - \frac{3(\alpha_1 + \alpha_2)}{8\pi} \ln \frac{\mu}{\Lambda} \right] \\
&\quad - \frac{3(\alpha_1 - \alpha_2)}{4\pi} C_{F, ABBD}^6(\Lambda) \ln \frac{\mu}{\Lambda} \\
&\quad - (9f_e^{BB}/4\pi) [C_{B, AD}^6(\Lambda)\alpha_1 + C_{W, AD}^6(\Lambda)\alpha_2] \ln \frac{\mu}{\Lambda}
\end{aligned}$$

$$C_{Q, AD, \alpha\beta}^6(\mu) = C_{Q, AD, \alpha\beta}^6(\Lambda) \left[ 1 + \left( \frac{173\alpha_1}{576\pi} - \frac{2\alpha_3}{\pi} \right) \ln \frac{\mu}{\Lambda} \right]$$

$$\begin{aligned}
C_{d1, AD, \alpha\beta}^{(6)} &= C_{d1, AD, \alpha\beta}^{(6)}(\Lambda) \left[ 1 + \left( \frac{13\alpha_1}{576\pi} - \frac{3\alpha_2}{8\pi} + \frac{2\alpha_3}{3\pi} \right) \ln \frac{\mu}{\Lambda} \right] \\
&\quad + C_{d2, AD, \alpha\beta}^6(\Lambda) \left[ \frac{5\alpha_1}{36\pi^2} + \frac{3\alpha_2}{4\pi} - \frac{4\alpha_3}{3\pi} \right] \ln \frac{\mu}{\Lambda} \\
&\quad + \left[ \frac{2\alpha_1 f_d^{\alpha\beta}}{9\pi} C_{B, AD}^6(\Lambda) + \frac{3\alpha_2 f_d^{\alpha\beta}}{4\pi^2} C_{W, AD}^6(\Lambda) \right] \ln \frac{\mu}{\Lambda}
\end{aligned}$$

$$\begin{aligned}
C_{d2, AD, \alpha\beta}^{(6)} &= C_{d2, AD, \alpha\beta}^{(6)}(\Lambda) \left[ 1 + \left( \frac{13\alpha_1}{576\pi} - \frac{3\alpha_2}{8\pi} + \frac{2\alpha_3}{3\pi} \right) \ln \frac{\mu}{\Lambda} \right] \\
&\quad + C_{d1, AD, \alpha\beta}^6(\Lambda) \left[ \frac{5\alpha_1}{36\pi^2} + \frac{3\alpha_2}{4\pi} - \frac{4\alpha_3}{3\pi} \right] \ln \frac{\mu}{\Lambda} \\
&\quad + \left[ \frac{\alpha_1 f_d^{\alpha\beta}}{3\pi} C_{B, AD}^6(\Lambda) - \frac{3\alpha_2 f_d^{\alpha\beta}}{4\pi} C_{W, AD}^6(\Lambda) \right] \ln \frac{\mu}{\Lambda}
\end{aligned}$$

where

$$\begin{aligned}
C_{\pm}^6(\mu) &\equiv C_{B, AD}^6(\mu) \pm C_{W, AD}^6(\mu) \\
\tilde{C}^6(\mu) &\equiv \alpha_1 C_{B, AD}^6(\mu) - 3\alpha_2 C_{W, AD}^6(\mu) \\
\gamma_{\pm} &\equiv (\gamma_{13} \pm \gamma_{23}) / 2 \\
\tilde{\gamma} &\equiv 3(\alpha_1 + 3\alpha_2) / 16\pi.
\end{aligned} \tag{3.26}$$

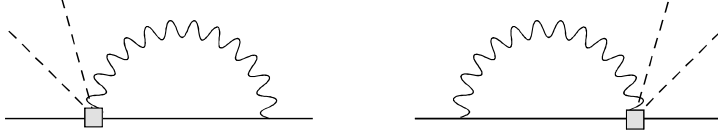


Figure 3.10: One-loop graphs for the matching of  $\mathcal{O}_{B,W}^{(7)}$  (denoted by the black box) into  $\mathcal{O}_{M,AD}^{(5)}$

We observe that to linear order in the lepton Yukawa couplings,  $C_{M,AD}^6(\mu)$  receives contributions from the two magnetic moment operators and  $\mathcal{O}_{\tilde{V}}^{(6)}$  but not from the four fermion operators.

### 3.2.3 Majorana Case

Although we have less operators in the Majorana case than in the Dirac case, it turns out that the flavor structure is far more complicated. In the Dirac case, we specify a flavor  $D$  for RH neutrino but this flavor is indeed inactive in our analysis. Unlike the Dirac case, we have  $\nu_L^c$  to play the role of  $\nu_R$ . The flavor of  $\nu_L^c$  plays an important role. Consider magnetic moment operator for Majorana neutrino

$$O_{MM}^{\alpha\beta} = \frac{\mu_{\alpha\beta}}{2} \overline{\nu_L^{\alpha c}} \sigma^{\mu\nu} \nu_L^{\beta} F_{\mu\nu} \quad (3.27)$$

where  $\alpha$  and  $\beta$  are flavors for neutrinos. We find that  $O_{MM}^{\alpha\alpha} = 0$  and the only non-diagonal operator could be nonzero. We only have a so-called transition magnetic moment operator for Majorana neutrinos. This doesn't happen in the Dirac case.

#### 3.2.3.1 Matching with $\mathcal{O}_{M,AD}^{(5)}$

First, we define

$$O_{W,AB}^{\pm} = \frac{1}{2} \left\{ O_{W,AB}^{(7)} \pm O_{W,BA}^{(7)} \right\}. \quad (3.28)$$

In this way, we can express  $O_{W,AB}^{(7)}$  in terms of operators with explicit flavor symmetry  $O_{W,AB}^{\pm}$ .

The one-loop graphs for matching  $O_{W,AB}^{\pm}$  and  $\mathcal{O}_{B,AB}^{(7)}$  with  $\mathcal{O}_{M,AB}^{(5)}$  are shown in Fig. 3.10. The mixing of  $O_{W,AB}^+$  and  $\mathcal{O}_{B,AB}^{(7)}$  are zero since  $O_{W,AB}^+$  and  $\mathcal{O}_{B,AB}^{(7)}$  are flavor antisymmetric while  $\mathcal{O}_{M,AB}^{(7)}$  is flavor symmetric. The  $7D$  operators  $\mathcal{O}_u^{(7)}$  and  $\mathcal{O}_d^{(7)}$  can contribute to

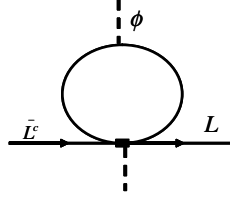


Figure 3.11: One-loop graphs for the matching of  $\mathcal{O}_{L,u,d}^{(7)}$  (denoted by the shaded box) into  $\mathcal{O}_{M,AD}^{(5)}$

$\mathcal{O}_M^{(5)}$  through the one-loop graphs of Fig. 3.2. Using NDA we can estimate the contributions from the coefficients of  $7D$  operators to the coefficient of the  $5D$  neutrino Majorana mass operator

$$\mathcal{O}_{W,AB}^+ \rightarrow C_{M,AB}^5 \simeq \frac{\alpha}{4\pi \sin^2 \theta_W} C_{W,AB}^+ \quad (3.29)$$

$$\mathcal{O}_{\tilde{V},AB}^{(7)} \rightarrow C_{M,AB}^5 \sim -\frac{f_e^{BB*}}{16\pi^2} C_{\tilde{V},AB}^{(7)}$$

$$\mathcal{O}_{L1,AB,BD}^{(7)} \rightarrow C_{M,AD}^5 \sim -\frac{f_e^{BB}}{16\pi^2} C_{L1,AB,BD}^{(7)}$$

$$\mathcal{O}_{L1,AB,AD}^{(7)} \rightarrow C_{M,BD}^5 \sim \frac{f_e^{AA}}{16\pi^2} C_{L1,AB,AD}^{(7)} \quad (3.30)$$

$$\mathcal{O}_{L2,AB,DD}^{(7)} \rightarrow C_{M,AB}^5 \sim \frac{f_e^{DD}}{8\pi^2} C_{L1,AB,DD}^{(7)}$$

$$\mathcal{O}_{L2,AB,AD}^{(7)} \rightarrow C_{M,BD}^5 \sim \frac{f_e^{AA}}{16\pi^2} C_{L2,ABAD}^{(7)}$$

$$\mathcal{O}_{d2,AB,\alpha B}^{(7)} \rightarrow C_{M,AB}^5 \sim \frac{f_d^{\alpha\beta} N_C}{16\pi^2} C_{d2,AB,\alpha B}^{(7)}$$

$$\mathcal{O}_{d2,AB,\alpha\beta}^{(7)} \rightarrow C_{M,AB}^5 \sim \frac{f_d^{\alpha\beta} N_C}{8\pi^2} C_{d2,AB,\alpha\beta}^{(7)} \quad (3.31)$$

$$\mathcal{O}_{u2,AB,\alpha\beta}^{(7)} \rightarrow C_{M,AB}^5 \sim \frac{f_u^{\alpha\beta*} N_C}{8\pi^2} C_{u2,AB,\alpha\beta}^{(7)}$$

$$\mathcal{O}_{u2,AB,\alpha B}^{(7)} \rightarrow C_{M,AB}^5 \sim \frac{f_d^{\alpha\beta} N_C}{16\pi^2} C_{u2,AB,\alpha B}^{(7)}$$

Please note  $\mathcal{O}_{L,AB,CD}^{(7)}$  could contribute to both  $\mathcal{O}_{M,AD}^{(5)}$  and  $\mathcal{O}_{M,BD}^{(5)}$ . We already see that flavor structure make our analysis of Majorana case very different than the Dirac case. Due

to flavor structure difference, Dirac neutrinos and Majorana neutrinos could have different implications.

### 3.2.3.2 Mixing with $\mathcal{O}_{M,AD}^{(7)}$

We could carry out our analysis just as in the Dirac case, but due to the complex flavor structure, a basis of operators close under renormalizations, including  $\mathcal{O}_{M,AD}^{(7)}$ , would include an intolerable number of operators. So we are not going to calculate the full anomalous dimension matrix  $\gamma$ . If  $\gamma$  is assumed constant, the solution to RGE up to the leading logarithms  $\ln \frac{\mu}{\Lambda}$  is

$$\mathbf{C}(\mu) = \exp(-\gamma^T \ln \frac{\mu}{\Lambda}) \mathbf{C}(\Lambda). \quad (3.32)$$

So if we are only interested in how one operator,  $\mathcal{O}_i$ , will contribute to  $\mathcal{O}_{M,AD}^{(7)}$ , we don't need to calculate the full  $\gamma$ .  $\gamma_{iM}$ , which stands for mixing of  $\mathcal{O}_i$  into  $\mathcal{O}_{M,AD}^{(7)}$ , will be enough; we then have

$$C_M^7(\mu) \sim -\gamma_{iM} C_i(\mu) \ln \frac{\mu}{\Lambda} \quad (3.33)$$

Just like in the Dirac case, the mixing of the four-fermion operators into  $\mathcal{O}_{M,AD}^{(7)}$  contains three powers of the lepton Yukawa couplings and is highly suppressed. And it turns out  $\mathcal{O}_{W,AB}^+$  will not contribute to neutrino magnetic moment. As for  $\mathcal{O}_{B,AB}^{(7)}$ , it is antisymmetric in flavor while  $\mathcal{O}_{M,AB}^{7D}$  is symmetric. So its contribution to  $C_{M,AB}^{7D}$  vanishes. At the end of the day, we are only left with  $\mathcal{O}_{W,AB}^-$  and  $\mathcal{O}_{\tilde{V},AB}^{(7)}$ .

As the operator  $\mathcal{O}_{W,AB}^-$  is flavor antisymmetric, it must be multiplied by another flavor antisymmetric contribution in order to produce a flavor symmetric mass term. This can be accomplished through insertion of Yukawa couplings in the diagram shown in Fig. 3.12 [53]. This diagram provides a logarithmically divergent contribution to the  $7D$  mass term, given by

$$C_{M,AB}^{7D}(v) \simeq \frac{3\alpha_2}{4\pi} \frac{m_A^2 - m_B^2}{v^2} \ln \frac{\Lambda}{v} C_{W,AB}^-(\Lambda) \quad (3.34)$$

where  $m_A$  are the charged lepton masses, and the exact coefficient has been computed using dimensional regularization, and renormalized with modified minimal subtraction.

As for  $\mathcal{O}_{\tilde{V},AB}^{(7)}$ , its mixing into  $\mathcal{O}_{M,AB}^{(7)}$  is very similar to how  $\mathcal{O}_{\tilde{V},AB}^{(6)}$  mixes into  $\mathcal{O}_{M,AB}^{(6)}$ .

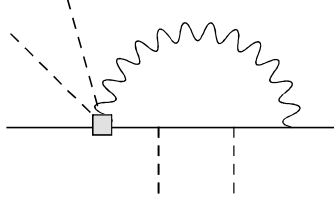


Figure 3.12: Contribution of  $O_W^-$  to the  $7D$  neutrino mass operator

After our calculation, we find

$$C_{M,AD}^7(\mu) \sim \left( \frac{9\alpha_2 f_e^{AA}}{8\pi} - \frac{3f_e^{AA}\lambda}{8\pi^2} \right) C_{V,AD}^7(\Lambda) \ln \frac{\mu}{\Lambda} \quad (3.35)$$

which is exactly as the Dirac case.

## Chapter 4

# Neutrino Mass Constraints

After SSB, the operators  $\mathcal{O}_M^{(4)}$  and  $\mathcal{O}_M^{(6)}$  generate a contribution to the Dirac neutrino mass

$$\begin{aligned}\delta m_\nu &= -C_M^4(v) \frac{v}{\sqrt{2}} \\ \delta m_\nu &= -C_M^6(v) \frac{v^3}{2\sqrt{2}\Lambda^2},\end{aligned}\tag{4.1}$$

and the operators  $\mathcal{O}_M^{(5)}$  and  $\mathcal{O}_M^{(7)}$  to the Majorana neutrino mass

$$\begin{aligned}\delta m_\nu &= -C_M^5(v) \frac{v^2}{2\Lambda} \\ \delta m_\nu &= -C_M^7(v) \frac{v^4}{4\Lambda^3}.\end{aligned}\tag{4.2}$$

Assuming there is no fine-tuning, the upper limit on  $m_\nu$  would put the same order of bound  $\delta m_\nu$  as well, namely,  $\delta m_\nu \lesssim m_\nu$ . In this way, we can use neutrino mass to constrain  $C_M(v)$  as follows:

$$\begin{aligned}|C_M^4(v)| &\lesssim \frac{m_\nu}{v/\sqrt{2}}, & |C_M^6(v)| &\lesssim \frac{m_\nu}{v/\sqrt{2}} \frac{\Lambda^2}{v^2/2}, \\ |C_M^5(v)| &\lesssim \frac{m_\nu}{v/\sqrt{2}} \frac{\Lambda}{v/\sqrt{2}}, & |C_M^7(v)| &\lesssim \frac{m_\nu}{v/\sqrt{2}} \frac{\Lambda^3}{v^3/2\sqrt{2}}.\end{aligned}\tag{4.3}$$

So, through the operator mixing and matching discussed in Section 3.2, we are going to constrain neutrino magnetic moment in Section 4.1, some parameters of  $\mu$ -decay in Section 4.2, and  $\beta$ -decay in Section 4.3. Finally, we constrain  $\pi \rightarrow \bar{\nu}\nu$  in Section 4.4

## 4.1 Constraints on Neutrino Magnetic Moment

In the Standard Model (minimally extended to include non-zero neutrino mass) the neutrino magnetic moment is given by [24]

$$\mu_\nu \approx 3 \times 10^{-19} \left( \frac{m_\nu}{1\text{eV}} \right) \mu_B. \quad (4.4)$$

An experimental observation of a magnetic moment larger than that given in Eq. (4.4) would be an unequivocal indication of physics beyond the minimally extended Standard Model. Current laboratory limits are determined via neutrino-electron scattering at low energies, with  $\mu_\nu < 1.5 \times 10^{-10} \mu_B$  [25] and  $\mu_\nu < 0.7 \times 10^{-10} \mu_B$  [26] obtained from solar and reactor experiments, respectively. Slightly stronger bounds are obtained from astrophysics. Constraints on energy loss from astrophysical objects via the decay of plasmons into  $\nu\bar{\nu}$  pairs restricts the neutrino magnetic moment to be  $\mu_\nu < 3 \times 10^{-12}$  [27]. Neutrino magnetic moments are reviewed in [29, 30, 31], and recent work can be found in [32, 28].

In general, contributions to  $m_\nu^{AD}$  involving  $\mathcal{O}_{M,AD}^{(6)}$  ( $\mathcal{O}_{M,AD}^{(7)}$ ) will be smaller than those that involve mixing with  $\mathcal{O}_{M,AD}^{(4)}$  ( $\mathcal{O}_{M,AD}^{(5)}$ ) by  $\sim (v/\Lambda)^2$ , since  $\mathcal{O}_{M,AD}^{(6)}$  ( $\mathcal{O}_{M,AD}^{(7)}$ ) contains an additional factor of  $(\phi^\dagger\phi)/\Lambda^2$ . For  $v$  not too different from  $\Lambda$ , the impact of the mixing with  $\mathcal{O}_{M,AD}^{(6)}$  ( $\mathcal{O}_{M,AD}^{(7)}$ ) can also be important.

### 4.1.1 Dirac Case

After SSB we have

$$\mathcal{O}_B^{(6)} \rightarrow \frac{v}{\sqrt{2}} g_1 \bar{\nu}_L \sigma^{\mu\nu} \nu_R B_{\mu\nu} \quad (4.5)$$

$$\mathcal{O}_W^{(6)} \rightarrow g_2 \frac{v}{\sqrt{2}} \bar{\nu}_L \sigma^{\mu\nu} \nu_R W_{\mu\nu}^3 + \dots \quad (4.6)$$

Using  $g_2 \sin \theta_W = g_1 \cos \theta_W = e$ , it is straightforward to see that the combination  $C_B^6 \mathcal{O}_B^{(6)} + C_W^6 \mathcal{O}_W^{(6)}$  appearing in  $\mathcal{L}_{\text{eff}}$  contains the magnetic moment operator

$$-\frac{\mu_\nu}{4} \bar{\nu} \sigma^{\mu\nu} \nu F_{\mu\nu} \quad (4.7)$$

where  $F_{\mu\nu}$  is the photon field strength tensor and

$$\frac{\mu_\nu}{\mu_B} = -4\sqrt{2} \left( \frac{m_e v}{\Lambda^2} \right) [C_B^6(v) + C_W^6(v)] \quad . \quad (4.8)$$

Matching with  $\mathcal{O}_{M,AD}^{(4)}$ ,  $\mathcal{O}_B^{(6)}$  and  $\mathcal{O}_W^{(6)}$  contribute to  $\mathcal{O}_M^{(6)}$  with

$$\begin{aligned} C_M^4 &\sim \frac{\alpha}{4\pi \cos^2 \theta_W} C_B^6 \\ C_M^4 &\sim \frac{3\alpha}{4\pi \sin^2 \theta_W} C_W^6 \end{aligned} \quad (4.9)$$

from which we find

$$\frac{\mu_\nu}{\mu_B} \lesssim 4 \left( \frac{m_e m_\nu}{\Lambda^2} \right) \left( \frac{\alpha}{4\pi \cos^2 \theta_W} + \frac{3\alpha}{4\pi \sin^2 \theta_W} \right). \quad (4.10)$$

For  $\Lambda = v \approx 250\text{GeV}$ , we have

$$\left| \frac{\mu_\nu}{\mu_B} \right| \lesssim 10^{-14}, \quad (4.11)$$

which is several orders of magnitude more stringent than current experimental constraints.

However, for  $\Lambda$  not too different from the weak scale, the 6D mixing can be of comparable importance to the 4D case. The solution to RGE allows us to relate  $\mu_\nu$  to the corresponding neutrino mass matrix element in terms of  $C_\pm(\Lambda)$  and  $C_M^6(\Lambda)$

$$\delta m_\nu = \frac{v^2}{16m_e} \frac{C_M^6(v)}{C_+(v)} \frac{\mu_\nu}{\mu_B} \quad , \quad (4.12)$$

To obtain a natural upper bound on  $\mu_\nu$ , we assume first that  $C_i^6(\Lambda) = 0$  ( $i \neq B, W$ ) so that  $\delta m_\nu$  is generated entirely by radiative corrections involving insertions of  $\mathcal{O}_{B,W}^{(6)}$ . Doing so in Eq. (4.12) and solving for  $\mu_\nu/\mu_B$  leads directly to

$$\frac{|\mu_\nu|}{\mu_B} = \frac{G_F m_e}{\sqrt{2}\pi\alpha} \left[ \frac{\delta m_\nu}{\alpha \ln(\Lambda/v)} \right] \frac{32\pi \sin^4 \theta_W}{9|f|} \quad , \quad (4.13)$$

where  $\theta_W$  is the weak mixing angle,

$$f = (1-r) - \frac{2}{3}r \tan^2 \theta_W - \frac{1}{3}(1+r) \tan^4 \theta_W \quad , \quad (4.14)$$

and  $r = C_-/C_+$  is a ratio of effective operator coefficients defined at the scale  $\Lambda$  (see below)

that one expects to be of order unity. To arrive at a numerical estimate of this bound, we substitute  $\Lambda = v$  into the logarithms appearing in Eq. (4.13) and obtain

$$\frac{|\mu_\nu|}{\mu_B} \lesssim 8 \times 10^{-15} \times \left( \frac{m_\nu}{1 \text{ eV}} \right) \frac{1}{|f|} . \quad (4.15)$$

It is interesting to consider the bound for the special case that only the magnetic moment operator is generated at the scale  $\Lambda$ , i.e.,  $C_+(\Lambda) \neq 0$  and  $C_- = 0$ , with  $f \simeq 1$ . For this case, considering a nearly degenerate neutrino spectrum with masses  $\sim 1$  eV leads to the  $|\mu_\nu| \lesssim 8 \times 10^{-15} \mu_B$ —a limit that is two orders of magnitude stronger than the astrophysical bound [27] and  $10^4$  stronger than those obtained from solar and reactor neutrinos. For a hierarchical neutrino mass spectrum, the bound would be even more stringent.

#### 4.1.2 Majorana Case

Table 4.1: Summary of constraints on the magnitude of the magnetic moment of Majorana neutrinos. The upper two lines correspond to a magnetic moment generated by the  $O_W$  operator, while the lower two lines correspond to the  $O_B^-$  operator.

i) 1-loop, 7D	$\mu_{\alpha\beta}^W$	$\leq 1 \times 10^{-10} \mu_B \left( \frac{[m_\nu]_{\alpha\beta}}{1 \text{ eV}} \right) \ln^{-1} \frac{\Lambda^2}{M_W^2} R_{\alpha\beta}$
ii) 2-loop, 5D	$\mu_{\alpha\beta}^W$	$\leq 1 \times 10^{-9} \mu_B \left( \frac{[m_\nu]_{\alpha\beta}}{1 \text{ eV}} \right) \left( \frac{1 \text{ TeV}}{\Lambda} \right)^2 R_{\alpha\beta}$
iii) 2-loop, 7D	$\mu_{\alpha\beta}^B$	$\leq 1 \times 10^{-7} \mu_B \left( \frac{[m_\nu]_{\alpha\beta}}{1 \text{ eV}} \right) \ln^{-1} \frac{\Lambda^2}{M_W^2} R_{\alpha\beta}$
iv) 2-loop, 5D	$\mu_{\alpha\beta}^B$	$\leq 4 \times 10^{-9} \mu_B \left( \frac{[m_\nu]_{\alpha\beta}}{1 \text{ eV}} \right) \left( \frac{1 \text{ TeV}}{\Lambda} \right)^2 R_{\alpha\beta}$

After spontaneous symmetry breaking, the flavor antisymmetric operators  $\mathcal{O}_B$  and  $\mathcal{O}_W^-$  contribute to the magnetic moment interaction

$$\frac{1}{2} [\mu_\nu]_{AB} \overline{\nu_L^{Ac}} \sigma^{\mu\nu} \nu_L^B F_{\mu\nu}, \quad (4.16)$$

where  $F_{\mu\nu}$  is the electromagnetic field strength tensor,

$$\frac{[\mu_\nu]_{AB}}{\mu_B} = \frac{2m_e v^2}{\Lambda^3} \left( C_{B,AB}^7(v) + C_{W,AB}^-(v) \right). \quad (4.17)$$

The flavor symmetric operator  $\mathcal{O}_W^+$  does not contribute to this interaction at tree-level.

One-loop matching yields a contribution to  $\mathcal{O}_M^{5D}$  associated with  $\mathcal{O}_W^+$  of order

$$C_M^{5D} \simeq \frac{\alpha}{4\pi \sin^2 \theta_W} C_W^+, \quad (4.18)$$

while contribution to  $\mathcal{O}_M^{5D}$  associated with  $\mathcal{O}_W^-$  is zero, as mentioned in Section 3.2.

We see that the one-loop contribution to the  $5D$  mass term provides a strong constraint on  $C_W^+$  but no constraint on the parameter  $C_W^-$ . In general,  $C_W^\pm$  are unrelated parameters in the theory. If the new physics were to have no specific flavor symmetry/antisymmetry it might be natural for  $C_W^\pm$  to be of similar magnitude. Alternatively, given the strong constraint on  $C_W^+$  arising from Eq. (4.18), a sizable magnetic moment requires  $|C_W^-| \gg |C_W^+|$ . We have seen that the flavor antisymmetric operator  $\mathcal{O}_W^-$  does not contribute to the  $5D$  neutrino mass term at 1-loop order, thus a direct constraint on the magnetic moment is not obtained from the diagrams in Fig. 3.10. However, suppose we had a theory in which the coefficients of  $\mathcal{O}_W^+$  and  $\mathcal{O}_W^-$  were of similar magnitude,  $C_W^+ \sim C_W^-$ . Then, using Eqs. (4.17, 4.18) we have

$$\begin{aligned} m_\nu &\sim \frac{\alpha}{8\pi \sin^2 \theta_W} \frac{\Lambda^2}{m_e \mu_B} \mu_\nu, \\ &\sim \frac{\mu_\nu}{0.4 \times 10^{-15} \mu_B} [\Lambda(\text{TeV})]^2 \text{ eV}, \end{aligned} \quad (4.19)$$

and thus obtain a stringent  $\mu_\nu$  bound similar to that for Dirac neutrinos.

We emphasize that Eq. (4.19) is not a model-independent constraint, as in general  $\mathcal{O}_W^+$  and  $\mathcal{O}_W^-$  are unrelated. While it might seem natural for the the new physics to generate coefficients of similar size for both operators, we could obtain finite  $C_W^-$  and vanishing  $C_W^+$  (at tree-level) by imposing an appropriate flavor symmetry.

We now consider the more general case where  $C_W^+$  and  $C_W^-$  are unrelated, and directly derive constraints on the the coefficient of the flavor antisymmetric operator,  $C_W^-$ . As the operator  $\mathcal{O}_W^-$  is flavor antisymmetric, it must be multiplied by another flavor antisymmetric contribution in order to produce a flavor symmetric mass term. This is given by Eq. (3.34). We note that Eq. (3.34) gives the  $\mathcal{O}_W^-$  contribution to the neutrino mass from all scales between  $\Lambda$  and the scale of electroweak symmetry breaking to leading log order. Using this result—as well as Eq. (4.17), to relate  $C_W^-$  and  $C_M^{7D}$  to  $\mu_\mu$  and  $m_\nu$ , respectively – leads to bound (i) in Table 4.1.

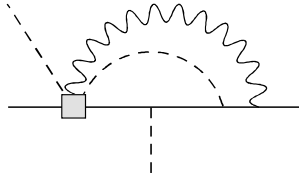


Figure 4.1: Representative contribution of  $O_W^-$  to the 5D neutrino mass operator

Note that this provides a weaker constraint than that in Eq. (4.19), as it is suppressed by the charged lepton masses, and also only logarithmically dependent on the scale of new physics  $\Lambda$ .

The neutrino magnetic moment operator  $\mathcal{O}_W^-$  will also contribute to the 5D mass operator *via* two-loop matching of the effective theory onto the full theory at  $\mu \sim \Lambda$ .

An illustrative contribution is shown in Fig. 4.1. As with the diagrams in Fig. 3.12, we require two Yukawa insertions in order to obtain a flavor symmetric result. This diagram contributes to the 5D mass operator, and we again provide an NDA estimate:

$$C_{M,AB}^{5D} \simeq \frac{g^2}{(16\pi^2)^2} \frac{m_A^2 - m_B^2}{v^2} C_{W,AB}^- \quad (4.20)$$

Again, using Eqs. (4.17, 4.20), this leads to bound (ii) in Table 4.1. In doing so, we have neglected the running of the operator coefficients from the scale  $\Lambda$  to  $v$ , since the effects are higher order in the gauge couplings and have a negligible numerical impact on our analysis.

Compared to the 1-loop (7D) case of Eq. (3.34), the 2-loop (5D) matching leads to a mass contribution that is suppressed by a factor of  $1/16\pi^2$  arising from the additional loop, but enhanced by a factor of  $\Lambda^2/v^2$  arising from the lower operator dimension. Thus, as we increase the new physics scale,  $\Lambda$ , this two-loop constraint rapidly becomes more restrictive and nominally provides a stronger constraint than the 1-loop result once  $\Lambda \approx 4\pi v \sim 4$  TeV. Inclusion of the logarithmic  $\Lambda$ -dependence of one-loop mixing implies that the "crossover" scale between the two effects is closer to  $\sim 10$  TeV.

Unlike the case of the  $SU(2)_L$  gauge boson, where a flavor symmetric operator  $\mathcal{O}_W^+$  exists, the operator  $\mathcal{O}_B^{(7)}$  is purely flavor antisymmetric. Therefore, it cannot contribute to the  $\mathcal{O}_M^{(5)}$  mass term at one loop. As was noticed in [53], the one-loop contribution of  $\mathcal{O}_B^{(7)}$  to the  $\mathcal{O}_M^{(7)}$  mass term also vanishes.

If we insert  $O_B$  in the diagram in Fig. 3.12, the contribution vanishes, due to the  $SU(2)$

structure of the graph. Therefore, to obtain a non-zero contribution to  $\mathcal{O}_M^{(7)}$  from  $\mathcal{O}_B^{(7)}$  we require the presence of some non-trivial  $SU(2)$  structure. This can arise, for instance, from a virtual  $W$  boson loop.

This mechanism gives the leading contribution of the operator  $\mathcal{O}_B^{(7)}$  to the  $7D$  mass term. The  $\mathcal{O}_B^{(7)}$  and  $\mathcal{O}_W^{(7)}$  contributions to the  $7D$  mass term are thus related by

$$\frac{(\delta m_\nu)^B}{(\delta m_\nu)^W} \approx \frac{\alpha}{4\pi \cos^2 \theta_W}, \quad (4.21)$$

where  $\theta_W$  is the weak mixing angle and where the factor on the RHS is due to the additional  $SU(2)_L$  boson loop. This additional loop suppression for the  $\mathcal{O}_B^{(7)}$  contribution results in a significantly weaker neutrino magnetic moment constraint than that obtained above  $\mathcal{O}_W^-$ . The corresponding limit is shown as bound (iii) in Table 4.1.

However, the leading contribution of  $\mathcal{O}_B^{(7)}$  to the 5D mass term arises from the same 2-loop matching considerations (Fig. 4.1) that we discussed in connection with the  $\mathcal{O}_W^-$  operator. Therefore, the contribution to the 5D mass term is the same as that for  $\mathcal{O}_W$ , except for a factor of  $(g_1/g_2)^2 = \tan^2 \theta_W$ . We thus obtain

$$C_{M,AB}^{(5)} \simeq \frac{g_1^2}{(16\pi^2)^2} \frac{m_\alpha^2 - m_\beta^2}{v^2} C_{B,AB}^{(7)} \quad (4.22)$$

corresponding to bound (iv) in Table 4.1. Importantly, this is the strongest constraint on the  $\mathcal{O}_B^{(7)}$  contribution to the neutrino magnetic moment for any value of  $\Lambda$ .

Our results are summarized in Table 4.1 below, where the quantity  $R_{\alpha\beta}$  is defined as

$$R_{\alpha\beta} = \left| \frac{m_\tau^2}{m_\alpha^2 - m_\beta^2} \right|, \quad (4.23)$$

with  $m_\alpha$  being the masses of charged lepton masses. Numerically, one has  $R_{\tau e} \simeq R_{\tau\mu} \simeq 1$  and  $R_{\mu e} \simeq 283$ .

The limit on the magnetic moment of a Dirac neutrino is considerably more stringent than for Majorana neutrino. This is due to the different flavor symmetries involved. In the Dirac case, no insertion of Yukawa couplings is needed to convert a flavor antisymmetric operator into a flavor symmetric operator, and the stringent limit  $\mu \leq 10^{-15} \mu_B$  holds (in the absence of strong cancellations). A significant implication is that if a magnetic moment

$\mu \geq 10^{-15} \mu_B$  were measured, it would indicate that neutrinos are Majorana fermions, rather than Dirac. Moreover, the scale of lepton number violation would be well below the conventional see-saw scale.

## 4.2 Implications for Muon Decay Parameters

### 4.2.1 Introduction

Precision studies of muon decay continue to play an important role in testing SM and searching for physics beyond it. In the gauge sector of SM, the Fermi constant  $G_\mu$  that characterizes the strength of the low-energy, four-lepton  $\mu$ -decay operator is determined from the  $\mu$  lifetime, and gives one of the three most precisely-known inputs into the theory. Analyses of the spectral shape, angular distribution, and polarization of the decay electrons (or positrons) probe for contributions from operators that deviate from the  $(V - A) \otimes (V - A)$  structure of the SM decay operator. In the absence of time-reversal (T) violating interactions, there exist seven independent parameters—the so-called Michel parameters [33, 34]—that characterize the final state charged leptons: two  $(\rho, \eta)$  that describe the spatially isotropic component of the lepton spectrum; two  $(\xi, \delta)$  that characterize the spatially anisotropic distribution; and three additional quantities  $(\xi', \xi'', \eta'')$  that are needed to describe the lepton's transverse and longitudinal polarization. Two additional parameters  $(\alpha'/A, \beta'/A)$  characterize a T-odd correlation between the final state lepton spin and momenta with the muon polarization:  $\hat{S}_e \cdot \hat{k}_e \times \hat{S}_\mu$ .

Recently, new experimental efforts have been devoted to more precise determinations of these parameters. The TWIST Collaboration has measured  $\rho$  and  $\delta$  at TRIUMF [35, 36], improving the uncertainty over previously reported values by factors of  $\sim 2.5$  and  $\sim 3$ , respectively. An experiment to measure the transverse positron polarization has been carried out at the Paul Scherrer Institute (PSI), leading to similar improvements in sensitivity over the results of earlier measurements [37]. A new determination of  $P_\mu \xi$  with a similar degree of improved precision is expected from the TWIST Collaboration, and one anticipates additional reductions in the uncertainties in  $\rho$  and  $\delta$  [38].

At present, there exists no evidence for deviations from SM predictions for the Michel parameters (MPs). It is interesting, nevertheless, to ask what constraints these new measurements can provide on possible contributions from physics beyond the SM. It has been

conventional to characterize these contributions in terms of a set of ten four-fermion operators

$$\mathcal{L}^{\mu\text{-decay}} = -\frac{4G_\mu}{\sqrt{2}} \sum_{\gamma, \epsilon, \mu} g_{\epsilon\mu}^\gamma \bar{e}_\epsilon \Gamma^\gamma \nu \bar{\nu} \Gamma_\gamma \mu_\mu \quad (4.24)$$

where the sum runs over Dirac matrices  $\Gamma^\gamma = 1$  (S),  $\gamma^\alpha$  (V), and  $\sigma^{\alpha\beta}/\sqrt{2}$  (T), and the subscripts  $\mu$  and  $\epsilon$  denote the chirality ( $R, L$ ) of the muon and final state lepton, respectively. In the Majorana case,  $\nu_R$  is substituted by  $\nu_L^c$ . In the SM, one has  $g_{LL}^V = 1$  and all other  $g_{\epsilon\mu}^\gamma = 0$ . A recent, global analysis by Gagliardi, Tribble, and Williams [40] give the present experimental bounds on the  $g_{\epsilon\mu}^\gamma$  that include the impact of the latest TRIUMF and PSI measurements. In the following sections, 1 stands for electron flavor and 2 for muon flavor.

### 4.2.2 Dirac Case

To arrive at neutrino mass naturalness constraints on the  $g_{\epsilon\mu}^\gamma$  coefficients, it is useful to tabulate their relationships with the dimension six operator coefficients. In some cases, one must perform a Fierz transformation in order to obtain the operator structures in Eq. (4.24). Letting

$$g_{\epsilon\mu}^\gamma = -\kappa \left(\frac{v}{\Lambda}\right)^2 C_k^6, \quad (4.25)$$

we give in Table 4.3 the  $\kappa$ s corresponding to the various dimension six operators.

We use the entries in Table 4.3 and the estimates in Eq. (3.20) to obtain the bounds in Table 4.2. Note that the bounds become smaller as  $\Lambda$  is increased from  $v$ .

The constraints on the  $g_{LR,RL}^V$  follow from mixing among the  $6D$  operators and Table 4.3. Assuming no fine-tuning,  $\delta m_\nu^{2D} \lesssim m_\nu^{2D}$ , we obtain

$$g_{LR}^V \lesssim \left(\frac{m_\nu^{2D}}{m_\mu}\right) \left(\frac{8\pi \sin^2 \theta_W}{9}\right) \left(\alpha - \frac{\lambda \sin^2 \theta_W}{3\pi}\right)^{-1} \left(\ln \frac{v}{\Lambda}\right)^{-1}. \quad (4.26)$$

A similar expression holds for  $g_{RL}^V$ , but with  $m_\mu \rightarrow m_e$  and  $m_\nu^{2D} \rightarrow m_\nu^{1D}$ . Note that in arriving at Eq. (4.26) we have ignored the running of the  $C_{\bar{V},AD}^6(\mu)$  between  $\Lambda$  and  $v$ , since the impact on the  $g_{LR,RL}^V$  is higher order in the gauge and Yukawa couplings. To derive numerical bounds on the  $g_{LR,RL}^V$  from Eq. (4.26) we use the running couplings in the  $\overline{\text{MS}}$  scheme  $\alpha = \hat{\alpha}(M_Z) \approx 1/127.9$ ,  $\sin^2 \hat{\theta}_W(M_Z) \approx 0.2312$  and the tree-level relation between the Higgs quartic coupling  $\lambda$ , the Higgs mass  $m_H$ , and  $v$ :  $2\lambda = (m_H/v)^2$ . We quote two results, corresponding to the direct search lower bound on  $m_H \geq 114$  GeV and the one-sided

Table 4.2: Constraints on  $\mu$ -decay couplings  $g_{e\mu}^\gamma$  in the Dirac case. The first eight rows give naturalness bounds in units of  $(v/\Lambda)^2 \times (m_\nu/1 \text{ eV})$  on contributions from  $6D$  muon decay operators based on one-loop mixing with the  $4D$  neutrino mass operators. The ninth row gives upper bounds derived from a recent global analysis of [40], while the last row gives estimated bounds from [44] derived from two-loop mixing of  $6D$  muon decay and mass operators. A “-” indicates that the operator does not contribute to the given  $g_{e\mu}^\gamma$ , while “None” indicates that the operator gives a contribution unconstrained by neutrino mass. The subscript  $D$  runs over the two generations of RH Dirac neutrinos

Source	$ g_{LR}^S $	$ g_{LR}^T $	$ g_{RL}^S $	$ g_{RL}^T $	$ g_{LR}^V $	$ g_{RL}^V $
$\mathcal{O}_{F,122D}^{(6)}$	$4 \times 10^{-7}$	$2 \times 10^{-7}$	-	-	-	-
$\mathcal{O}_{F,212D}^{(6)}$	$4 \times 10^{-7}$	-	-	-	-	-
$\mathcal{O}_{F,112D}^{(6)}$	None	None	-	-	-	-
$\mathcal{O}_{F,211D}^{(6)}$	-	-	$8 \times 10^{-5}$	$4 \times 10^{-5}$	-	-
$\mathcal{O}_{F,121D}^{(6)}$	-	-	$8 \times 10^{-5}$	-	-	-
$\mathcal{O}_{F,221D}^{(6)}$	-	-	None	None	-	-
$\mathcal{O}_{\tilde{V},2D}^{(6)}$	-	-	-	-	$8 \times 10^{-7}$	-
$\mathcal{O}_{\tilde{V},1D}^{(6)}$	-	-	-	-	-	$2 \times 10^{-4}$
Global [40]	0.088	0.025	0.417	0.104	0.036	0.104
Two-loop [44]	$10^{-4}$	$10^{-4}$	$10^{-2}$	$10^{-2}$	$10^{-4}$	$10^{-2}$

Table 4.3: Coefficients  $\kappa$  that relate  $g_{e\mu}^\gamma$  to the dimension six operator coefficients  $C_k^6$

$\kappa$	$g_{LR}^S$	$g_{LR}^T$	$g_{RL}^S$	$g_{RL}^T$	$g_{LR}^V$	$g_{RL}^V$
$C_{F,122D}^6$	1/4	1/8	-	-	-	-
$C_{F,212D}^6$	1/2	-	-	-	-	-
$C_{F,112D}^6$	3/4	1/8	-	-	-	-
$C_{F,211D}^6$	-	-	1/4	1/8	-	-
$C_{F,121D}^6$	-	-	1/2	-	-	-
$C_{F,221D}^6$	-	-	3/4	1/8	-	-
$C_{\tilde{V},2D}^6$	-	-	-	-	-1/2	-
$C_{\tilde{V},1D}^6$	-	-	-	-	-	-1/2

95 % C.L. upper bound from analysis of precision electroweak measurements,  $m_H \leq 186$  GeV[54]. We obtain

$$|g_{LR}^V| \lesssim \left(\frac{m_\nu^{2D}}{1 \text{ eV}}\right) \left(\ln \frac{\Lambda}{v}\right)^{-1} \begin{cases} 1.2 \times 10^{-6}, & m_H = 114 \text{ GeV} \\ 7.5 \times 10^{-6}, & m_H = 186 \text{ GeV} \end{cases} \quad (4.27)$$

$$|g_{RL}^V| \lesssim \left(\frac{m_\nu^{1D}}{1 \text{ eV}}\right) \left(\ln \frac{\Lambda}{v}\right)^{-1} \begin{cases} 2.5 \times 10^{-4}, & m_H = 114 \text{ GeV} \\ 1.5 \times 10^{-3}, & m_H = 186 \text{ GeV} \end{cases}. \quad (4.28)$$

For  $\Lambda \sim 1$  TeV, the logarithms are  $\mathcal{O}(1)$  so that for  $m_\nu \sim 1$  eV, the bounds on the  $g_{LR,RL}^V$  derived from  $6D$  mixing are comparable in magnitude to those estimated from mixing with the  $4D$  mass operators.

Although the four fermion operators do not mix with  $\mathcal{O}_{M,AD}^{(6)}$  at linear order in the Yukawa couplings, they do contribute to the magnetic moment operators  $\mathcal{O}_{B,AD}^{(6)}$  and  $\mathcal{O}_{W,AD}^{(6)}$  at this order. From  $6D$  mixing, we have

$$\frac{\delta\mu_\nu^{AD}}{\mu_B} = \frac{\sqrt{2}}{8\pi^2} \left(\frac{m_e}{v}\right) \left(\frac{v}{\Lambda}\right)^2 \text{Re} [f_{AA}^* C_{F,AAAD}^6 + f_{BB}^* C_{F,ABBD}^6] \ln \frac{\Lambda}{v}, \quad (4.29)$$

where  $\delta\mu_\nu^{AD}$  denotes the contribution to the magnetic moment matrix and  $\mu_B$  is a Bohr magneton. While  $\mathcal{O}_{F,AAAD}^{(6)}$  does not contribute to  $\mu$ -decay, the operator  $\mathcal{O}_{F,ABBD}^{(6)}$  does, and its presence in Eq. (4.29) implies constraints on its coefficient from current bounds on neutrino magnetic moments. The most stringent constraints arise for  $A = 1$ ,  $B = 2$  for which we find

$$|C_{F,122D}^6| \left(\frac{v}{\Lambda}\right)^2 \leq 5 \times 10^{10} \left(\ln \frac{\Lambda}{v}\right)^{-1} \left(\frac{\mu_\nu^{1D}}{\mu_B}\right). \quad (4.30)$$

Current experimental bounds on  $|\mu_\nu^{\text{exp}}/\mu_B|$  range from  $\sim 10^{-10}$  from observations of solar and reactor neutrinos [25] to  $\sim 3 \times 10^{-12}$  from the non-observation of plasmon decay into  $\bar{\nu}\nu$  in astrophysical objects [27]. Assuming that the logarithm in Eq. (4.30) is of order unity, these limits translate into bounds on  $g_{LR}^S$  and  $g_{LR}^T$  ranging from  $\sim 1 \rightarrow 0.03$  and  $\sim 0.3 \rightarrow 0.01$ , respectively. The solar and reactor neutrino limits on  $|\mu_\nu^{\text{exp}}/\mu_B|$  imply bounds on the  $g_{LR}^{S,T}$  that are weaker than those obtained from the global analysis of  $\mu$ -decay measurements, while those associated with the astrophysical magnetic moment limits are comparable to the global values. Nevertheless, the bounds derived from neutrino magnetic moments are

several orders of magnitude weaker than those derived from the scale of neutrino mass.

The naturalness bounds on the  $C_k^6$  associated with the scale of  $m_\nu$  have implications for the interpretation of  $\mu$ -decay experiments. Because the coefficients  $C_{F,112D}^6$  and  $C_{F,221D}^6$  that contribute to  $g_{LR,RL}^{S,T}$  are not directly constrained by  $m_\nu$ , none of the eleven Michel parameters is directly constrained by neutrino mass alone. Instead, it is more relevant to compare the results of global analyses from which limits on the  $g_{\epsilon\mu}^\gamma$  are obtained with the  $m_\nu$  naturalness bounds, since the latter imply tiny values for the couplings  $g_{LR,RL}^V$ . Should future experiments yield a value for either of these couplings that is considerably larger than our bounds in Table 4.2, the new physics above  $\Lambda$  would have to exhibit either fine-tuning or a symmetry in order to evade unacceptably large contributions to  $m_\nu$ . In addition, should future global analyses find evidence for non-zero  $g_{LR,RL}^{S,T}$  with magnitudes considerably larger than those given by the  $m_\nu$ -constrained contributions listed in Table 4.2, then one would have evidence for a non-trivial flavor structure in the new physics that allows considerably larger effects from the operators  $\mathcal{O}_{F,112D}^{(6)}$  and  $\mathcal{O}_{F,221D}^{(6)}$  than from the other four fermion operators.

### 4.2.3 Majorana Case

Just as in the Dirac case, we define  $\kappa$  as in

$$g_{\epsilon\mu}^\gamma = -\kappa \left(\frac{v}{\Lambda}\right)^3 C_k^7 \quad (4.31)$$

and we give in Table 4.5 the  $\kappa$  corresponding to the various dimension seven operators. Since seven dimension operators contribute to  $g_{\epsilon\mu}^\gamma$ ,  $g_{\epsilon\mu}^\gamma$  is proportional to  $(\frac{v}{\Lambda})^3$ . We notice that  $\mathcal{O}_{L2,2B,12}^{(7)}$  ( $\mathcal{O}_{L2,1B,21}^{(7)}$ ) only contributes to  $g_{RL}^T$  ( $g_{LR}^T$ ) due to a special flavor structure for Majorana neutrinos. Let take  $\mathcal{O}_{L2,2B,12}^{(7)}$  as an example to illustrate this

$$\begin{aligned} \mathcal{O}_{L2,2B,12}^{(7)} &= \epsilon^{ij} \epsilon^{km} (\overline{L^{2c}}_i L_k^B) (\overline{l_R^1} L_j^2) \phi_m \\ &\xrightarrow{\text{After SSB}} \frac{v}{\sqrt{2}} (\overline{\nu_L^{\mu c}} \nu_L^B) (\overline{e_R} \mu_L) - \frac{v}{\sqrt{2}} (\overline{\mu_L^c} \nu_L^B) (\overline{e_R} \nu_L^\mu) \end{aligned} \quad (4.32)$$

Table 4.4: Constraints on  $\mu$ -decay couplings  $g_{e\mu}^\gamma$  in the Majorana case. The naturalness bounds are given in units of  $(v/\Lambda)^2 \times (m_\nu/1\text{eV})$  on contributions from  $7D$  muon decay operators based on one-loop mixing with the  $5D$  neutrino mass operators

Source	$ g_{LR}^S $	$ g_{LR}^T $	$ g_{RL}^S $	$ g_{RL}^T $	$ g_{LR}^V $	$ g_{RL}^V $
$O_{L1,21,1B}^{(7)}$	-	-	$1.6 \times 10^{-4}$	-	-	-
$O_{L1,21,2B}^{(7)}$	$8 \times 10^{-7}$	-	-	-	-	-
$O_{L2,2B,11}^{(7)}$	-	-	$4 \times 10^{-5}$	$2 \times 10^{-5}$	-	-
$O_{L2,2B,21}^{(7)}$	$4 \times 10^{-7}$	$2 \times 10^{-7}$	-	-	-	-
$O_{L2,1B,22}^{(7)}$	$2 \times 10^{-7}$	$1 \times 10^{-7}$	-	-	-	-
$O_{L2,1B,12}^{(7)}$	-	-	$8 \times 10^{-5}$	$4 \times 10^{-5}$	-	-
$O_{L2,2B,12}^{(7)}$	-	-	-	None	-	-
$O_{L2,1B,21}^{(7)}$	-	None	-	-	-	-
$O_{\tilde{V},B1}^{(7)}$	-	-	-	-	-	$1.6 \times 10^{-4}$
$O_{\tilde{V},B2}^{(7)}$	-	-	-	-	$8 \times 10^{-7}$	-
Global [40]	0.088	0.025	0.417	0.104	0.036	0.104
Two-loop [44]	$10^{-4}$	$10^{-4}$	$10^{-2}$	$10^{-2}$	$10^{-4}$	$10^{-2}$

Table 4.5: Coefficients  $\kappa$  that relate  $g_{e\mu}^\gamma$  to the dimension six operator coefficients  $C_k^7$

$\kappa$	$g_{LR}^S$	$g_{LR}^T$	$g_{RL}^S$	$g_{RL}^T$	$g_{LR}^V$	$g_{RL}^V$
$C_{L1,21,1B}^7$	-	-	$-\frac{1}{2\sqrt{2}}$	-	-	-
$C_{L1,21,2B}^7$	$\frac{1}{2\sqrt{2}}$	-	-	-	-	-
$C_{L2,2B,11}^7$	-	-	$\frac{1}{4\sqrt{2}}$	$\frac{1}{8\sqrt{2}}$	-	-
$C_{L2,2B,21}^7$	$-\frac{1}{4\sqrt{2}}$	$-\frac{1}{8\sqrt{2}}$	-	-	-	-
$C_{L2,1B,22}^7$	$\frac{1}{4\sqrt{2}}$	$-\frac{1}{8\sqrt{2}}$	-	-	-	-
$C_{L2,1B,12}^7$	-	-	$-\frac{1}{4\sqrt{2}}$	$\frac{1}{8\sqrt{2}}$	-	-
$C_{L2,2B,12}^7$	-	-	-	$-\frac{1}{8\sqrt{2}}$	-	-
$C_{L2,1B,21}^7$	-	$\frac{1}{8\sqrt{2}}$	-	-	-	-
$C_{\tilde{V},B1}^7$	-	-	-	-	-	$\frac{1}{2\sqrt{2}}$
$C_{\tilde{V},B2}^7$	-	-	-	-	$\frac{1}{2\sqrt{2}}$	-

$$\begin{aligned}
&= -\frac{1}{2} \frac{v}{\sqrt{2}} (\overline{\nu_L^{\mu c}} \mu_L) (\overline{e_R} \nu_L^B) - \frac{1}{4} \frac{v}{\sqrt{2}} (\overline{\nu_L^{\mu c}} \frac{\sigma^{\mu\nu}}{\sqrt{2}} \mu_L) (\overline{e_R} \frac{\sigma_{\mu\nu}}{\sqrt{2}} \nu_L^B) \\
&+ \frac{1}{2} \frac{v}{\sqrt{2}} (\overline{\mu_L^c} \nu_L^\mu) (\overline{e_R} \nu_L^B) + \frac{1}{4} \frac{v}{\sqrt{2}} (\overline{\mu_L^c} \frac{\sigma^{\mu\nu}}{\sqrt{2}} \nu_L^\mu) (\overline{e_R} \frac{\sigma_{\mu\nu}}{\sqrt{2}} \nu_L^B)
\end{aligned}$$

where we perform a Fierz transformation in the third and fourth lines. For Majorana particles  $\psi$  and  $\chi$ , we have

$$\begin{aligned}
\overline{\psi^c} \chi &= \overline{\chi^c} \psi \\
\overline{\psi^c} \sigma^{\mu\nu} \chi &= -\overline{\chi^c} \sigma^{\mu\nu} \psi.
\end{aligned} \tag{4.33}$$

So Eq. (4.32) becomes

$$\mathcal{O}_{L2,2B,12}^{(7)} \xrightarrow{\text{After SSB}} -\frac{v}{2\sqrt{2}} (\overline{\nu_L^{\mu c}} \frac{\sigma^{\mu\nu}}{\sqrt{2}} \mu_L) (\overline{e_R} \frac{\sigma_{\mu\nu}}{\sqrt{2}} \nu_L^B).$$

We see  $\mathcal{O}_{L2,2B,12}^{(7)}$  indeed only contributes  $g_{RL}^T$ .

We use the entries in Table 4.5 and the estimates in Eq. (3.29) and Eq. (3.30) to obtain the bounds in Table 4.4.

From Table 4.4, we find  $g_{LR,RL}^S$  in the Majorana case are fully constrained, while they are not in the Dirac case, due to  $\mathcal{O}_{F,221D}^{(6)}$  and  $\mathcal{O}_{F,112D}^{(6)}$ . This happens because of Eq. (4.33) for Majorana neutrinos. So the experimental measurements of  $g_{LR,RL}^S$  might give us hints if neutrinos are Dirac or Majorana. If we find  $|g_{LR,RL}^S|$  is greater than the bounds obtained here, it should mean that neutrinos are Dirac ones and contributions to  $\mathcal{O}_M^{(4)}$  from  $\mathcal{O}_{F,221D}^{(6)}$  and  $\mathcal{O}_{F,112D}^{(6)}$  are much more than these from the other four-fermion operators constrained by neutrino mass, which means flavour structure is non-trivial in new physics. And as in the Dirac case,  $g_{LR,RL}^T$  can't be fully bounded by neutrino mass in the Majorana case.

The constraints on the  $g_{LR,RL}^V$  follow from mixing among the  $7D$  operators and Table 4.5. We use in Eq. (3.35) to obtain

$$g_{LR}^V \lesssim \left( \frac{m_\nu^{2D}}{m_\mu} \right) \left( \frac{8\pi \sin^2 \theta_W}{9} \right) \left( \alpha - \frac{\lambda \sin^2 \theta_W}{3\pi} \right)^{-1} \left( \ln \frac{v}{\Lambda} \right)^{-1}. \tag{4.34}$$

which is the same as in the Dirac case. A similar expression holds for  $g_{RL}^V$ , but with

$m_\mu \rightarrow m_e$  and  $m_\nu^{2D} \rightarrow m_\nu^{1D}$ . We again have

$$|g_{LR}^V| \lesssim \left( \frac{m_\nu^{2D}}{1 \text{ eV}} \right) \left( \ln \frac{\Lambda}{v} \right)^{-1} \begin{cases} 1.2 \times 10^{-6}, & m_H = 114 \text{ GeV} \\ 7.5 \times 10^{-6}, & m_H = 186 \text{ GeV} \end{cases} \quad (4.35)$$

$$|g_{RL}^V| \lesssim \left( \frac{m_\nu^{1D}}{1 \text{ eV}} \right) \left( \ln \frac{\Lambda}{v} \right)^{-1} \begin{cases} 2.5 \times 10^{-4}, & m_H = 114 \text{ GeV} \\ 1.5 \times 10^{-3}, & m_H = 186 \text{ GeV} \end{cases} \quad (4.36)$$

The constraints on  $|g_{LR}^V|$  and  $|g_{RL}^V|$  from the  $7D$  neutrino mass operator in the Majorana case is the same as constraints from the  $6D$  neutrino mass operator. What is more, constraints on  $g_{e\mu}^\gamma$  from  $\mathcal{O}_M^{(5)}$  are the same order as ones from  $\mathcal{O}_M^{(4)}$ .

#### 4.2.4 Constraints from Experiments

Finally, we note that one may use a combination of neutrino mass and direct studies of the Michel spectrum to derive bounds on a subset of the Michel parameters that are more stringent than one obtains from  $\mu$ -decay experiments alone. To illustrate, we consider the parameters  $\delta$  and  $\alpha$ , for which one has

$$\frac{3}{4} - \rho = \frac{3}{4} |g_{LR}^V|^2 + \frac{3}{2} |g_{LR}^T|^2 + \frac{3}{4} \text{Re} (g_{LR}^S g_{LR}^{T*}) + (L \leftrightarrow R) \quad (4.37)$$

$$\alpha = 8 \text{Re} \{ g_{RL}^V (g_{LR}^{S*} + 6g_{LR}^{T*}) + (L \leftrightarrow R) \} \quad . \quad (4.38)$$

If neutrinos are Dirac particles (Majorana particles), from Table 4.2 (Table 4.4), we observe that the magnitudes of the  $g_{LR,RL}^V$  contributions to  $\rho$  and  $\alpha$  are constrained to be several orders of magnitude below the current experimental sensitivities, whereas the contributions  $g_{LR,RL}^{S,T}$  that arise from  $\mathcal{O}_{F,112D}^{(6)}$  and  $\mathcal{O}_{F,221D}^{(6)}$  ( $g_{LR,RL}^T$  that arise from  $\mathcal{O}_{L2,2B,12}^{(7)}$  and  $\mathcal{O}_{L2,1B,21}^{(7)}$ ) are only directly constrained by experiment. Thus, we may use the current experimental results for  $\rho$  to constrain the operator coefficients  $C_{F,112D}^6$  and  $C_{F,221D}^6$  ( $C_{L2,2B,12}^{(7)}$  and  $C_{L2,1B,21}^{(7)}$ ) and subsequently employ the results—together with the  $m_\nu$  bounds on the  $g_{LR,RL}^V$ —to derive expectations for the magnitude of  $\alpha$ . For simplicity, we consider only the contributions from  $C_{F,112D}^6$  to  $\rho$  in the Dirac case. We think the same results hold for Majorana case because of similarities between the constraints from the Dirac case and those from the Majorana case. Using the current experimental uncertainty in this parameter, we

find

$$|C_{F,112D}^6| \left(\frac{v}{\Lambda}\right)^2 \leq 0.1. \quad (4.39)$$

In the parameter  $\alpha$ , this coefficient interferes with  $C_{\tilde{V},1D}^6$ :

$$\alpha = -6 \left(\frac{v}{\Lambda}\right)^4 \text{Re} \left( C_{\tilde{V},1D}^6 C_{F,112D}^{6*} + \dots \right), \quad (4.40)$$

where the " $+\dots$ " indicates contributions from the other coefficients that we will assume to be zero for purposes of this discussion. From Eq. (4.39) and the  $m_\nu$  limits on  $C_{\tilde{V},1D}^6$  we obtain

$$|\alpha| \leq 2 \times 10^{-4} \left(\frac{v}{\Lambda}\right)^2 \left(\frac{m_\nu^{1D}}{1 \text{ eV}}\right). \quad (4.41)$$

For  $\Lambda = v$ , this expectation for  $|\alpha|$  is more than two orders of magnitude below the present experimental sensitivity and will fall rapidly as  $\Lambda$  increases from  $v$ . A similar line of reasoning can be used to constrain the parameter  $\alpha'$  in terms of  $m_\nu$  and the CP-violating phases that may enter the effective operator coefficients.

## 4.3 Implications for Beta Decay Parameters

### 4.3.1 Introduction

Precision studies of nuclear and neutron beta decay, which once played an important role in the developments of the Standard Model, have been used to test the SM and look for the physics beyond it. Measurements of various correlation coefficients provide constraints on the deviations from what the SM predicts. Several experiments have been carried out to measure the correlation coefficients with improved precision. The abBA collaboration will make it possible to measure the correlations  $a$ ,  $b$ ,  $A$ , and  $B$  with precision of approximately  $10^{-4}$ , using a pulsed cold neutron beam at the SNS in OAK Ridge. The WITCH (Weak Interaction Trap for CHarged particles) experiment[39] aims to measure the recoil energy spectrum of the daughter ions from  $\beta$ -decay with a precision on  $a$  of about 0.5% or better. It will be used to search for both scalar and tensor weak interaction types.

In analogy with the effective four fermion Lagrangian for  $\mu$ -decay, we use (as in [43])

$$\mathcal{L}^{\beta\text{-decay}} = -\frac{4G_\mu}{\sqrt{2}} \sum_{\gamma,\epsilon,\delta} a_{\epsilon\delta}^\gamma \bar{e}_\epsilon \Gamma^\gamma \nu_e \bar{u} \Gamma_\gamma d_\delta \quad (4.42)$$

where  $\nu_R$  is substituted by  $\nu_L^c$  in the Majorana case. In SM, one has  $a_{LL}^V = V_{ud}$ , the (1,1) element of the Cabibbo-Kobayashi-Maskawa (CKM) matrix, and all other  $a_{e\delta}^\gamma = 0$ . In the literature, there exist several equivalent parameterizations of non-Standard-Model contributions to light quark  $\beta$ -decay [46, 52]. Theoretically, the couplings  $a_{e\delta}^\gamma$  can be generated in various models beyond the SM. The left-right symmetric model, the exotic fermions, and the leptoquark exchange and the limits that they put on the couplings are discussed in [46].

Besides neutrino mass constraints, we also find that  $a_{LL}^S$ ,  $a_{LR}^S$ ,  $a_{LR}^T$ , and  $a_{RL}^V$  can also be constrained by the unitarity of the Cabibbo-Kobayashi-Maskawa (CKM) matrix,  $R_{e/\mu} = \frac{\Gamma(\pi^+ \rightarrow e^+ \nu_e + \pi^+ \rightarrow e^+ \nu_e \gamma)}{\Gamma(\pi^+ \rightarrow \mu^+ \nu_\mu + \pi^+ \rightarrow \mu^+ \nu_\mu \gamma)}$ , and pion beta decay ( $\pi_\beta$ ), which can constrain other  $a_{e\delta}^\gamma$  as well. In fact, constraints on  $a_{LR,LL}^V$ ,  $a_{RL,RR}^S$ , and  $a_{RL}^T$  by CKM unitarity and  $R_{e/\mu}$  are discussed in [46]. In our paper, special attention goes to constraints on  $a_{LL}^S$ ,  $a_{LR}^S$ ,  $a_{LR}^T$ , and  $a_{RL}^V$  that involve the right-handed (RH) neutrino. Since no RH neutrino exists in SM, there is no interference between the amplitudes from SM and the ones with RH neutrino. So the new physics' contributions to  $\beta$ -decay's correlation coefficients are much more sensitive to  $a_{RL,RR}^S$ ,  $a_{RL}^T$ , and  $a_{LR,LL}^V$  than to  $a_{LL,LR}^S$ ,  $a_{LR}^T$ , and  $a_{RL}^V$ . The constraints on  $a_{LL,LR}^S$ ,  $a_{LR}^T$ , and  $a_{RL}^V$  could not constrain the correlation coefficients as much as are complementary to their measurements. In this section,  $e$  stands for electron flavor and 1 for the first generation of quarks.

### 4.3.2 Correlation coefficients

The coupling constant  $a_{e\delta}^\gamma$  has to be determined from experiments. The distribution in the electron and neutrino directions and in the electron energy from oriented nuclei is given by [55]

$$\begin{aligned}
\omega(\langle \mathbf{J} \rangle | E_e, \Omega_e, \Omega_\nu) dE_e d\Omega_e d\Omega_\nu = & \\
& \frac{F(\pm Z, E_e)}{(2\pi)^5} p_e E_e (E_0 - E_e)^2 dE_e d\Omega_e d\Omega_\nu \times \\
& \frac{1}{2} \xi \left\{ 1 + a \frac{\mathbf{p}_e \cdot \mathbf{p}_\nu}{E_e E_\nu} + b \frac{m_e}{E_e} \right. \\
& + c \left[ \frac{\mathbf{p}_e \cdot \mathbf{p}_\nu}{3E_e E_\nu} - \frac{(\mathbf{p}_e \cdot \mathbf{j})(\mathbf{p}_\nu \cdot \mathbf{j})}{E_e E_\nu} \right] \left[ \frac{J(J+1) - 3\langle \mathbf{J} \cdot \mathbf{j} \rangle}{J(2J-1)} \right] \\
& \left. + \frac{\mathbf{J}}{J} \cdot \left[ A \frac{\mathbf{p}_e}{E_e} + B \frac{\mathbf{p}_\nu}{E_\nu} + D \frac{\mathbf{p}_e \times \mathbf{p}_\nu}{E_e E_\nu} \right] \right\} \quad (4.43)
\end{aligned}$$

where  $E_e$ ,  $p_e$ , and  $\Omega_e$  denote the total energy, momentum, and angular coordination of the  $\beta$  particle, and similarly for the neutrino;  $\langle \mathbf{J} \rangle$  is the nuclear polarization of the initial nuclear state with spin  $\mathbf{J}$ ;  $\mathbf{j}$  is a unit vector in the direction of  $\mathbf{J}$ ;  $E_0$  is the total energy available in the transition; and  $F(\pm Z, E_e)$  is the Fermi-function. The  $a$ ,  $b$ ,  $c$ ,  $A$ ,  $B$ , etc., are the correlation coefficients that can be related to  $a_{e\delta}^\gamma$ .

Conventionally, people often use the effective  $n \rightarrow pe^- \bar{\nu}$  interaction, which, neglecting the induced form factors, is given by [46]

$$H_\beta^{(N)} \sim H_{V,A}^{(N)} + H_S^{(N)} + H_T^{(N)}, \quad (4.44)$$

$$H_{V,A}^{(N)} = \bar{e} \gamma_\lambda (C_V + C'_V \gamma_5) \nu_e \bar{p} \gamma^\lambda n + \bar{e} \gamma_\lambda \gamma_5 (C_A + C'_A \gamma_5) \nu_e \bar{p} \gamma^\lambda \gamma_5 n + h.c., \quad (4.45)$$

$$H_S^{(N)} = \bar{e} (C_S + C'_S \gamma_5) \nu_e \bar{p} n + h.c., \quad (4.46)$$

$$H_T^{(N)} = \bar{e} \frac{\sigma^{\lambda\mu}}{\sqrt{2}} (C_T + C'_T \gamma_5) \nu_e \bar{p} \frac{\sigma^{\lambda\mu}}{\sqrt{2}} n + h.c., \quad (4.47)$$

where the pseudo-scalar contribution is neglected since this vanishes in the nonrelativistic approximation for the nucleons. The relation between the couplings  $a_{e\delta}^\gamma$  in Eqs. (4.42) and those in Eqs. (4.45–4.47) are given by

$$C_V = \frac{4G_\mu}{\sqrt{2}} g_V (a_{LL}^V + a_{LR}^V + a_{RR}^V + a_{RL}^V) \quad (4.48)$$

$$C'_V = \frac{4G_\mu}{\sqrt{2}} g_V (-a_{LL}^V - a_{LR}^V + a_{RR}^V + a_{RL}^V) \quad (4.49)$$

$$C_A = \frac{4G_\mu}{\sqrt{2}} g_A (a_{LL}^V - a_{LR}^V + a_{RR}^V - a_{RL}^V) \quad (4.50)$$

$$C'_A = \frac{4G_\mu}{\sqrt{2}} g_A (-a_{LL}^V + a_{LR}^V + a_{RR}^V - a_{RL}^V) \quad (4.51)$$

$$C_S = \frac{4G_\mu}{\sqrt{2}} g_S (a_{RL}^S + a_{RR}^S + a_{LR}^S + a_{LL}^S) \quad (4.52)$$

$$C'_S = \frac{4G_\mu}{\sqrt{2}} g_S (-a_{RL}^S - a_{RR}^S + a_{LR}^S + a_{LL}^S) \quad (4.53)$$

$$C_T = \frac{8G_\mu}{\sqrt{2}} g_T (a_{RL}^T + a_{LR}^T) \quad (4.54)$$

$$C'_T = \frac{8G_\mu}{\sqrt{2}} g_T (-a_{RL}^T + a_{LR}^T) \quad (4.55)$$

where the constant  $g_i \equiv g_i(0)$ ,  $i = V, A, S, T$  are defined by

$$\langle p | \bar{u} \Gamma_i d | n \rangle = g_i(q^2) \bar{p} \Gamma_i n \quad q^2 \rightarrow 0. \quad (4.56)$$

If we assume exotic interactions are small—i.e.,  $C_i \ll 1$  and  $C'_i \ll 1$ , with  $i = S, T$ —the Fierz interference term  $b$  and the beta-neutrino correlation coefficient  $a$  can be written as

$$b \simeq \pm \gamma \frac{1}{1 + \rho^2} \left[ \text{Re} \left( \frac{C_S - C'_S}{C_V} \right) + \rho^2 \text{Re} \left( \frac{C_T - C'_T}{C_A} \right) \right] \quad (4.57)$$

$$a \simeq \frac{1 - \rho^2/3}{1 + \rho^2} \left[ -\frac{1}{(1 + \rho^2)^2} \left( 1 + \frac{1}{3} \rho^2 \right) \frac{|C_S|^2 + |C'_S|^2}{|C_V|^2} + \frac{1}{3} \rho^2 (1 - \rho^2) \frac{|C_T|^2 + |C'_T|^2}{|C_A|^2} \right] \quad (4.58)$$

where we ignore the T-odd terms in  $a$  and  $\rho = \frac{C_A M_{GT}}{C_V M_F}$ ,  $\gamma = \sqrt{1 - \alpha^2 Z^2}$ , and  $M_F$  and  $M_{GT}$  are the Fermi and Gamov-Teller matrix elements respectively.

We will see below that neutrino masses would put bounds on  $a_{LL}^S, a_{LR}^S, a_{LR}^T$ , and  $a_{RL}^V$ . From Eqs. (4.50–4.55),  $a_{LL}^S, a_{LR}^S$ , and  $a_{LR}^T$  are related to the  $n \rightarrow pe^{-\bar{\nu}}$  couplings

$$\frac{8G_\mu}{\sqrt{2}} g_S (a_{LR}^S + a_{LL}^S) = C_S + C'_S \quad (4.59)$$

$$\frac{8G_\mu}{\sqrt{2}} g_T a_{LR}^T = C_T + C'_T. \quad (4.60)$$

So our paper will constrain  $(C_S + C'_S)$  and  $(C_T + C'_T)$ . These results are complementary to those from measurements of  $b$ , which are sensitive to  $(C_S - C'_S)$  and  $(C_T - C'_T)$  from Eq. (4.57) and measurements of  $a$ , which are sensitive to  $|C_S|^2 + |C'_S|^2$  and  $|C_T|^2 + |C'_T|^2$  from Eq. (4.58).

### 4.3.3 Dirac Case

#### 4.3.3.1 Effective Hamiltonian Below the Weak Scale

We are going to relate  $C_j^6$  to  $a_{e\mu}^\gamma$ . First, we start with the effective Lagrangian valid below  $\Lambda$  that takes the form

$$L_{eff} = L_4 + \frac{1}{\Lambda^2} L_6 + \dots \quad (4.61)$$

where  $L_n$  is the sum of all the independent dimension  $n$  operators. Specifically  $L_6$  is

$$\begin{aligned} L_6 = & +C_{Q,AD,\alpha\beta}^6(\mu)\mathcal{O}_{Q,AD,\alpha\beta}^{(6)} + C_{d1,AD,\alpha\beta}^6(\mu)\mathcal{O}_{d1,AD,\alpha\beta}^{(6)} \\ & + C_{d2,AD,\alpha\beta}^6(\mu)\mathcal{O}_{d2,AD,\alpha\beta}^{(6)} + C_{\tilde{V},AB}^6(\mu)\mathcal{O}_{\tilde{V},AB}^{(6)} + \dots \end{aligned} \quad (4.62)$$

where we just write down the interesting operators which can contribute to both  $\beta$ -decay and neutrino mass via loop graphs, and  $+\dots$  are other operators. In general the Wilson coefficients are denoted by  $C'$ s, depending on the indices, and  $\mu$  is the renormalization scale. After spontaneous symmetry breaking, all the fermions and  $W, Z$  gauge bosons become massive. The fermions' masses (except top quark) are much smaller than the weak scale. But  $W, Z$  gauge bosons' masses are comparable to the weak scale. So when we evolve  $\mu$  down to the weak scale, massive gauge bosons need to be integrated out. The effective Hamiltonian valid below the weak scale generated by Eq. (4.62) to the leading order in new physics cutoff  $\Lambda$  writes

$$\begin{aligned} -H_{eff}(\mu) = & \frac{a_{AD,\alpha\beta}^{S1}(\mu)}{\Lambda^2} \overline{l}_L^A \nu_R^D \overline{u}_L^\alpha d_R^\beta + \frac{a_{AD,\alpha\beta}^{S2}(\mu)}{\Lambda^2} \overline{l}_L^A \nu_R^D \overline{u}_R^\alpha d_L^\beta \\ & + \frac{a_{AD,\alpha\beta}^{S3}(\mu)}{\Lambda^2} \nu_L^A \nu_R^D \overline{u}_R^\alpha u_L^\beta + \frac{a_{AD,\alpha\beta}^{S4}(\mu)}{\Lambda^2} \nu_L^A \nu_R^D \overline{d}_L^\alpha d_R^\beta \\ & + \frac{a_{AD,\alpha\beta}^{T1}(\mu)}{\Lambda^2} \overline{l}_L^A \frac{\sigma^{\mu\nu}}{\sqrt{2}} \nu_R^D \overline{u}_L^\alpha \frac{\sigma_{\mu\nu}}{\sqrt{2}} d_R^\beta + \frac{a_{AD,\alpha\beta}^{T2}(\mu)}{\Lambda^2} \nu_L^A \frac{\sigma^{\mu\nu}}{\sqrt{2}} \nu_R^D \overline{d}_L^\alpha \frac{\sigma_{\mu\nu}}{\sqrt{2}} d_R^\beta \\ & + \frac{a_{AD,\alpha\beta}^V(\mu)}{\Lambda^2} \overline{l}_R^A \gamma^\mu \nu_R^D \overline{u}_L^\alpha \gamma^\mu d_L^\beta + h.c. + \dots \end{aligned} \quad (4.63)$$

where the boundary conditions for coefficients  $a_{AD,\alpha\beta}^{S1,S2,S3,S4,T1,T2,V}$  at  $v$  are given by

$$\begin{aligned} a_{AD,\alpha\beta}^{S1}(v) &= C_{d2,AD,\alpha\beta}^6(v) + \frac{C_{d1,AD,\alpha\beta}^6(v)}{2} \\ a_{AD,\alpha\beta}^{S2}(v) &= C_{Q,AD,\alpha\beta}^6(v) V_{CKM}^{\gamma\beta} \\ a_{AD,\alpha\beta}^{S3}(v) &= C_{Q,AD,\alpha\beta}^6(v) \\ a_{AD,\alpha\beta}^{S4}(v) &= - \left( C_{d2,AD,\gamma\beta}^6(v) + \frac{C_{d1,AD,\gamma\beta}^6(v)}{2} \right) V^{\gamma\alpha} \\ a_{AD,\alpha\beta}^{T1}(v) &= \frac{C_{d1,AD,\alpha\beta}^6(v)}{4} \end{aligned} \quad (4.64)$$

$$a_{AD,\alpha\beta}^{T2}(v) = -\frac{C_{d1,AD,\gamma\beta}^6(v)V^{\gamma\alpha}}{4}$$

$$a_{AD,\alpha\beta}^v(v) = -C_{\tilde{V},AD}^6(v)V_{CKM}^{\alpha\beta}$$

which is obtained by matching Eq. (4.63) with Eq. (4.62) at the weak scale. In Eq. (4.63), we just write the operators containing  $\nu_R$ , since the ones with  $\nu_L$  won't contribute to neutrino mass or mix with other relevant operators. Among 6D operators in Section 2.3.1, only  $\mathcal{O}_{Q,AD,\alpha\beta}^{(6)}$ ,  $\mathcal{O}_{d1,AD,\alpha\beta}^{(6)}$ ,  $\mathcal{O}_{d2,AD,\alpha\beta}^{(6)}$ , and  $\mathcal{O}_{\tilde{V},AB}^{(6)}$  that contribute to neutrino mass generate the operators containing only one  $\nu_R$  in Eq. (4.63). And  $\dots$  in Eq. (4.63) are generated by  $\dots$  in Eq. (4.62).

We need to evolve  $\mu$  from the weak scale  $v$ , where  $C_{Q,AD,\alpha\beta}^6$ ,  $C_{d1,AD,\alpha\beta}^{(6)}$ ,  $C_{d2,AD,\alpha\beta}^{(6)}$ , and  $C_{\tilde{V},AB}^{(6)}$  can be related to neutrino masses, down to nucleon mass  $m_N$  in order to calculate various semileptonic processes. The evolutions of  $C_{Q,AD,\alpha\beta}^6(\mu)$ ,  $C_{d1,AD,\alpha\beta}^{(6)}(\mu)$ ,  $C_{d2,AD,\alpha\beta}^{(6)}(\mu)$ , and  $C_{\tilde{V},AB}^{(6)}(\mu)$  from  $\Lambda$  to  $v$  were calculated in Chapter 3. The QED running of  $a_{AD,\alpha\beta}^{S1,S2,S3,S4,T1,T2,V}(\mu)$  is ignored, since the correcting due to the running is around  $\frac{\alpha}{4\pi} \ln \frac{v}{m_N} \sim 3 \times 10^{-2}$ , which is negligible when we are only interested in order of magnitudes. We calculate the QCD running of  $a_{AD,\alpha\beta}^{S1\dots S4,T1,T2,V}(\mu)$  by solving the renormalization group equation (RGE) for these coefficients. The RGE for  $a_{AD,\alpha\beta}^{S1\dots S4,T1,T2,V}(\mu)$  is

$$\mu \frac{d}{d\mu} a_i + \sum_k a_k \gamma_{ki}^{QCD} = 0 \quad (4.65)$$

where  $\gamma^{QCD}$  is the anomalous dimension matrix and superscript  $QCD$  reminds us that the renormalization of the operators in Eq. (4.63) are only given by gluon exchanges between the quark fields. A standard calculation gives the following result for  $\gamma^{QCD}$ :

$$\gamma^{QCD} = \frac{\alpha_3}{4\pi} \gamma^{(0)} \equiv \frac{\alpha_3}{4\pi} \begin{pmatrix} 8 & 0 & 0 & 0 & 0 & 0 & 0 \\ 0 & 8 & 0 & 0 & 0 & 0 & 0 \\ 0 & 0 & 8 & 0 & 0 & 0 & 0 \\ 0 & 0 & 0 & 8 & 0 & 0 & 0 \\ 0 & 0 & 0 & 0 & \frac{-8}{3} & 0 & 0 \\ 0 & 0 & 0 & 0 & 0 & \frac{-8}{3} & 0 \\ 0 & 0 & 0 & 0 & 0 & 0 & 0 \end{pmatrix} \quad (4.66)$$

in the basis of  $\{a_{AD,\alpha\beta}^{S1\dots S4}, a_{AD,\alpha\beta}^{T1}, a_{AD,\alpha\beta}^{T2}, a_{AD,\alpha\beta}^V\}$ . Using the renormalization group equation for  $\alpha_3(\mu)$  to the leading term

$$\mu \frac{d\alpha_3}{d\mu} = -2\beta_0 \frac{\alpha_3^2}{4\pi} \quad (4.67)$$

where  $\beta_0 = \frac{11N_c - 2f}{3}$  and  $N_c$  is the number of colors and  $f$  the number of quark flavors, we solve the RGE for  $a_{AD,\alpha\beta}^{S1\dots S4,T1,T2,V}(\mu)$  and have

$$a_{AD,\alpha\beta}^i(\mu) = \left( \frac{\alpha_3(v)}{\alpha_3(\mu)} \right)^{-\frac{\gamma_i^{(0)}}{2\beta_0}} a_{AD,\alpha\beta}^i(v) \quad i = S1 \dots S4, T1, T2, V. \quad (4.68)$$

When  $\mu$  evolves from  $v$  down to  $m_N$ , the top quark, the bottom quark, and the charm quark are integrated out one by one and so  $f = 6 \rightarrow 5 \rightarrow 4 \rightarrow 3$  which implies

$$\begin{aligned} a_{AD,\alpha\beta}^{S1\dots S4}(m_N) &= \left( \frac{\alpha_3(m_c)}{\alpha_3(m_N)} \right)^{-\frac{4}{9}} \left( \frac{\alpha_3(m_b)}{\alpha_3(m_c)} \right)^{-\frac{12}{25}} \\ &\quad \left( \frac{\alpha_3(m_t)}{\alpha_3(m_b)} \right)^{-\frac{12}{23}} \left( \frac{\alpha_3(v)}{\alpha_3(m_t)} \right)^{-\frac{4}{7}} a_{AD,\alpha\beta}^{S1\dots S4}(v) \\ &\equiv K_S a_{AD,\alpha\beta}^{S1\dots S4}(v) \end{aligned} \quad (4.69)$$

$$\begin{aligned} a_{AD,\alpha\beta}^{T1,T2}(m_N) &= \left( \frac{\alpha_3(m_c)}{\alpha_3(m_N)} \right)^{\frac{4}{27}} \left( \frac{\alpha_3(m_b)}{\alpha_3(m_c)} \right)^{\frac{3}{25}} \\ &\quad \left( \frac{\alpha_3(m_t)}{\alpha_3(m_b)} \right)^{\frac{4}{23}} \left( \frac{\alpha_3(v)}{\alpha_3(m_t)} \right)^{\frac{4}{21}} a_{AD,\alpha\beta}^{T1,T2}(v) \\ &\equiv K_T a_{AD,\alpha\beta}^{T1,T2}(v) \end{aligned} \quad (4.70)$$

$$a_{AD,\alpha\beta}^V(m_N) \equiv K_V a_{AD,\alpha\beta}^V(v). \quad (4.71)$$

Using  $\alpha_3(m_Z) = 0.120$  and the 1-loop QCD beta function, we get

$$\begin{aligned} \alpha_3(v) &= 0.105 \\ \alpha_3(m_t) &= 0.110 \\ \alpha_3(m_b) &= 0.212 \\ \alpha_3(m_c) &= 0.338 \\ \alpha_3(m_N) &= 0.378 \end{aligned} \quad (4.72)$$

and

$$\begin{aligned}
K_S &= 1.90 \\
K_T &= 0.81 \\
K_V &= 1.
\end{aligned} \tag{4.73}$$

Comparing Eq. (4.62) with Eq. (4.42), we have

$$\begin{aligned}
|a_{LL}^S| &\sim \left| \frac{a_{eD,11}^{S3}(m_N) v^2}{\Lambda^2} \frac{v^2}{2} \right| \sim \left| K_S \frac{a_{eD,11}^{S3}(v) v^2}{\Lambda^2} \frac{v^2}{2} \right| \\
&\sim \left| K_S \frac{C_{Q,eD,1\gamma}^6(v) V^{\gamma 1} v^2}{\Lambda^2} \frac{v^2}{2} \right| \\
|a_{LR}^S| &\sim \left| \frac{a_{eD,11}^{S1}(m_N) v^2}{\Lambda^2} \frac{v^2}{2} \right| \sim \left| K_S \left( \frac{C_{d2,eD,11}^6(v)}{\Lambda^2} + \frac{C_{d1,eD,11}^6(v)}{2\Lambda^2} \right) \frac{v^2}{2} \right| \\
|a_{LR}^T| &\sim \left| \frac{a_{eD,11}^{T1}(m_N) v^2}{\Lambda^2} \frac{v^2}{2} \right| \sim \left| K_T \frac{C_{d1,eD,11}^6(v) v^2}{4\Lambda^2} \frac{v^2}{2} \right| \\
|a_{RL}^V| &\sim \left| \frac{a_{eD,11}^V(m_N) v^2}{\Lambda^2} \frac{v^2}{2} \right| \sim \left| K_V \frac{C_{\tilde{V},eD}^6(v) V_{ud} v^2}{\Lambda^2} \frac{v^2}{2} \right|.
\end{aligned} \tag{4.74}$$

#### 4.3.3.2 4D Case

If we look closely at Eq. (4.74), it is obvious that  $|a_{LL}^S|$  depends on  $C_{Q,eD,1\gamma}^{(6)}$  and  $|a_{LR}^S|$ , and  $|a_{LR}^T|$  only depends on the diagonal coefficients  $C_{d1,d2,eD,11}^6$ . However, only  $C_{Q,eD,11}^6$  and  $C_{d1,d2,eD,11}^6$  are constrained through Eq. (3.20), and  $C_{Q,eD,1\gamma}^6$  with  $\gamma \neq 1$  are unconstrained. It seems to imply that neutrino mass could put bounds on  $|a_{LR}^S|$  and  $|a_{LR}^T|$  but not on  $|a_{LL}^S|$ . Actually there are some subtleties here. We can just as well carry out the calculations in the basis of  $Q'^\alpha$ ,  $u_R'^\alpha$ , and  $d_R'^\alpha$  defined in Section 2.3 wherein  $f_d$  is diagonal. The operators involving just lepton fields and their corresponding coefficients won't change under the redefinition. So substituting Eq. (3.17–3.19) into Eq. (4.74) and Eq. (3.20) gives us

$$|a_{LL}^S| \sim \left| K_S \frac{C_{Q,eD,11}^{(6)}(v) v^2}{\Lambda^2} \frac{v^2}{2V_{ud}} \right|$$

$$|a_{LR}^S| \sim \left| K_S (V_{CKM})^{1\gamma} \left( \frac{C'_{d2,eD,\gamma 1}(v)}{\Lambda^2} + \frac{C'_{d1,eD,\gamma 1}(v)}{2\Lambda^2} \right) \frac{v^2}{2V_{ud}} \right| \quad (4.75)$$

$$|a_{LR}^T| \sim \left| K_T (V_{CKM})^{1\gamma} \frac{C'_{d1,eD,\gamma 1}(v)}{4\Lambda^2} \frac{v^2}{2V_{ud}} \right|$$

and

$$\begin{aligned} C_{M,AD}^4 &\sim \frac{2N_C}{(4\pi)^2} \frac{m_u^\beta}{v/\sqrt{2}} V^{*\beta\alpha} C'_{Q,AD,\alpha\beta}{}^6 \\ C_{M,AD}^4 &\sim \frac{N_C}{(4\pi)^2} \frac{m_d^\beta}{v/\sqrt{2}} \delta^{\alpha\beta} C'_{d1,AD,\alpha\beta}{}^6 \\ C_{M,AD}^4 &\sim \frac{2N_C}{(4\pi)^2} \frac{m_d^\beta}{v/\sqrt{2}} \delta^{\alpha\beta} C'_{d2,AD,\alpha\beta}{}^6 \end{aligned} \quad (4.76)$$

in terms of new coefficients  $C'_{Q,AD,\alpha\beta}{}^6$ ,  $C'_{d1,AD,\alpha\beta}{}^6$ , and  $C'_{d2,AD,\alpha\beta}{}^6$ .

This time we find that  $|a_{LL}^S|$  is constrained but  $|a_{LR}^S|$  and  $|a_{LR}^T|$  are not, because  $C'_{Q,AD,11}{}^6$  is bounded by neutrino mass and  $C'_{d1,d2,AD,1\gamma}{}^6$  with  $\gamma \neq 1$  is not.

Now we have a contradiction here. What happened? Let us illustrate it with a simple example. Suppose we have a effective Lagragian

$$L_{eff} = C_1 \mathcal{O}_1 + C_2 \mathcal{O}_2 + \dots \quad (4.77)$$

where  $\mathcal{O}_1$  and  $\mathcal{O}_2$  are two independent operators and  $C_1$  and  $C_2$  are their coefficients. And we also assume they both contribute to some mass operator  $\mathcal{O}_M$  through loop effects

$$C_M \sim C_1 A \quad (4.78)$$

$$C_M \sim C_2 A$$

where  $A$  is a constant.

Somehow the operator  $\mathcal{O}_1$  can relate to some observable  $g$ , namely  $g = C_1 B$ , where  $B$  is a constant. It is clear  $g$  can be constrained by  $\mathcal{O}_M$ .

Now we use another basis  $\{\mathcal{O}_+, \mathcal{O}_-\}$  where  $\mathcal{O}_\pm = \frac{1}{2}(\mathcal{O}_1 \pm \mathcal{O}_2)$ . Under this basis the effective Lagragian becomes

$$L_{eff} = C_+ \mathcal{O}_+ + C_- \mathcal{O}_- \quad (4.79)$$

where  $C_\pm = C_1 \pm C_2$ .

$\mathcal{O}_-$  doesn't contribute to  $\mathcal{O}_M$  since  $\mathcal{O}_1$  and  $\mathcal{O}_2$  are assumed to contribute the same amount to  $\mathcal{O}_M$  by assumption. For  $\mathcal{O}_+$  we have  $C_M \sim C_+ A$ . The observable  $g = \frac{C_+ + C_-}{2} B$ . It seems  $g$  is unbounded since  $\mathcal{O}_M$  can't constrain  $C_-$ . With the basis  $\{\mathcal{O}_1, \mathcal{O}_2\}$ , we can separately constrain  $C_i$  because we use no fine-tuning assumption which implies that there is no cancellation between contributions from  $\mathcal{O}_1$  and  $\mathcal{O}_2$ . Therefore, we can put bounds on  $C_-$ . So if we assume there is no fine tuning,  $g$  is also constrained under  $\{\mathcal{O}_+, \mathcal{O}_-\}$ . The same thing happens to  $|a_{LL}^S|$ ,  $|a_{LR}^S|$ , and  $|a_{LR}^T|$ , since there is a relation between  $\mathcal{O}_{Q,d1,d2,AD,\alpha\beta}$  and  $\mathcal{O}'_{Q,d1,d2,AD,\alpha\beta}$  by  $\mathcal{O}_{Q,d1,d2,AD,\alpha\beta} = V_{CKM}^{\alpha\gamma} \mathcal{O}'_{Q,d1,d2,AD,\alpha\beta}$ . So as long as we assume no fine tuning happens,  $|a_{LL}^S|$ ,  $|a_{LR}^S|$ , and  $|a_{LR}^T|$  should be bounded no matter what basis we choose.

So Eq. (3.20) yields

$$\begin{aligned}
|a_{LL}^S| &\sim \left| \frac{a_{eD,11}^{S3}(m_N) v^2}{\Lambda^2} \frac{v^2}{2} \right| \sim \left| K_S \frac{a_{eD,11}^{S3}(v) v^2}{\Lambda^2} \frac{v^2}{2} \right| \\
&\sim \left| K_S \frac{C_{Q,eD,1\gamma}^6(v) V^{\gamma 1} v^2}{\Lambda^2} \frac{v^2}{2} \right| \\
|a_{LR}^S| &\sim \left| \frac{a_{eD,11}^{S1}(m_N) v^2}{\Lambda^2} \frac{v^2}{2} \right| \sim \left| K_S \left( \frac{C_{d2,eD,11}^6(v)}{\Lambda^2} + \frac{C_{d1,eD,11}^6(v)}{2\Lambda^2} \right) \frac{v^2}{2} \right| \quad (4.80) \\
|a_{LR}^T| &\sim \left| \frac{a_{eD,11}^{T1}(m_N) v^2}{\Lambda^2} \frac{v^2}{2} \right| \sim \left| K_T \frac{C_{d1,eD,11}^6(v) v^2}{4\Lambda^2} \frac{v^2}{2} \right| \\
|a_{RL}^V| &\sim \left| \frac{a_{eD,11}^V(m_N) v^2}{\Lambda^2} \frac{v^2}{2} \right| \sim \left| K_V \frac{C_{\tilde{V},eD}^6(v) V_{ud} v^2}{\Lambda^2} \frac{v^2}{2} \right|
\end{aligned}$$

and

$$\begin{aligned}
C_{Q,eD,11}^6 &\lesssim \frac{m_\nu (4\pi)^2}{m_u 2N_C} \Rightarrow |a_{LL}^S| \lesssim \frac{4\pi^2 m_\nu}{N_C m_u} K_S \left( \frac{v^2}{\Lambda^2} \right) \sim 5 \times 10^{-6} \frac{v^2}{\Lambda^2} \frac{m_\nu}{1 \text{ eV}} \quad (4.81) \\
C_{d1,eD,11}^6 &\lesssim \frac{(4\pi)^2 m_\nu}{N_C m_d V^{ud}} \Rightarrow \begin{cases} |a_{LR}^S| \lesssim \frac{8\pi^2 m_\nu}{N_C m_d} K_S \left( \frac{v^2}{\Lambda^2} \right) \sim 1.2 \times 10^{-5} \frac{v^2}{\Lambda^2} \frac{m_\nu}{1 \text{ eV}} \\ |a_{LR}^T| \lesssim \frac{2\pi^2 m_\nu}{N_C m_d} K_T \left( \frac{v^2}{\Lambda^2} \right) \sim 3 \times 10^{-6} \frac{v^2}{\Lambda^2} \frac{m_\nu}{1 \text{ eV}} \end{cases} \\
C_{d2,eD,11}^6 &\lesssim \frac{(4\pi)^2 m_\nu}{2N_C m_d V^{ud}} \Rightarrow |a_{LR}^S| \lesssim \frac{2\pi^2 m_\nu}{N_C m_d} K_T \left( \frac{v^2}{\Lambda^2} \right) \sim 3 \times 10^{-6} \frac{v^2}{\Lambda^2} \frac{m_\nu}{1 \text{ eV}} \\
C_{\tilde{V},eD}^6 &\lesssim (4\pi)^2 \frac{m_\nu}{m_e} \Rightarrow |a_{RL}^V| \lesssim 8\pi^2 \frac{m_\nu}{m_e} K_V \left( \frac{v^2}{\Lambda^2} \right) \sim 1.5 \times 10^{-4} \frac{v^2}{\Lambda^2} \frac{m_\nu}{1 \text{ eV}}.
\end{aligned}$$

Table 4.6: Constraints on  $\beta$ -decay couplings  $a_{e\mu}^\gamma$  in the Dirac case. The naturalness bounds are given in units of  $(v/\Lambda)^2 \times (m_\nu/1\text{eV})$  on contributions from  $6D$  beta decay operators based on one-loop mixing with the  $4D$  neutrino mass operators

Source	$ a_{LL}^S $	$ a_{LR}^S $	$ a_{LR}^T $	$ a_{RL}^V $
$O_{Q,eD,11}^{(6)}$	$5 \times 10^{-6}$	-	-	-
$O_{d1,eD,11}^{(6)}$	-	$1.2 \times 10^{-5}$	$3 \times 10^{-6}$	-
$O_{d2,eD,11}^{(6)}$	-	$3 \times 10^{-6}$	-	-
$O_{\bar{\nu},eD}^{(6)}$	-	-	-	$1.5 \times 10^{-4}$

The bounds in Table 4.6 become smaller as  $\Lambda$  increases.

Eqs. (4.59, 4.60) give us the constraints of

$$\begin{aligned} |\tilde{C}_S + \tilde{C}'_S| &\lesssim 4 \times 10^{-6} \\ |\tilde{C}_T + \tilde{C}'_T| &\lesssim 8 \times 10^{-5} \end{aligned} \quad (4.82)$$

where  $\tilde{C}_S \equiv \frac{C_S}{C_V}$ ,  $\tilde{C}'_S \equiv \frac{C'_S}{C_V}$ ,  $\tilde{C}_T \equiv \frac{C_T}{C_A}$ , and  $\tilde{C}'_T \equiv \frac{C'_T}{C_A}$ , and we use  $C_V \sim \frac{4G_\mu}{\sqrt{2}} g_V a_{LL}^{VSM}$  and  $C_A \sim \frac{4G_\mu}{\sqrt{2}} g_S a_{LL}^{VSM}$  approximately, and  $0.25 \lesssim g_S \lesssim 1$  [52] and  $0.6 \lesssim g_T \lesssim 2.3$  [52].

#### 4.3.3.3 $6D$ Case

Due to mixing among  $6D$  operators,  $|a_{RL}^V|$  can be constrained by neutrino mass. We obtain

$$|a_{RL}^V| \lesssim \left(\frac{m_\nu}{m_e}\right) \left(\frac{8\pi \sin^2 \theta_W}{9}\right) \left(\alpha - \frac{\lambda \sin^2 \theta_W}{3\pi}\right)^{-1} \left(\ln \frac{\Lambda}{v}\right)^{-1} \quad (4.83)$$

which is the same as the expression for  $|g_{RL}^V|$  in Section 4.2. so we just repeat it here:

$$|a_{RL}^V| \lesssim \left(\frac{m_\nu}{\text{1eV}}\right) \left(\ln \frac{\Lambda}{v}\right)^{-1} \begin{cases} 2.5 \times 10^{-4} & m_H = 114\text{GeV} \\ 1.5 \times 10^{-3} & m_H = 186\text{GeV}. \end{cases} \quad (4.84)$$

The constraints on  $|a_{RL}^V|$  from the  $4D$  mass operator is comparable to the one obtained from the  $6D$  mass operator.

### 4.3.4 Majorana Case

We carry out the same analysis in Section 4.3.3.1 and find relations between  $a_{e\delta}^\gamma$  and  $C_i^7$  as follow:

$$\begin{aligned}
\mathcal{O}_{d2,eB,11}^{(7)} &\rightarrow a_{LR}^S \sim -\frac{v^3}{2\sqrt{2}\Lambda^3 V_{ud}} K_S C_{d2,eB,11}^7(v) \\
\mathcal{O}_{d1,e1,1e}^{(7)} &\rightarrow a_{LR}^T \sim -\frac{v^3}{4\sqrt{2}\Lambda^3 V_{ud}} K_T C_{d1,e1,1e}^7(v) \\
\mathcal{O}_{d1,e1,1B}^{(7)} &\rightarrow \begin{cases} a_{LR}^S \sim \frac{v^3}{4\sqrt{2}\Lambda^3 V_{ud}} K_S C_{d1,e1,1B}^7(v) \\ a_{LR}^T \sim \frac{v^3}{8\sqrt{2}\Lambda^3 V_{ud}} K_T C_{d1,e1,1B}^7(v) \end{cases} \quad e \neq B \\
\mathcal{O}_{d1,B1,1e}^{(7)} &\rightarrow \begin{cases} a_{LR}^S \sim \frac{v^3}{4\sqrt{2}\Lambda^3 V_{ud}} K_S C_{d1,B1,1e}^7(v) \\ a_{LR}^T \sim \frac{-v^3}{8\sqrt{2}\Lambda^3 V_{ud}} K_T C_{d1,B1,1e}^7(v) \end{cases} \quad e \neq B \quad (4.85) \\
\mathcal{O}_{d2,e1,1B}^{(7)} &\rightarrow \begin{cases} a_{LR}^S \sim \frac{v^3}{4\sqrt{2}\Lambda^3 V_{ud}} K_S C_{d2,e1,1B}^7(v) \\ a_{LR}^T \sim \frac{v^3}{8\sqrt{2}\Lambda^3 V_{ud}} K_T C_{d2,e1,1B}^7(v) \end{cases} \\
\mathcal{O}_{d2,B1,1e}^{(7)} &\rightarrow \begin{cases} g_{LR}^S \sim \frac{v^3}{4\sqrt{2}\Lambda^3 V_{ud}} K_S C_{d2,B1,1e}^7(v) \\ g_{LR}^T \sim \frac{-v^3}{8\sqrt{2}\Lambda^3 V_{ud}} K_T C_{d2,B1,1e}^7(v) \end{cases} \\
\mathcal{O}_{u1,eB,\alpha 1}^{(7)} &\rightarrow a_{LL}^S \sim \frac{-v^3}{2\sqrt{2}\Lambda^3 V_{ud}} V^{*1\alpha} K_S C_{u1,eB,\alpha 1}^7(v) \quad e \neq B \\
\mathcal{O}_{u1,Be,\alpha 1}^{(7)} &\rightarrow a_{LL}^S \sim \frac{v^3}{2\sqrt{2}\Lambda^3 V_{ud}} V^{*1\alpha} K_S C_{u1,Be,\alpha 1}^7(v) \quad e \neq B \\
\mathcal{O}_{u2,eB,\alpha 1}^{(7)} &\rightarrow a_{LL}^S \sim \frac{v^3}{2\sqrt{2}\Lambda^3 V_{ud}} V^{*1\alpha} K_S C_{u2,eB,\alpha 1}^7(v) \\
\mathcal{O}_{R,Ae,11}^{(7)} &\rightarrow a_{RR}^V \sim \frac{v^3}{2\sqrt{2}\Lambda^3 V_{ud}} K_V C_{R,Ae,11}^7(v) \\
\mathcal{O}_{\tilde{V},Ae}^{(7)} &\rightarrow a_{RL}^V \sim \frac{v^3}{2\sqrt{2}\Lambda^3} K_V C_{\tilde{V},Ae}^7(v)
\end{aligned}$$

where we see some operators vanish with  $e = B$  due to the flavor structure of Majorana neutrinos, in which case the neutrinos in beta decay are not electron neutrinos.

Matching the above operators with  $\mathcal{O}_M^{(5)}$ , we find only some of them can contribute to  $\mathcal{O}_M^{(5)}$  using Eq. (3.31)

$$\mathcal{O}_{d2,eB,11}^{(7)} \rightarrow C_{M,eB}^5 \sim \frac{f_d^{11} N_C}{8\pi^2} C_{d2,eB,11}^7$$

Table 4.7: Constraints on  $\beta$ -decay couplings  $a_{\epsilon\mu}^\gamma$  in the Majorana case. Naturalness bounds are given in units of  $(v/\Lambda)^2 \times (m_\nu/1\text{eV})$  on contributions from  $7D$  beta decay operators based on one-loop mixing with the  $5D$  neutrino

Source	$ a_{LL}^S $	$ a_{LR}^S $	$ a_{LR}^T $	$ a_{RL}^V $
$O_{d1,B1,1e}^{(7)}$	-	None	-	-
$O_{d1,e1,1e}^{(7)}$	-	None	None	-
$O_{d1,e1,1B}^{(7)}$	-	None	None	-
$O_{d2,eB,11}^{(7)}$	-	$6 \times 10^{-6}$	$3 \times 10^{-6}$	-
$O_{d2,e1,1B}^{(7)}$	-	$6 \times 10^{-6}$	$3 \times 10^{-6}$	-
$O_{d2,B1,1e}^{(7)}$	-	$6 \times 10^{-6}$	$3 \times 10^{-6}$	-
$O_{u1,eB,\alpha1}^{(7)}$	None	-	-	-
$O_{u1,Be,\alpha1}^{(7)}$	None	-	-	-
$O_{u2,eB,\alpha1}^{(7)}$	$5 \times 10^{-6}$	-	-	-
$O_{\tilde{V},Ae}^{(7)}$				$1.5 \times 10^{-4}$

$$\begin{aligned}
\mathcal{O}_{d2,e1,1B}^{(7)} &\rightarrow C_{M,eB}^{(5)} \sim \frac{f_d^{11} N_C}{16\pi^2} C_{d2,e1,1B}^{(7)} \\
\mathcal{O}_{d2,B1,1e}^{(7)} &\rightarrow C_{M,eB}^{(5)} \sim \frac{f_d^{11} N_C}{16\pi^2} C_{d2,B1,1e}^{(7)} \\
\mathcal{O}_{u2,eB;\alpha1}^{(7)} &\rightarrow C_{M,eB}^{(5)} \sim \frac{f_u^{\alpha1*} N_C}{8\pi^2} C_{u2,eB;\alpha1}^{(7)} \\
\mathcal{O}_{\tilde{V},Ae}^{(7)} &\rightarrow C_{M,Ae}^{(5)} \sim \frac{f_e^{AA} N_C}{16\pi^2} C_{\tilde{V},Ae}^{(7)}.
\end{aligned} \tag{4.86}$$

The graphs of  $\mathcal{O}_{d1,u1}^{(7)}$  with Yukawa interaction inserted in the loop turn out to be proportional to  $\epsilon_{ij}\phi^i\phi^j$ , which is zero. We use the estimates in Eq. (3.20) to obtain the bounds in Table 4.7. We still assume there is no fine-tuning.

Consequently, the magnitudes of  $a_{LR}^S$ ,  $a_{LR}^T$ , and  $a_{LL}^S$  are not directly bounded by  $m_\nu$  and naturalness considerations, as indicated in Table 4.7. From a theoretical standpoint, one might expect the magnitudes of  $C_{d1}^7$  and  $C_{u1}^7$  to be comparable to those of the other four-fermion operator coefficients in models that are consistent with the scale of neutrino mass. Nevertheless, we cannot *a priori* rule out order of magnitude or more differences between operator coefficients. In contrast, the magnitudes of  $a_{LR}^S$ ,  $a_{LR}^T$ , and  $a_{LL}^S$  are bounded by  $m_\nu$  in the absence of fine-tuning. An implication is that if the magnitudes of  $a_{LR}^S$ ,  $a_{LR}^T$ ,

and  $a_{LL}^S$  greater than our bounds were measured, they would indicate that neutrinos are Dirac fermions, rather than Majorana ones. It also gives evidence that flavor structure is non-trivial in new physics. Using Eqs. (4.59, 4.60), we arrive to the same the constraints as Dirac case

$$\begin{aligned} \left| \tilde{C}_S + \tilde{C}'_S \right| &\lesssim 4 \times 10^{-6} \\ \left| \tilde{C}_T + \tilde{C}'_T \right| &\lesssim 8 \times 10^{-5} \end{aligned} \quad (4.87)$$

### 4.3.5 Status of Experiments

The current experiment limits on scalar and tensor couplings in  $\beta$ -decay usually comes from the Fierz interaction term  $b$  or from the  $\beta - \nu$  correlation coefficient  $a$ . The Fierz interaction term  $b$  always constrains the term  $\left| \tilde{C}_S - \tilde{C}'_S \right|$  or  $\left| \tilde{C}_T - \tilde{C}'_T \right|$ . The recent analysis yields  $\left| \tilde{C}_S - \tilde{C}'_S \right| < 0.0044$  (90% C.L.) [60] and  $\tilde{C}_T - \tilde{C}'_T = -(1.5 \pm 12) \times 10^{-3}$  [61]. These results are complementary to our analysis. The  $\beta - \nu$  correlation coefficient  $a$  depends quadratically on the scalar and tensor couplings. The scalar couplings were studied by measuring the beta-neutrino correlation coefficient  $a$  in the superallowed pure Fermi  $\beta$  transition  $^{18}\text{Ne}(0^+) \rightarrow ^{18}\text{F}(0^+, 1040\text{keV})$  ( $T_{1/2} = 1.67\text{s}$ ) [62]. It yielded the limit  $\sqrt{\left| \tilde{C}_S \right|^2 + \left| \tilde{C}'_S \right|^2} < 0.29$  (95% C.L.) for the scalar coupling constant. A recent experiment was carried out at ISOLDE to measure the positron-neutrino correlation in the  $0^+ \rightarrow 0^+$   $\beta$ -decay of  $^{32}\text{Ar}$  [63]. Combined with the results from [64], it gives us  $\left| \tilde{C}_S \right|^2 < 3.6 \times 10^{-3}$  and  $\left| \tilde{C}'_S \right|^2 < 3.6 \times 10^{-3}$ , which means  $\left| \tilde{C}_S + \tilde{C}'_S \right| < 10^{-1}$ . The present limit on the tensor couplings is obtained by determining the  $\beta - \nu$  correlation coefficient in the decay of  $^6\text{He}$  [65], which is a pure GT transition and is thus sensitive to the tensor couplings. It gives us  $\frac{|C_T|^2 + |C'_T|^2}{|C_A|^2 + |C'_A|^2} < 0.8\%$  (68% C.L.), which implies  $\left| \tilde{C}_T + \tilde{C}'_T \right| < 1.6 \times 10^{-1}$ . Recently, a comprehensive analysis of experimental data was carried out in [52]. The general fit with seven free real parameters in [52] results in the following 95.5% C.L. limits

$$\begin{aligned} \left| \tilde{C}_S \right| &< 0.070, \quad \left| \tilde{C}'_S \right| < 0.067, \\ \left| \tilde{C}_T \right| &< 0.090, \quad \left| \tilde{C}'_T \right| < 0.089. \end{aligned} \quad (4.88)$$

Our constraints are more stringent by one or two orders of magnitude and are compared

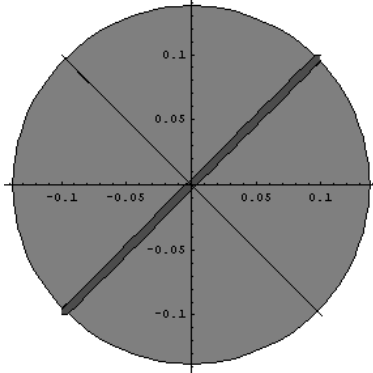


Figure 4.2: Constraints on  $\tilde{C}_S = C_S/C_V$  and  $\tilde{C}'_S = C'_S/C_V$ . The narrow diagonal band at  $-45^\circ$  is from this work. The gray circle is a 95% C.L. limit from Ref. [62]. The diagonal band at  $45^\circ$  is a 90% C.L. limit from Ref. [60]

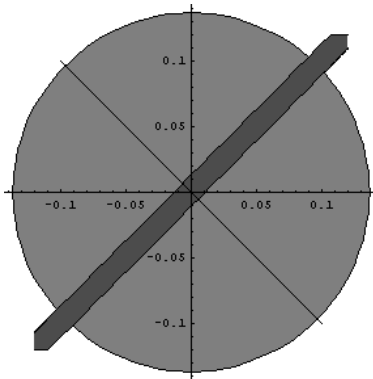


Figure 4.3: Constraints on  $\tilde{C}_T = C_T/C_A$  and  $\tilde{C}'_T = C'_T/C_A$ . The diagonal band at  $-45^\circ$  is from this work. The gray circle is a 68% C.L. limit from Ref. [65]. The diagonal band at  $45^\circ$  is a 90% C.L. limit from Ref. [61]

with the existing limits in Fig. 4.2 and Fig. 4.3 where it is seen that they are complimentary to the existing limits. Combining our results with the existing limits yields

$$|\tilde{C}_S| \lesssim 2 \times 10^{-3}, |\tilde{C}'_S| \lesssim 2 \times 10^{-3},$$

$$|\tilde{C}_T| \lesssim 6 \times 10^{-3}, |\tilde{C}'_T| \lesssim 6 \times 10^{-3}.$$

#### 4.3.6 Constraints From CKM Unitarity, $R_{e/\mu}$ , and $\pi_\beta$

Besides neutrino mass constraints, we also find that  $a_{LL}^S$ ,  $a_{LR}^S$ ,  $a_{LR}^T$ , and  $a_{RL}^V$  can also be constrained by the unitarity of the Cabibbo-Kobayashi-Maskawa (CKM) matrix,  $R_{e/\mu} =$

Table 4.8: Constraints on  $\beta$ -decay couplings  $a_{e\mu}^\gamma$ 

	$ a_{LL}^S $	$ a_{LR}^S $	$ a_{LR}^T $	$ a_{RL}^V $
Neutrino Mass	$5 \times 10^{-6}$	$1.2 \times 10^{-5}$	$10^{-6}$	$10^{-3} \sim 10^{-4}$
CKM Unitarity	0.066	0.066	0.031	0.021
$R_{e/\mu}$	$2 \times 10^{-5}$	$2 \times 10^{-5}$	$1 \times 10^{-3}$	$5 \times 10^{-2}$
$\pi_\beta$	0.13	0.13	-	0.13
Two-loop[51]	$10^{-4}$	$10^{-4}$	$10^{-4}$	$10^{-3}$
Current Limits[52][46]	-	-	-	$3.7 \times 10^{-2}$

$\frac{\Gamma(\pi^+ \rightarrow e^+ \nu_e + \pi^+ \rightarrow e^+ \nu_e \gamma)}{\Gamma(\pi^+ \rightarrow \mu^+ \nu_\mu + \pi^+ \rightarrow \mu^+ \nu_\mu \gamma)}$ , and pion beta decay ( $\pi_\beta$ ), which can constrain other  $a_{e\delta}^\gamma$  as well.

In fact, constraints on  $a_{LR,LL}^V$ ,  $a_{RL,RR}^S$ , and  $a_{RL}^T$  by CKM unitarity and  $R_{e/\mu}$  are discussed in [46]. In our paper, special attention goes to constraints on  $a_{LL}^S$ ,  $a_{LR}^S$ ,  $a_{LR}^T$ , and  $a_{RL}^V$  that involve the right-handed (RH) neutrino. Our analysis could apply to both Dirac and Majorana cases. Our results are summarized in Table 4.8.

#### 4.3.6.1 CKM Unitarity

The Cabibbo-Kobayashi-Maskawa matrix relates the quark eigenstates of the weak interaction with the quark mass eigenstates and therefore it is unitary. The test of CKM matrix unitarity, specially the first row relation

$$|V_{ud}|^2 + |V_{us}|^2 + |V_{ub}|^2 = 1, \quad (4.89)$$

would give us a hint of new physics. For example, the author of [72] discussed its implications for R-parity violating (RPV) extensions of the minimal supersymmetric Standard Model. The most precise determination of  $|V_{ud}|$  comes from the study of superallowed  $0^+ \rightarrow 0^+$  nuclear beta decays. Taking the average of the nine most precise determinations yields [67]

$$|V_{ud}|_{EX} = 0.97377 \pm 0.00027. \quad (4.90)$$

The precise value of  $|V_{us}|^2$  is somewhat controversial. The Particle Data Group 2005 (PDG05) [68] recommended for  $V_{us}$  only the value determined from Ke3 decay,

$$|V_{us}|_{EX} = 0.2200 \pm 0.0026 \quad \text{PDG05}, \quad (4.91)$$

ignoring the value obtained from hyperon decays due to large theoretical uncertainties. However, recent measurements of  $K \rightarrow \pi e \nu$  branching ratio [67] yields a different value for  $|V_{us}|$  than previous PDG averages

$$|V_{us}|_{EX} = 0.2257 \pm 0.0021 \quad \text{PDG06.} \quad (4.92)$$

As for  $V_{ub}$ , its value is small,  $|V_{ub}|^2 \sim 1 \times 10^{-5}$ , and consequently it has a negligible impact on the unitarity test, Eq. (4.89). We follow the notations in [72] and then one has

$$\frac{|V_{ud}|_{EX}^2 - |V_{ud}|_{SM}^2}{|V_{ud}|_{SM}^2} = \begin{cases} -0.0035 \pm 0.0017 & \text{PDG05} \\ -0.0008 \pm 0.0015 & \text{PDG06} \end{cases}, \quad (4.93)$$

where  $|V_{ud}|_{SM}$  denotes the value implied by CKM unitarity. We note  $|V_{ud}|_{EX}$  from PDG05 deviates from the Standard Model predictions by  $2\sigma$ , while  $|V_{ud}|_{EX}$  from PDG06 is consistent with the Standard Model predictions.

In order to constrain the effects of new physics in  $\beta$ -decay, we can define effective Fermi constants as in [72]

$$G_F^\beta = G_\mu |V_{ud}| (1 - \Delta r_\mu + \Delta r_\beta - \Delta_\mu + \Delta_\beta) \quad (4.94)$$

where  $\Delta r_\beta$  and  $\Delta r_\mu$  denote the appropriate SM radiative corrections to the tree-level  $\beta$ -decay and  $\mu$ -decay, respectively, and where  $\Delta_\beta$  and  $\Delta_\mu$  denote the new physics correction to tree-level SM  $\beta$ -decay and  $\mu$ -decay amplitude.  $G_\beta$  can be related to Eq. (4.93) by

$$\frac{G_F^{\beta 2}}{G_F^{\beta, SM 2}} - 1 = \frac{|V_{ud}|_{EX}^2 - |V_{ud}|_{SM}^2}{|V_{ud}|_{SM}^2} \sim 2\Delta_\beta - 2\Delta_\mu \quad (4.95)$$

where the SM values are computed using  $\Delta r_\mu = \Delta r_\beta = 0$ . Analogous to  $\mu$ -decay, Eq. (4.44) can be rewritten as

$$\mathcal{H}^{\beta\text{-decay}} = \frac{4G_\mu}{\sqrt{2}} \sum_{\gamma, \epsilon, \delta} \tilde{a}_{\epsilon\delta}^\gamma \bar{e}_\epsilon \Gamma^\gamma \nu_e \bar{p} \Gamma_\gamma n_\delta \quad (4.96)$$

where

$$\begin{aligned} \tilde{a}_{\epsilon L}^V &= \left( \frac{g_V + g_A}{2} \right) a_{\epsilon L}^V + \left( \frac{g_V - g_A}{2} \right) a_{\epsilon R}^V \\ \tilde{a}_{\epsilon R}^V &= \left( \frac{g_V - g_A}{2} \right) a_{\epsilon L}^V + \left( \frac{g_V + g_A}{2} \right) a_{\epsilon R}^V \end{aligned}$$

$$\begin{aligned}
\tilde{a}_{\epsilon L}^S &= \frac{g_S}{2} a_{\epsilon L}^S + \frac{g_S}{2} a_{\epsilon R}^S \\
\tilde{a}_{\epsilon R}^S &= \frac{g_S}{2} a_{\epsilon L}^S + \frac{g_S}{2} a_{\epsilon R}^S \\
\tilde{a}_{\epsilon L}^T &= \frac{g_T}{2} a_{\epsilon L}^T + \frac{g_T}{2} a_{\epsilon R}^T \\
\tilde{a}_{\epsilon R}^T &= \frac{g_T}{2} a_{\epsilon L}^T + \frac{g_T}{2} a_{\epsilon R}^T.
\end{aligned} \tag{4.97}$$

We find

$$\begin{aligned}
\Delta_\beta &= |\tilde{a}_{RR}^V|^2 + |\tilde{a}_{LR}^V|^2 + |\tilde{a}_{RL}^V|^2 + |\tilde{a}_{LL}^V|^2 \\
&+ 4 \left( |\tilde{a}_{RR}^S|^2 + |\tilde{a}_{LR}^S|^2 + |\tilde{a}_{RL}^S|^2 + |\tilde{a}_{LL}^S|^2 \right) \\
&+ 3 \left( |\tilde{a}_{RL}^T|^2 + |\tilde{a}_{LR}^T|^2 \right) - 1.
\end{aligned} \tag{4.98}$$

It follows, using PDG06 result from Eq. (4.93), that

$$\begin{aligned}
|a_{LR}^S|, |a_{LL}^S| &\lesssim 0.066 \quad (95\% \text{C.L.}) \\
|a_{LR}^T| &\lesssim 0.031 \quad (95\% \text{C.L.}) \\
|a_{RL}^V| &\lesssim 0.021 \quad (95\% \text{C.L.}),
\end{aligned} \tag{4.99}$$

which are  $10^3$  greater than the bounds from neutrino mass. The contributions from  $|a_{LR}^S|$ ,  $|a_{LL}^S|$ ,  $|a_{LR}^T|$ , and  $|a_{RL}^V|$  alone don't explain the PDG05 result from Eq. (4.93). So we need to include  $\Delta r_\mu$  or  $\tilde{a}_{RL}^V$ . However, when  $\Delta r_\beta \sim \Delta r_\mu$ , we can safely assume  $\Delta r_\beta \lesssim 10^{-3}$  which still yields the same bounds.

#### 4.3.6.2 $R_{e/\mu}$

Constraints on  $|a_{LR}^S|$ ,  $|a_{LL}^S|$ , and  $|a_{LR}^T|$  can also be obtained by studying the results of  $\pi_{\ell 2}$  decays. The ratio

$$R_{e/\mu} = \frac{\Gamma(\pi^+ \rightarrow e^+ \nu_e) + \Gamma(\pi^+ \rightarrow e^+ \nu_e \gamma)}{\Gamma(\pi^+ \rightarrow \mu^+ \nu_\mu) + \Gamma(\pi^+ \rightarrow \mu^+ \nu_\mu \gamma)} \tag{4.100}$$

has been measured precisely at PSI [73] and TRIUMF [74]. Comparing the Particle Data Group average [67] with the SM value as calculated in [75], one has

$$\frac{R_{e/\mu}^{EX}}{R_{e/\mu}^{SM}} = 0.9958 \pm 0.0033 \pm 0.0004 \tag{4.101}$$

where the first error is experimental and the second is theoretical. In terms of couplings in Eq. (4.42), one has [71]

$$\frac{R_{e/\mu}}{R_{e/\mu}^{SM}} = \left| 1 + \eta'_{LL} - \eta_{LR} + \omega_e(\eta_{RP} + 2k_0\alpha_{RL}^T) \right|^2 + \left| \eta_{RL} - \eta_{RR} + \omega_e(\eta_{LP} - 2k_0\alpha_{LR}^T) \right|^2 \quad (4.102)$$

where  $\eta'_{LL} = \frac{a_{LL}^V}{V_{ud}} - 1$ ,  $\eta_{ik} = \frac{a_{ik}^V}{V_{ud}}$  ( $ik = LR, RL, RR$ ),  $\eta_{iP} = \frac{a_{iL}^S - a_{iR}^S}{V_{ud}}$  ( $i = L, R$ ),  $\omega_e = \frac{m_\pi}{m_e} \frac{m_\pi}{m_u + m_d} \sim 2.6 \times 10^3$ , and  $k_0 \sim e_e(e_u + e_d) \frac{3\alpha}{\pi} \ln \frac{M_W^2}{\mu^2} \sim 10^{-2}$ . The  $\alpha_{RL}^T$  and  $\alpha_{LR}^T$  appear in Eq. (4.102) because the tensor interactions can induce the scalar ones by exchanging photons between quarks and charged leptons[78]. The corresponding  $2\sigma$  bounds on  $|a_{LR}^S|$ ,  $|a_{LL}^S|$ , and  $|a_{LR}^T|$  are

$$\begin{aligned} |a_{LL}^S - a_{LR}^S| &\lesssim 2 \times 10^{-5} \quad (95\% \text{C.L.}) \\ |a_{LR}^T| &\lesssim 1 \times 10^{-3} \quad (95\% \text{C.L.}) \\ |a_{RL}^V| &\lesssim 5 \times 10^{-2} \quad (95\% \text{C.L.}) \end{aligned} \quad (4.103)$$

where the bounds on scalar couplings are roughly comparable to the ones from neutrino mass and the bounds on tensor coupling is  $10^2$  greater than the one from neutrino mass. It should be noted that the bounds (4.103) would become insignificant, if there were also a contribution from new S and T interactions to  $\pi^+ \rightarrow \mu\nu$  with coupling constants comparable to  $a_{LL}^S$ ,  $a_{LR}^S$ , and  $a_{LR}^T$ . Future experiments will make more precise measurements of  $R_{e/\mu}$ , aiming for precision at the level of  $< 1 \times 10^{-3}$  (TRIUMF [76]) and  $5 \times 10^{-4}$  (PSI [77]). With higher precision on  $R_{e/\mu}$ , the constraints on  $a_{LL}^S$  and  $a_{LR}^S$  would be stronger than those from neutrino mass.

### 4.3.6.3 $\pi_\beta$

We note that operators associated with  $a_{LL}^S$ ,  $a_{LR}^S$ , and  $a_{RL}^V$  in the effective Lagrangian Eq. (4.42) could contribute to pion beta decay. So a precise measurement of its branching ratio, together with the SM prediction, would imply bounds on  $a_{LL}^S$ ,  $a_{LR}^S$ , and  $a_{RL}^V$ . We calculate the correction due to  $a_{LL}^S$ ,  $a_{LR}^S$ , and  $a_{RL}^V$  terms in the effective Lagrangian Eq. (4.42) to pion beta decay rate as follows:

We note that the part of Effective Lagragian (4.42) associated with  $a_{LL}^S$ ,  $a_{LR}^S$ , and  $a_{RL}^V$

$$\frac{4G_\mu}{\sqrt{2}} (a_{LR}^S \bar{e}_L \nu_e \bar{u} d_R + a_{LL}^S \bar{e}_L \nu_e \bar{u} d_L) + \frac{4G_\mu}{\sqrt{2}} (a_{RL}^V \bar{e}_R \gamma^\mu \nu_e \bar{u} \gamma_\mu d_R) \quad (4.104)$$

would contribute to  $\pi^+ \rightarrow \pi^0 e^+ \nu$ . The amplitude is of the form

$$\begin{aligned} \delta \mathcal{M} = & \frac{4G_\mu}{\sqrt{2}} \frac{(a_{LR}^S + a_{LL}^S)}{2} \langle \pi^0 | \bar{u} d | \pi^+ \rangle \bar{u}_e \left( \frac{1 + \gamma^5}{2} \right) v_\nu \\ & + \frac{4G_\mu}{\sqrt{2}} \frac{a_{RL}^V}{2} \langle \pi^0 | \bar{u} \gamma_\mu d | \pi^+ \rangle \bar{u}_e \gamma^\mu \left( \frac{1 + \gamma^5}{2} \right) v_\nu \end{aligned} \quad (4.105)$$

where we set  $\langle \pi^0 | \bar{u} \gamma^5 d | \pi^+ \rangle = \langle \pi^0 | \bar{u} \gamma^5 \gamma_\mu d | \pi^+ \rangle = 0$  due to the parity symmetry. The hadronic matrix element  $\langle \pi^0 | \bar{u}(x) \gamma_\mu d(x) | \pi^+ \rangle$  is

$$\begin{aligned} & \langle \pi^0 | \bar{u}(x) \gamma_\mu d(x) | \pi^+ \rangle \\ & = \left[ f_+ (Q^2) (p_{\pi^0} + p_{\pi^+})_\mu + f_- (Q^2) (p_{\pi^0} - p_{\pi^+})_\mu \right] e^{-i(p_{\pi^+} - p_{\pi^0}) \cdot x} \end{aligned} \quad (4.106)$$

where  $Q^2 = (p_{\pi^+} - p_{\pi^0})^2$  and  $f_- = 0$  due to conservation of the current  $\bar{u}(x) \gamma_\mu d(x)$  and isospin symmetry and  $f_+(0) = \sqrt{2}$  given by CVC. Taking the derivative on both sides of Eq. (4.106) gives us

$$\begin{aligned} \partial^\mu \langle \pi^0 | \bar{u}(x) \gamma_\mu d(x) | \pi^+ \rangle & = i(m_u - m_d) \langle \pi^0 | \bar{u}(x) d(x) | \pi^+ \rangle \\ & = -i f_+ (p_{\pi^+} - p_{\pi^0})^\mu (p_{\pi^0} + p_{\pi^+})_\mu e^{-i(p_{\pi^+} - p_{\pi^0}) \cdot x} \\ \implies \langle \pi^0 | \bar{u}(x) d(x) | \pi^+ \rangle & = \frac{m_{\pi^0}^2 - m_{\pi^+}^2}{m_u - m_d} f_+ e^{-i(p_{\pi^+} - p_{\pi^0}) \cdot x} \end{aligned} \quad (4.107)$$

where we use

$$\partial^\mu (\bar{u}(x) \gamma_\mu d(x)) = i(m_u - m_d) \bar{u}(x) d(x). \quad (4.108)$$

So the amplitude becomes

$$\begin{aligned} \delta \mathcal{M} = & \frac{4G_\mu f_+}{\sqrt{2}} \left( \frac{(a_{LR}^S + a_{LL}^S)}{2} \frac{m_{\pi^0}^2 - m_{\pi^+}^2}{m_u - m_d} \bar{u}_e \left( \frac{1 + \gamma^5}{2} \right) v_\nu \right. \\ & \left. + \frac{a_{RL}^V}{2} (p_{\pi^0} + p_{\pi^+})_\mu \bar{u}_e \gamma^\mu \left( \frac{1 + \gamma^5}{2} \right) v_\nu \right). \end{aligned} \quad (4.109)$$

Considering that the pion mass is much greater than the pion momenta, the momentum

terms can be neglected and so one has

$$\begin{aligned} \delta\mathcal{M} \approx & \frac{4G_\mu f_+}{\sqrt{2}} \left( -\frac{(a_{LR}^S + a_{LL}^S)}{2} \frac{2m_\pi^2 \Delta}{m_u - m_d} \bar{u}_e \left( \frac{1 + \gamma^5}{2} \right) v_\nu \right. \\ & \left. + \frac{a_{RL}^V}{2} 2m_\pi \bar{u}_e \gamma^0 \left( \frac{1 + \gamma^5}{2} \right) v_\nu \right) \end{aligned} \quad (4.110)$$

where  $\Delta = m_{\pi^+} - m_{\pi^0}$ ,  $m_\pi = \frac{m_{\pi^+} + m_{\pi^0}}{2}$ .

The total amplitude is  $\mathcal{M}_{tot} = \mathcal{M}_{SM} + \delta\mathcal{M}$ , where  $SM$  denotes contributions from the Standard Model. In computing  $|\mathcal{M}_{tot}|^2$  to obtain the differential rate, we find that the cross term involving  $\mathcal{M}_{SM}$  and  $\delta\mathcal{M}$  vanishes, since  $\mathcal{M}_{SM}$  contains no right-handed neutrino spinors. For  $|\delta\mathcal{M}|^2$ , we have

$$\begin{aligned} |\delta\mathcal{M}|^2 &= \left( \frac{4G_\mu f_+}{\sqrt{2}} \right)^2 \left[ \left| \frac{(a_{LR}^S + a_{LL}^S)}{2} \frac{2m_\pi^2 \Delta}{m_u - m_d} \right|^2 Tr \left( p_e \cdot \gamma \frac{1 + \gamma^5}{2} p_\nu \cdot \gamma \right) \right. \\ &\quad \left. + 4m_\pi^2 \left| \frac{a_{RL}^V}{2} \right|^2 Tr \left( p_e \cdot \gamma \gamma^0 \frac{1 + \gamma^5}{2} p_\nu \cdot \gamma \gamma^0 \right) \right] \\ &= \left( \frac{4G_\mu f_+}{\sqrt{2}} \right)^2 \left[ \left| \frac{(a_{LR}^S + a_{LL}^S)}{2} \frac{2m_\pi^2 \Delta}{m_u - m_d} \right|^2 2(E_e \cdot E_\nu - \mathbf{p}_e \cdot \mathbf{p}_\nu) \right. \\ &\quad \left. + 4m_\pi^2 \left| \frac{a_{RL}^V}{2} \right|^2 2(E_e \cdot E_\nu + \mathbf{p}_e \cdot \mathbf{p}_\nu) \right] \\ &\sim \left( \frac{4G_\mu f_+}{\sqrt{2}} \right)^2 \left[ \left| \frac{(a_{LR}^S + a_{LL}^S)}{2} \frac{2m_\pi^2 \Delta}{m_u - m_d} \right|^2 2(E_e \cdot E_\nu) \right. \\ &\quad \left. + 4m_\pi^2 \left| \frac{a_{RL}^V}{2} \right|^2 2(E_e \cdot E_\nu) \right] \\ &= \left( \frac{4G_\mu f_+}{\sqrt{2}} \right)^2 \left[ \left| \frac{(a_{LR}^S + a_{LL}^S)}{2} \frac{2m_\pi^2 \Delta}{m_u - m_d} \right|^2 2 + 8m_\pi^2 \left| \frac{a_{RL}^V}{2} \right|^2 \right] (E_e \cdot E_\nu) \end{aligned} \quad (4.111)$$

where  $\mathbf{p}_e \cdot \mathbf{p}_\nu$  would integrate to zero when calculating the decay rate so that only the  $E_e \cdot E_\nu$  term would contribute.

The decay rate of  $\pi^+ \rightarrow \pi^0 e^+ \nu$  is

$$\begin{aligned} d\delta\Gamma &= \frac{(2\pi)^4 |\delta\mathcal{M}|^2 \delta^{(4)}(p_{\pi^+} - p_{\pi^0} - p_e - p_\nu)}{2m_{\pi^+}} \frac{d^3\mathbf{p}_{\pi^0}}{(2\pi)^3 2E_{\pi^0}} \frac{d^3\mathbf{p}_e}{(2\pi)^3 2E_e} \frac{d^3\mathbf{p}_\nu}{(2\pi)^3 2E_\nu} \\ &\approx \frac{|\delta\mathcal{M}|^2 \delta(\Delta - E_e - E_\nu)}{16m_\pi^2 E_e E_\nu (2\pi)^5} d^3\mathbf{p}_e 4\pi E_\nu^2 dE_\nu \end{aligned} \quad (4.112)$$

where we integrate over the final state pion momentum  $\mathbf{p}_{\pi^0}$  and set  $E_{\pi^+} = m_{\pi^+}$  and  $E_{\pi^0} = m_{\pi^0}$  by neglecting the pion momenta. Then we have

$$\begin{aligned} \delta\Gamma &= \int \frac{|\delta\mathcal{M}|^2 \delta(\Delta - E_e - E_\nu)}{16m_\pi^2 E_e E_\nu (2\pi)^5} d^3\mathbf{p}_e 4\pi E_\nu^2 dE_\nu \\ &= \left( \frac{4G_\mu f_+}{\sqrt{2}} \right)^2 \left[ \left| \frac{(a_{LR}^S + a_{LL}^S)}{2} \frac{2m_\pi^2 \Delta}{m_u - m_d} \right|^2 + 8m_\pi^2 \left| \frac{a_{RL}^V}{2} \right|^2 \right] \\ &= \left( \left| (a_{LR}^S + a_{LR}^S) \frac{2\Delta}{m_u - m_d} \right|^2 + 4 |a_{RL}^V|^2 \right) \frac{G_\mu^2 \Delta^5}{15 (2\pi)^3}. \end{aligned} \quad (4.113)$$

Finally, taking the ratio of this to the decay rate of  $\pi^+ \rightarrow \mu^+ \nu$

$$\Gamma_{\pi^+ \rightarrow \mu^+ \nu} = \frac{G_\mu^2}{4\pi} F_\pi^2 m_\mu^2 m_\pi |V_{ud}|^2 \left( 1 - \frac{m_\mu^2}{m_\pi^2} \right)^2 \quad (4.114)$$

yields

$$\begin{aligned} \delta Br(\pi^+ \rightarrow \pi^0 e^+ \nu) &= \frac{2\Delta^5 \left( \left| (a_{LR}^S + a_{LR}^S) \frac{2\Delta}{m_u - m_d} \right|^2 + 4 |a_{RL}^V|^2 \right)}{15 (2\pi)^2 F_\pi^2 m_\mu^2 m_\pi |V_{ud}|^2 \left( 1 - \frac{m_\mu^2}{m_\pi^2} \right)^2} \\ &\approx 1.32 \times 10^{-8} \left( |a_{LR}^S + a_{LR}^S|^2 + |a_{RL}^V|^2 \right) \end{aligned} \quad (4.115)$$

where we use  $\Delta = m_{\pi^+} - m_{\pi^0} = 4.59$  MeV,  $m_\pi = \frac{m_{\pi^+} + m_{\pi^0}}{2} = 137.27$  MeV,  $F_\pi = 92.4$  MeV, and  $m_\mu = 105.66$  MeV. The predictions [79] of the SM and CVC, given the PDG recommended value range for  $V_{ud}$ , are

$$Br^{SM}(\pi^+ \rightarrow \pi^0 e^+ \nu) = (1.038 - 1.041) \times 10^{-8} \quad (4.116)$$

while the PIBETA collaboration's recent result [79] is

$$Br^{EX}(\pi^+ \rightarrow \pi^0 e^+ \nu) = [1.036 \pm 0.004(stat) \pm 0.005(syst)] \times 10^{-8} \quad (4.117)$$

which implies

$$|\delta Br(\pi^+ \rightarrow \pi^0 e^+ \nu)| \lesssim 0.023 \times 10^{-8} \quad (95\% \text{ C.L.}) \quad (4.118)$$

From Eq. (4.118), one has the bounds on  $a_{LL}^S$ ,  $a_{LR}^S$ , and  $a_{RL}^V$

$$\begin{aligned} |a_{LR}^S + a_{LR}^S| &\lesssim 0.13 \quad (95\% \text{C.L.}) \\ |a_{RL}^V| &\lesssim 0.13 \quad (95\% \text{C.L.}) \end{aligned} \quad (4.119)$$

#### 4.4 Constraints on $\pi \rightarrow \nu \bar{\nu}$

The decay  $\pi^0 \rightarrow \nu \bar{\nu}$  is forbidden by angular momentum conservation if the neutrino is massless. This is the case in SM. So the upper bound on neutrino masses would imply the upper limit for the branching ratio of  $\pi^0 \rightarrow \nu \bar{\nu}$ . The most general local nonderivative effective neutrino-quark interaction that could contribute to  $\pi^0 \rightarrow \nu \bar{\nu}$  is given in [69] by:

$$\mathcal{L} = \frac{G_\mu}{\sqrt{2}} [g_{AA} \bar{\nu} \gamma^\mu \gamma^5 \nu J_\mu^A + (g_{PP} \bar{\nu} \gamma^5 \nu + i g_{SP} \bar{\nu} \nu) J^P] \quad (4.120)$$

where  $J_\mu^A = \frac{1}{2} (\bar{u} \gamma_\mu \gamma_5 u - \bar{d} \gamma_\mu \gamma_5 d)$ ,  $J^P = \frac{1}{2} (\bar{u} \gamma_5 u - \bar{d} \gamma_5 d)$ , and a branching ratio is

$$B(\pi^0 \rightarrow \nu \bar{\nu}) \approx (9.6 \times 10^{-7}) \kappa \left[ \left( 0.2 g_{AA} \frac{m_\nu}{m_\pi} - g_{PP} \right)^2 + \kappa^2 g_{SP}^2 \right] \quad (4.121)$$

where  $\kappa = \sqrt{1 - \frac{4m_\nu^2}{m_\pi^2}}$ ,  $m_\nu$  and  $m_\pi$  denote the neutrino and the pion mass.

In Eq. (4.120), the first term comes from the Standard Model and new physics. Since the contribution from the SM to  $g_{AA}$  dominates over the one from new physics, we can safely assume  $g_{AA} = 1$ . The chirality-changing pseudoscalar interaction in Eq. (4.120) could induce the neutrino mass radiatively and thereby be generated by  $\mathcal{O}_{Q,AD,\alpha\beta}^{(6)}$ ,  $\mathcal{O}_{d1,AD,\alpha\beta}^{(6)}$ ,  $\mathcal{O}_{d2,AD,\alpha\beta}^{(6)}$ , and  $\mathcal{O}_{\tilde{\nu},AB}^{(6)}$ , after integrating out the massive gauge bosons below the weak scale. Matching

Eq. (4.120) with Eq. (4.63) at  $m_N$  gives

$$\begin{aligned}
g_{PP} &= -\frac{v^2}{\Lambda^2} \left( \frac{a_{AD,11}^{S3}(m_N) + a_{DA,11}^{S3*}(m_N)}{2} + \frac{a_{AD,11}^{S4}(m_N) + a_{DA,11}^{S4*}(m_N)}{2} \right) \\
g_{SP} &= \frac{v^2}{\Lambda^2} \left( \frac{a_{AD,11}^{S3}(m_N) - a_{DA,11}^{S3*}(m_N)}{2i} + \frac{a_{AD,11}^{S4}(m_N) - a_{DA,11}^{S4*}(m_N)}{2i} \right)
\end{aligned} \tag{4.122}$$

where  $A$  and  $D$  are the flavors of two neutrinos in the final products. Using Eq. (4.64) and Eq. (4.81), we have

$$\begin{aligned}
|g_{PP}| &\lesssim \frac{K_S v^2 (4\pi)^2}{\Lambda^2 2N_C} \left( \frac{m_\nu}{m_u} + \frac{3m_\nu}{m_d} \right) \sim 4 \times 10^{-5} \\
|g_{SP}| &\lesssim \frac{K_S v^2 (4\pi)^2}{\Lambda^2 2N_C} \left( \frac{m_\nu}{m_u} + \frac{3m_\nu}{m_d} \right) \sim 4 \times 10^{-5},
\end{aligned} \tag{4.123}$$

which implies  $B(\pi^0 \rightarrow \nu\bar{\nu}) < 3 \times 10^{-15}$  which we use  $m_\nu \sim 1\text{eV}$  and set  $\Lambda = v$ . Our result is eight orders of magnitude stronger than the current best experimental limit [70] and  $10^4$  stronger than the result obtained in [44]. While only carried out our analysis in the Dirac case, we believe the same result should hold for the Majorana case.

# Bibliography

- [1] S.L. Glashow, Nucl. Phys. 22, 579 (1961); S. Weinberg, Phys. Rev. Lett. 19, 1264 (1967).
- [2] Phys. Scripta T121 (2005) 17–22; A. Franklin, Are There Really Neutrinos?, Cambridge, Perseus Books (2001).
- [3] Super-Kamiokande Collaboration, S. Fukuda et al., Phys. Rev. Lett. 81, 1562 (1998); S. Fukuda et al., Phys. Rev. Lett. 82, 2644 (1999); S. Fukuda et al., Phys. Rev. Lett. 85, 3999 (2000).
- [4] SNO collaboration, Q.R. Ahmad *et al.*, Phys. Rev. Lett. 87, 071301 (2001); Q.R. Ahmad *et al.*, Phys. Rev. Lett. 89, 011301 (2002); Q.R. Ahmad *et al.*, Phys.Rev.Lett 89, 011302 (2002).
- [5] KamLAND collaboration, K. Eguchi et al., Phys. Rev. Lett. 90, 021802 (2003).
- [6] B. T. Cleveland et al., Astrophys. J. 496, 505 (1998).
- [7] GALLEX Collaboration, W. Hampel et al., Phys. Lett. B 447, 127 (1999); GNO Collaboration, M. Altmann et al., Phys. Lett. B 490, 16 (2000); Nucl. Phys. Proc. Suppl. 91, 44 (2001).
- [8] SAGE Collaboration, J. N. Abdurashitov et al., Phys. Rev. C 60, 055801 (1999); Nucl. Phys. Proc. Suppl. 110, 315 (2002).
- [9] Super-Kamiokande Collaboration, S. Fukuda et al., Phys. Rev. Lett. 86, 5651(2001).
- [10] Soudan 2 Collaboration, W.W.M.Allison et al., Physics Letters B 449, 137 (1999).
- [11] Phys. Lett. B 517, 59 (2001); M. Ambrosio et al. NATO Advanced Research Workshop on Cosmic Radiations, Oujda (Morocco), 21–23 March, 2001.

- [12] Mainz Collaboration, J. Bonn et al., Nucl. Phys. Proc. Suppl. 91, 273 (2001).
- [13] Katrin Collaboration, A. Osipowicz et al., Eur. Phys. J. C26, 457 (2003).
- [14] W.M. Yao et al., Journal of Physics G 33, 1 (2006).
- [15] M. Gell-Mann, P. Ramond and R. Slansky, in Supergravity, p. 315, edited by F. van Nieuwenhuizen and D. Freedman, North Holland, Amsterdam, 1979; T. Yanagida, Proc. of the Workshop on Unified Theory and the Baryon Number of the Universe, KEK, Japan (1979); R.N. Mohapatra and G. Senjanovi, Phys. Rev. Lett. 44, 912 (1980).
- [16] S. R. Elliott and P. Vogel, Annu. Rev. Nucl. Part. Sci. 52, 115 (2002).
- [17] S. P. Mikheyev, A. Y. Smirnov, Nuovo Cim. 9C 17 (1986); L. Wolfenstein, Phys. Rev. D 17, 2369 (1978).
- [18] M. B. Voloshin, Sov. J. Nucl. Phys. 48, 512 (1988). For a specific implementation, see R. Barbieri and R. N. Mohapatra, Phys. Lett. B 218, 225 (1989).
- [19] H. Georgi and L. Randall, Phys. Lett. B 244, 196 (1990).
- [20] W. Grimus and H. Neufeld, Nucl. Phys. B 351, 115 (1991).
- [21] K. S. Babu and R. N. Mohapatra, Phys. Rev. Lett. 64, 1705 (1990).
- [22] S. M. Barr, E. M. Freire and A. Zee, Phys. Rev. Lett. 65, 2626 (1990).
- [23] L. F. Abbott, Nucl. Phys. B 185, 189 (1981).
- [24] W. J. Marciano and A. I. Sanda, Phys. Lett. B 67, 303 (1977); B. W. Lee and R. E. Shrock, Phys. Rev. D 16, 1444 (1977); K. Fujikawa and R. Shrock, Phys. Rev. Lett. 45, 963 (1980).
- [25] J. F. Beacom and P. Vogel, Phys. Rev. Lett. 83, 5222 (1999); D. W. Liu et al., Phys. Rev. Lett. 93, 021802 (2004).
- [26] H. T. Wong [TEXONO Collaboration], [arXiv:hep-ex/0605006]; B. Xin et al. [TEXONO Collaboration], Phys. Rev. D 72, 012006 (2005); Z. Daraktchieva et al. [MUNU Collaboration], Phys. Lett. B 615, 153 (2005).

- [27] G.G. Raffelt, Phys. Rep. 320, 319 (1999).
- [28] A. B. Balantekin, [arXiv:hep-ph/0601113]; A. de Gouvea and J. Jenkins, [arXiv:hep-ph/0603036]; A. Friedland, [arXiv:hep-ph/0505165].
- [29] M. Fukugita and T. Yanagida, Physics of neutrinos and applications to astrophysics, Ch. 10, Springer, Berlin, (2003), and references therein.
- [30] B. Kayser, F. Gibrat-Debu and F. Perrier, World Sci. Lect. Notes Phys. 25, 1 (1989).
- [31] H. T. Wong and H. B. Li, Mod. Phys. Lett. A 20, 1103 (2005).
- [32] G. C. McLaughlin and J. N. Ng, Phys. Lett. B 470, 157 (1999); R. N. Mohapatra, S. P. Ng, and H. b. Yu, Phys. Rev. D 70, 057301 (2004).
- [33] L. Michel, Proc. Roy. Soc. Lond. A 63, 514 (1950); C. Bouchiat and L. Michel, Phys. Rev. 106, 170 (1957).
- [34] T. Kinoshita and A. Sirlin, Phys. Rev. 108, 844 (1957).
- [35] J. R. Musser [TWIST Collaboration], Phys. Rev. Lett. 94, 101805 (2005) [arXiv:hep-ex/0409063].
- [36] A. Gaponenko et al. [TWIST Collaboration], Phys. Rev. D 71, 071101 (2005) [arXiv:hep-ex/0410045].
- [37] N. Danneberg et al., Phys. Rev. Lett. 94, 021802 (2005).
- [38] R. Tribble and G. Marshall, private communication. See also Hu, J, Proceedings of the PANIC05 conference , Sante Fe, N.M., 2005.
- [39] Beck, M., et al., Nucl. Instr. and Meth. A 503, 567 (2003); Beck, M., et al., Nucl. Instr. and Meth. B 204, 521 (2003).
- [40] C. A. Gagliardi, R. E. Tribble and N. J. Williams, [arXiv:hep-ph/0509069].
- [41] R. J. Erwin, J. Kile, M. J. Ramsey-Musolf, and P. Wang, Phys. Rev. D 75, 033005 (2007) [arXiv:hep-ph/0602240].
- [42] Nicole F. Bell, Mikhail Gorchtein, Michael J. Ramsey-Musolf, Petr Vogel, and Peng Wang, Phys. Lett. B 642, 377 (2006).

- [43] S. Profumo, M. J. Ramsey-Musolf, and S. Tulin, [arXiv:hep-ph/0608064].
- [44] G. Prezeau and A. Kurylov, Phys. Rev. Lett. 95, 101802 (2005) [arXiv:hep-ph/0409193].
- [45] N. F. Bell, V. Cirigliano, M. J. Ramsey-Musolf, P. Vogel and M. B. Wise, Phys. Rev. Lett. 95, 151802 (2005) [arXiv:hep-ph/0504134].
- [46] P. Herczeg, Prog. Part. Nucl. Phys. 46, 413 (2001).
- [47] L. E. Ibanez, F. Marchesano, and R. Rabadan, JHEP 0111, 002 (2001).
- [48] I. Antoniadis, E. Kiritsis, J. Rizos, and T. N. Tomaras, Nucl. Phys. B 660, 81 (2003).
- [49] Paul Langacker and Brent D. Nelson, Phys. Rev. D 72, 053013 (2005).
- [50] M. Doi, T. Kotani and H. Nishiura, Prog. Theor. Phys. 114, 845 (2005) [arXiv:hepph/0502136].
- [51] T. M. Ito and G. Prezeau, Phys. Rev. Lett. 94, 161802 (2005) [arXiv:hep-ph/0410254].
- [52] N. Severijns, M. Beck and O. Naviliat-Cuncic, [arXiv:nucl-ex/0605029].
- [53] S. Davidson, M. Gorbahn, and A. Santamaria, Phys. Lett. B 626, 151 (2005) [arXiv:hep-ph/0506085].
- [54] LEP Electroweak Working Group, <http://lepewwg.web.cern.ch/LEPEWWG/>.
- [55] J. D Jackson, S. B. Treiman, and H. W. Wyld, Jr., Phys. Rev. 106, 517 (1957); Nucle. Phys. 4, 206 (1957).
- [56] C. P. Burgess and D. London, Phys. Rev. D 48, 4337 (1993).
- [57] V. M. Lobashev et al., Phys. Lett. B 460, 227 (1999).
- [58] C. Weinheimer et al., Phys. Lett. B 460, 219 (1999).
- [59] LEP Electroweak Working Group, <http://lepewwg.web.cern.ch/LEPEWWG/>
- [60] J. C. Hardy, and I. S. Towner, Phys. Rev. Lett. 94, 092502 (2005).
- [61] A. S. Carnoy et al., Phys. Rev. C 43, 2825 (1991).

- [62] V. Egorov, et al., Nucl. Phys. A 621, 745 (1997).
- [63] E. G. Adelberger, et al., Phys. Rev. Lett. 83, 1299 (1999).
- [64] W.E. Ormand, B.A. Brown, and B.R. Holstein, Phys. Rev. C 40, 2914 (1989).
- [65] C. H. Johnson, F. Pleasonton, and T. A. Carlson, Phys. Rev. 132, 1149 (1963).
- [66] J. Giedt, G. L. Kane, P. Langacker and B. D. Nelson, Phys. Rev. D 71, 115013 (2005)  
[arXiv:hep-th/0502032].
- [67] W.-M. Yao et al., Journal of Physics G 33, 1 (2006).
- [68] S. Eidelman et al., Phys. Lett. B592, 1 (2004).
- [69] P. Herczeg and C. M. Hoffman, Phys. Lett. 100, 347 (1981).
- [70] A. V. Artamonov et al., Phys. Rev. D 72, 091102 (2005).
- [71] P. Herczeg, Phys. Rev. D 52, 3949 (1995).
- [72] M. J. Ramsey-Musolf, Phys. Rev. D62, 056009 (2000).
- [73] C. Czapek et al., Phys. Rev. Lett. 70, 17 (1993).
- [74] D.I. Britton et al., Phys. Rev. Lett. 68, 3000 (1992).
- [75] W. Marciano and A. Sirlin, Phys. Rev. Lett. 71, 3629 (1993).
- [76] T. Numao and D. A. Bryman [PIENU collaboration], future experiment,  
<https://www.pienu.triumf.ca>.
- [77] D. Počanić and A. van der Shaaf [PEN collaboration], future experiment,  
<http://pen.phys.virginia.edu/>.
- [78] M. B. Voloshin, Phys. Lett. B 283, 120 (1992).
- [79] D. Pocanic et al., Phys. Rev. Lett. 93, 181803 (2004).